

Striking many-body effects in a simple (B_2O_3) oxide

Guillaume Ferlat

IMPMC, Sorbonne Université, Paris, France

Michele Casula



IMPMC,
Sorbonne Univ.

Maria Hellgren



IMPMC,
Sorbonne Univ.

Mathieu Salanne



PHENIX,
Sorbonne Univ.

1^{ère} réunion générale du GDR NBODY

8-10 janvier 2020, Lille, France



Striking many-body effects in a simple (B_2O_3) oxide

PHYSICAL REVIEW MATERIALS 3, 063603 (2019)

van der Waals forces stabilize low-energy polymorphism in B_2O_3 : Implications for the crystallization anomaly

Guillaume Ferlat,¹ Maria Hellgren,¹ François-Xavier Coudert,² Henri Hay,¹ Francesco Mauri,^{1,3} and Michele Casula¹

¹Sorbonne Université, MNHN, UMR CNRS 7590, IRD, IMPMC, F-75005 Paris, France

²Chimie ParisTech, PSL University, CNRS, Institut de Recherche de Chimie Paris, 75005 Paris, France

³Dipartimento di Fisica, Università di Roma La Sapienza, Piazzale Aldo Moro 5, I-00185 Roma, Italy



(Received 13 December 2018; published 10 June 2019)

Many-body effects at the origin of structural transitions in B_2O_3

Cite as: J. Chem. Phys. 151, 224508 (2019); doi: 10.1063/1.5131763

Submitted: 15 October 2019 • Accepted: 27 November 2019 •

Published Online: 12 December 2019



Axelle Baroni,^{1,2,3} Fabien Pacaud,^{1,4} Mathieu Salanne,^{1,a)} Matthieu Micoulaut,² Jean-Marc Delaeye,⁴ Anita Zeidler,⁵ Philip S. Salmon,⁵ and Guillaume Ferlat^{1,b)}

AFFILIATIONS

¹Sorbonne Université, CNRS, PHENIX, F-75005 Paris, France

²Sorbonne Université, CNRS, LPTMC, F-75005 Paris, France

³Sorbonne Université, CNRS, MNHN, IRD, IMPMC, F-75005 Paris, France

⁴CEA, DEN, Laboratoire d'Etude des Matériaux et Procédés Actifs, 30207 Bagnols-sur-Cèze, France

Striking many-body effects in a simple (B_2O_3) oxide

nature
materials

LETTERS

PUBLISHED ONLINE: 2 SEPTEMBER 2012 | DOI:10.1038/NMAT3416

Hidden polymorphs drive vitrification in B_2O_3

Guillaume Ferlat^{1*}, Ari Paavo Seitsonen^{1,2}, Michele Lazzeri¹ and Francesco Mauri^{1*}

PHYSICAL REVIEW MATERIALS 3, 063603 (2019)

van der Waals forces stabilize low-energy polymorphism in B_2O_3 : Implications for the crystallization anomaly

Guillaume Ferlat,¹ Maria Hellgren,¹ François-Xavier Coudert,² Henri Hay,¹ Francesco Mauri,^{1,3} and Michele Casula¹

¹Sorbonne Université, MNHN, UMR CNRS 7590, IRD, IMPMC, F-75005 Paris, France

²Chimie ParisTech, PSL University, CNRS, Institut de Recherche de Chimie Paris, 75005 Paris, France

³Dipartimento di Fisica, Università di Roma La Sapienza, Piazzale Aldo Moro 5, I-00185 Roma, Italy



(Received 13 December 2018; published 10 June 2019)

Many-body effects at the origin of structural transitions in B_2O_3

Cite as: J. Chem. Phys. 151, 224508 (2019); doi: 10.1063/1.5131763

Submitted: 15 October 2019 • Accepted: 27 November 2019 •

Published Online: 12 December 2019



Axelle Baroni,^{1,2,3} Fabien Pacaud,^{1,4} Mathieu Salanne,^{1,5} Matthieu Micoulaut,² Jean-Marc Delaeye,⁴

Anita Zeidler,⁵ Philip S. Salmon,⁵ and Guillaume Ferlat^{1,6}

AFFILIATIONS

¹Sorbonne Université, CNRS, PHENIX, F-75005 Paris, France

²Sorbonne Université, CNRS, LPTMC, F-75005 Paris, France

³Sorbonne Université, CNRS, MNHN, IRD, IMPMC, F-75005 Paris, France

⁴CEA, DEN, Laboratoire d'Etude des Matériaux et Procédés Actifs, 30207 Bagnols-sur-Cèze, France

Striking many-body effects in a simple (B_2O_3) oxide

nature
materials

LETTERS

PUBLISHED ONLINE: 2 SEPTEMBER 2012 | DOI:10.1038/NMAT3416

Hidden polymorphs drive vitrification in B_2O_3

Guillaume Ferlat^{1*}, Ari Paavo Seitsonen^{1,2}, Michele Lazzari¹ and Francesc... ^{1,2,3,4} ^{1,2,3,4} ^{1,2,3,4} ^{1,2,3,4}

PHYSICAL REVIEW B 92, 144111 (2015)

Dispersion effects in SiO_2 polymorphs: An *ab initio* study

Henri Hay,^{1,*} Guillaume Ferlat,¹ Michele Casula,¹ Ari Paavo Seitsonen,^{1,2,3} and Francesco Mauri¹

¹Institut de Minéralogie, Physique des Matériaux et Cosmochimie, Sorbonne Universités - UPMC Univ Paris 06, UMR CNRS 7590, 4 Place Jussieu, F-75005 Paris, France

²Institut für Chemie, Universität Zürich, Winterthurerstrasse 190, CH-8057 Zürich, Switzerland

³École Normale Supérieure, Paris Sciences et Lettres (PSL) Research University, Département de Chimie, Sorbonne Universités, Université Pierre et Marie Curie (UPMC), Université Paris 06, CNRS UMR 8640 Pasteur, F-75005 Paris, France

(Received 22 July 2015; revised manuscript received 5 October 2015; published 30 October 2015)

PHYSICAL REVIEW MAT

van der Waals forces stabilize low-e
Implications for the crystallization anomaly

Guillaume Ferlat,¹ Maria Hellgren,¹ François-Xavier Coudert,² Henri Hay,¹ Francesco Mauri,^{1,3} and Michele Casula¹

¹Sorbonne Université, MNHN, UMR CNRS 7590, IRD, IMPMC, F-75005 Paris, France

²Chimie ParisTech, PSL University, CNRS, Institut de Recherche de Chimie Paris, 75005 Paris, France

³Dipartimento di Fisica, Università di Roma La Sapienza, Piazzale Aldo Moro 5, I-00185 Roma, Italy



(Received 13 December 2018; published 10 June 2019)

Many-body effects at the origin of structural transitions in B_2O_3

Cite as: J. Chem. Phys. 151, 224508 (2019); doi: 10.1063/1.5131763

Submitted: 15 October 2019 • Accepted: 27 November 2019 •

Published Online: 12 December 2019



Axelle Baroni,^{1,2,3} Fabien Pacaud,^{1,4} Mathieu Salanne,^{1,5} Matthieu Micoulaut,² Jean-Marc Delaeye,⁴ Anita Zeidler,⁵ Philip S. Salmon,⁵ and Guillaume Ferlat^{1,2,3}

AFFILIATIONS

¹Sorbonne Université, CNRS, PHENIX, F-75005 Paris, France

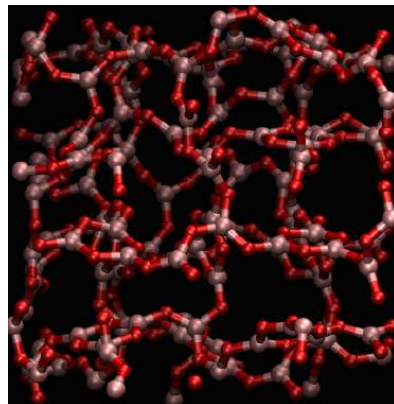
²Sorbonne Université, CNRS, LPTMC, F-75005 Paris, France

³Sorbonne Université, CNRS, MNHN, IRD, IMPMC, F-75005 Paris, France

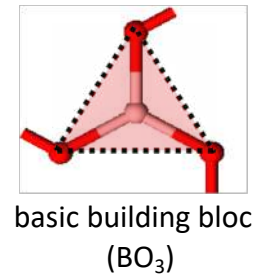
⁴CEA, DEN, Laboratoire d'Etude des Matériaux et Procédés Actifs, 30207 Bagnols-sur-Cèze, France

B₂O₃ (and borates): Motivations

- Major component of industrial glasses (ceramics, biomaterials, optical fibers, waste storage matrix, ...)
- A prototypical **network-forming** system based on **trigonal units**



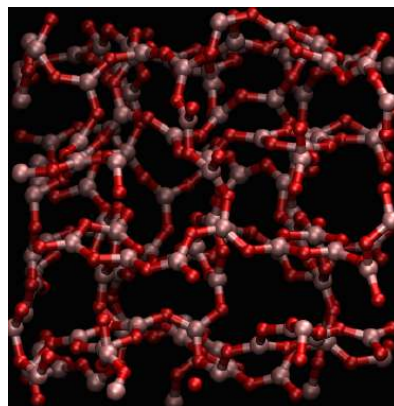
(simulated) glass configuration



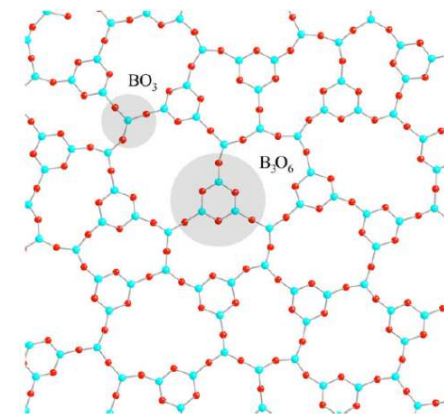
basic building block
(BO₃)

B_2O_3 (and borates): Motivations

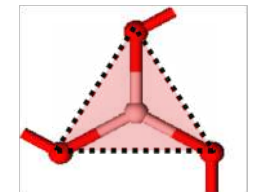
- Major component of industrial glasses (ceramics, biomaterials, optical fibers, waste storage matrix, ...)
- A prototypical **network-forming** system based on **trigonal units**



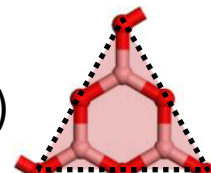
(simulated) glass configuration



2D schematic representation of the glass structure (from A.C. Hannon)



basic building block
(BO_3)

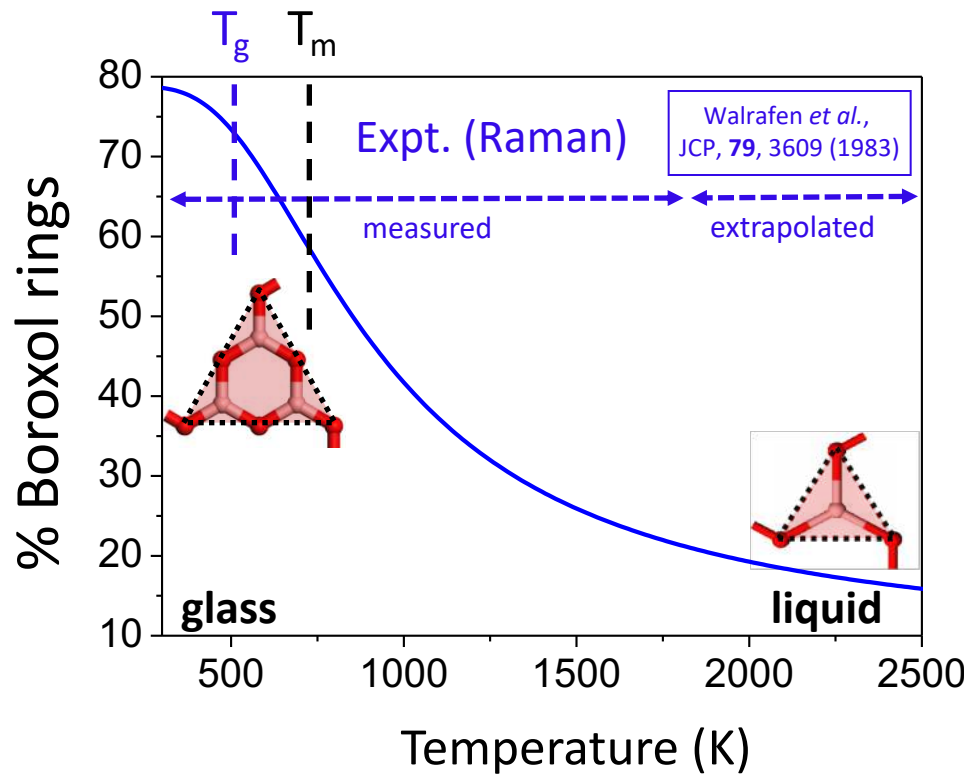
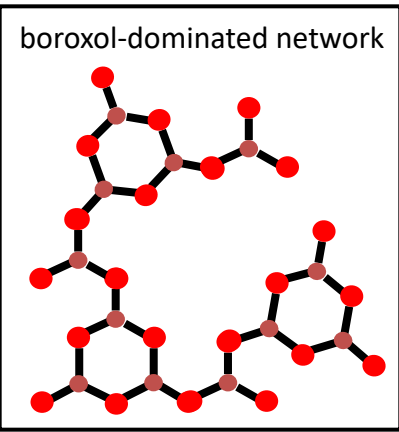


boroxol ring

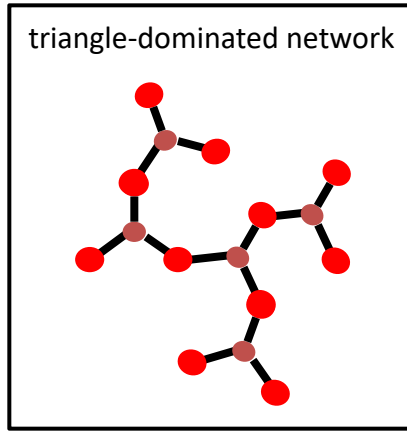
- A glass with significant **medium-range order (superstructural units)**
G. Ferlat et al., Phys. Rev. Lett., 101, 065504 (2008)
- The **glass former par excellence** (abnormal reluctance to crystallisation)

Experimental facts

Glass



Liquid



✓ Marked **structural transformation** (for $500 < T < 1500$ K)

[Existence of a boroxol ring stabilisation energy: $\Delta E \approx -6$ kcal/mol]

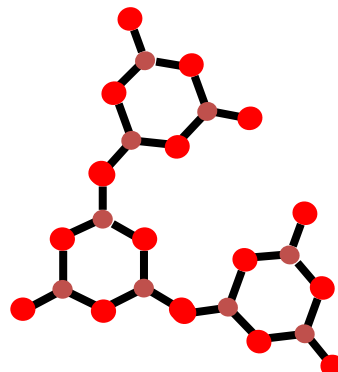
What is the driving force ? ...

Experimental facts

Why is the glass so (structurally) different from the known crystal?

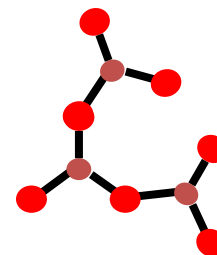
B₂O₃ anomaly n°1: the glass has a very different medium-range structure, dominated by **boroxol** rings

In the glass:



✓ Large amounts (~70%) of boroxol rings

In the crystal:

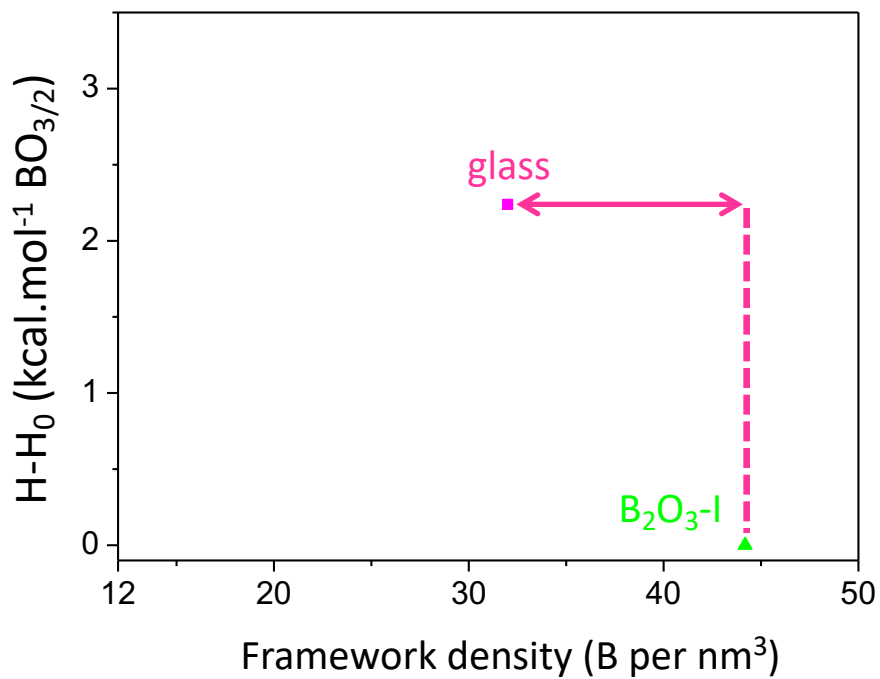


✓ NO boroxols at all in B₂O₃-I

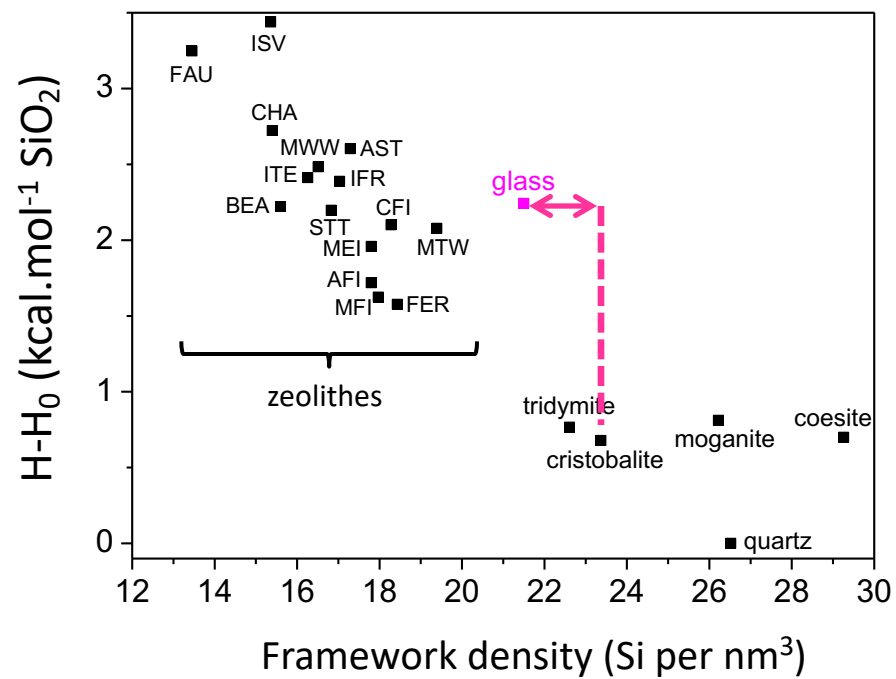
B₂O₃ anomaly n°2: the glass has a **low density** (1.84 g.cm⁻³) compared to the known crystal (B₂O₃-I: 2.55 g.cm⁻³)

Experimental facts

B_2O_3



SiO_2



$$\rho_{\text{glass}} \sim 0.71 \rho_{\text{crystal}}$$

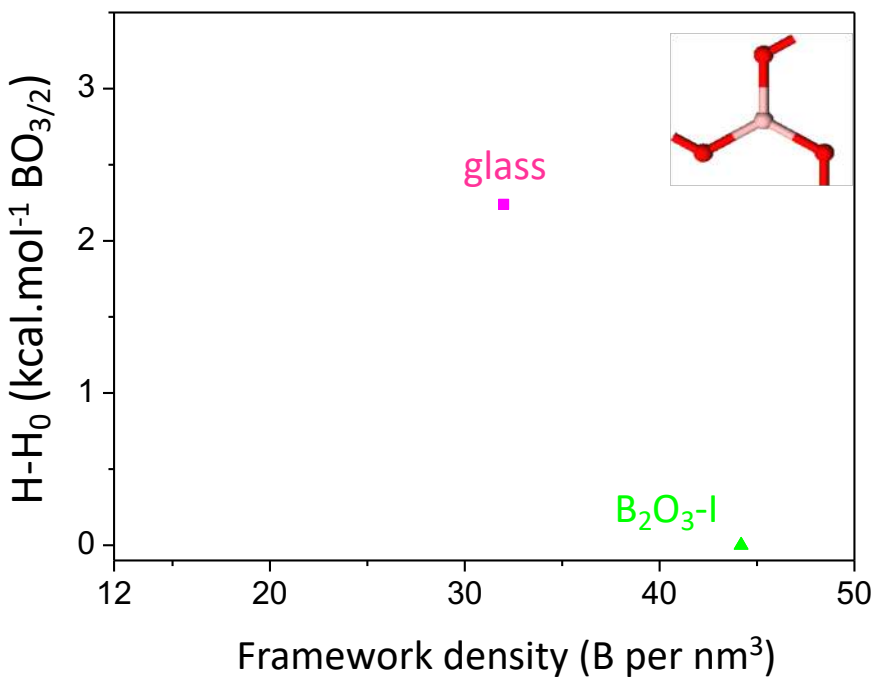
$$\rho_{\text{glass}} \sim 0.95 \rho_{\text{tridymite}}$$

$$\rho_{\text{glass}} \sim 0.92 \rho_{\text{cristobalite}}$$

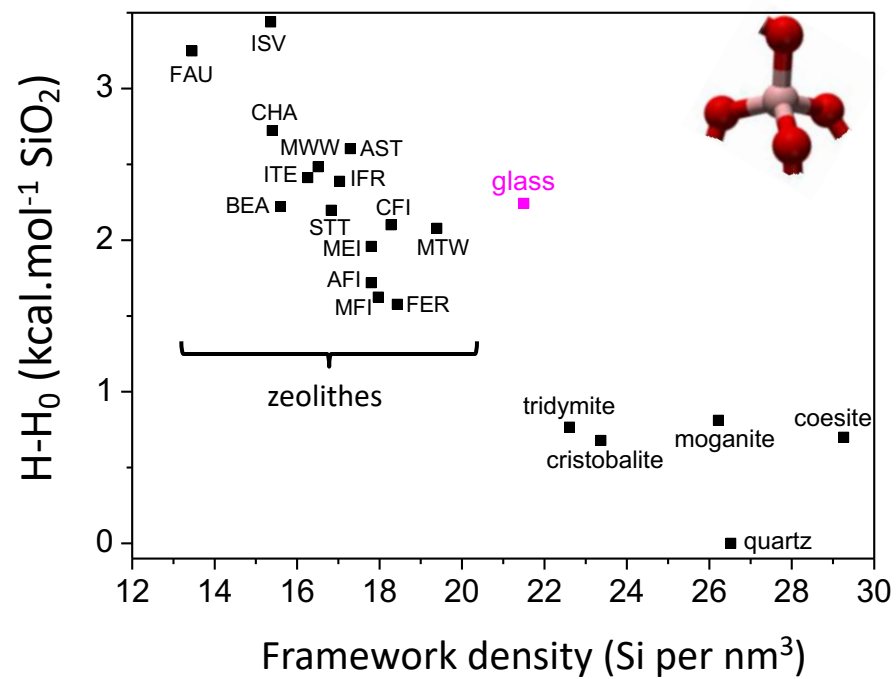
B_2O_3 anomaly n°2: the glass has a low density compared to the known crystal

Experimental facts

B_2O_3



SiO_2

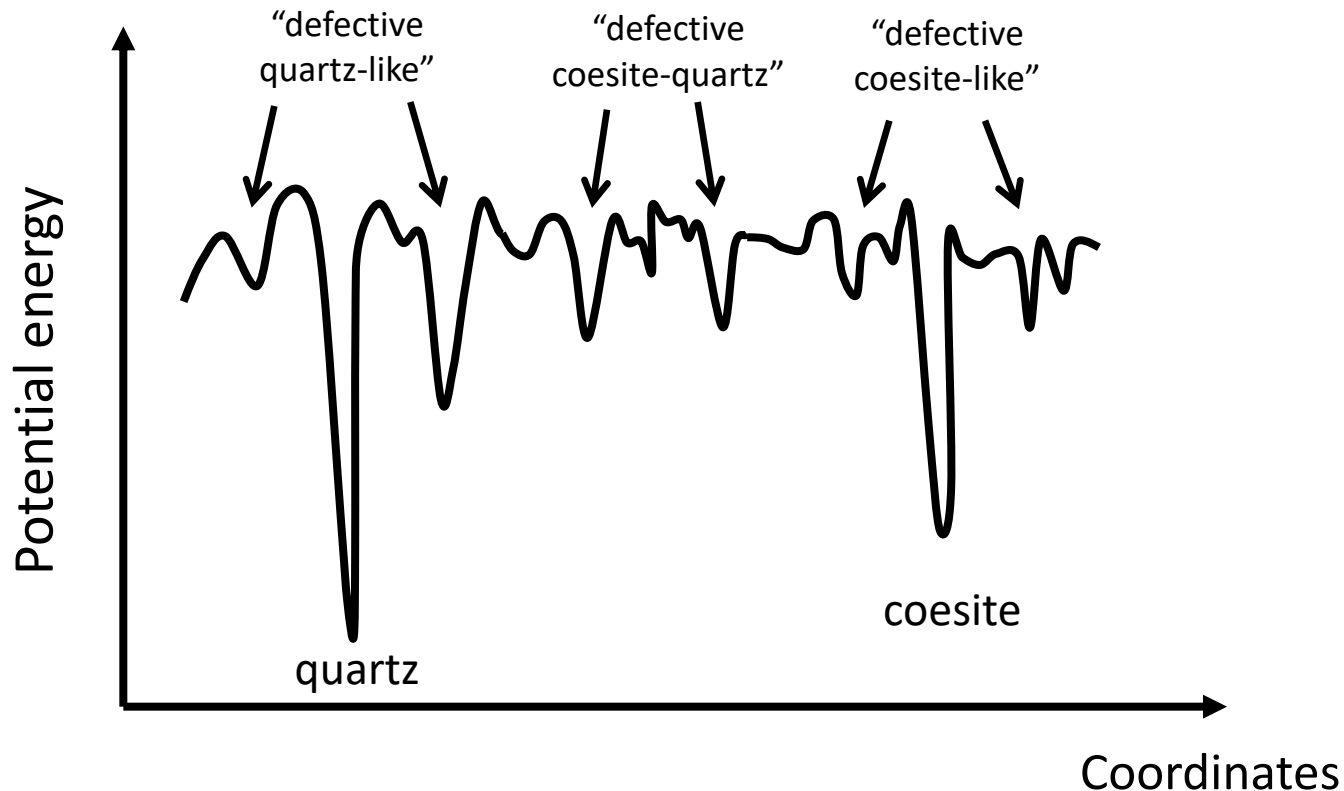


- ✓ B_2O_3 : - poor polymorphism
- (very) good glass former

- ✓ SiO_2 : - rich polymorphism
- good glass former

B_2O_3 anomaly n°3: Poor polymorphism (despite very high aptitude to vitrify)

Polymorphism and ease of vitrification

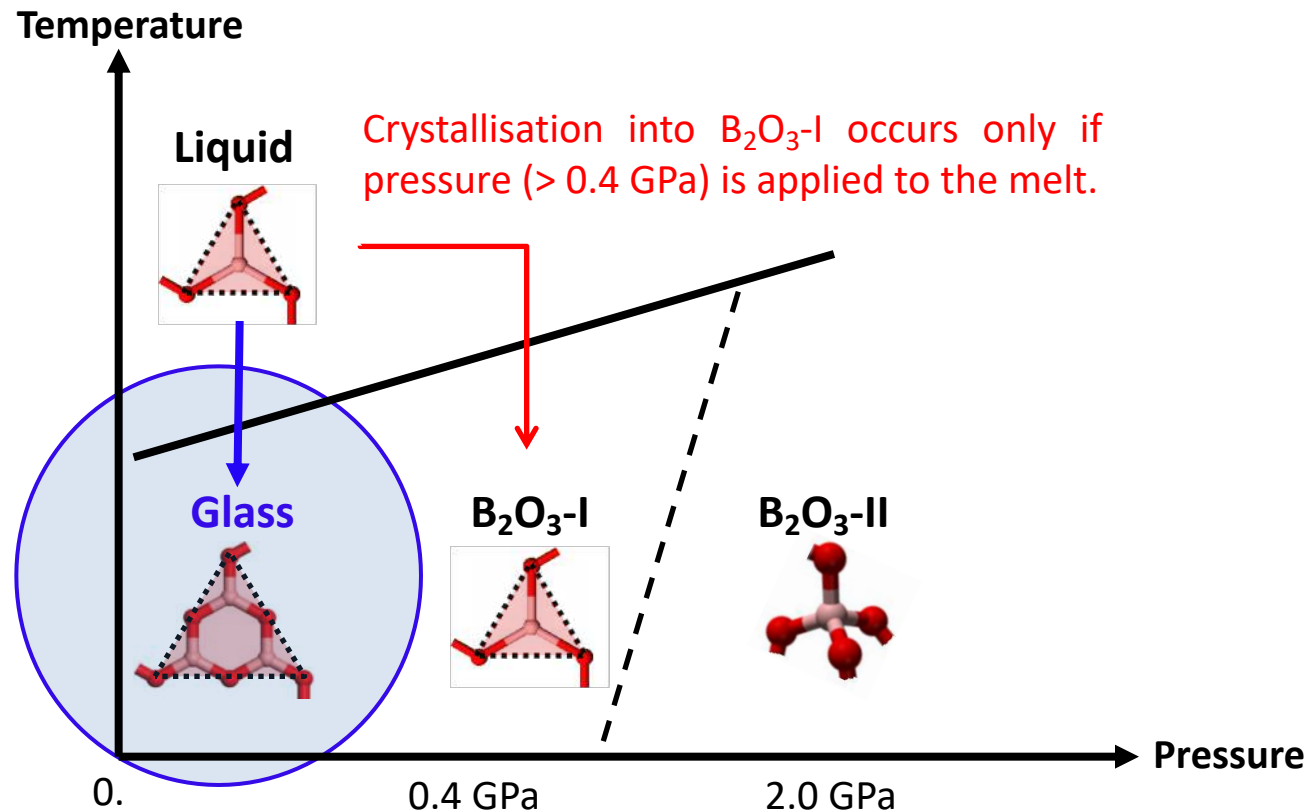


Rich (low-energy) polymorphism (many competing crystals)
→ *rugged* energy landscape → favours amorphisation

See e.g. Goodman, Nature (1975), Wang & Merz, Nature (1976), Perrin *et al.* Nature Comm. (2016), ...

Experimental facts

Anomaly n°4: The crystallisation of B_2O_3 -I from the melt at ambient pressure has never been observed (even if seeded with crystals). No crystal growth (of B_2O_3 -I) at any imposed cooling rate unless pressure is applied (*crystallisation anomaly*).



The B_2O_3 anomalies: summary

Why is the glass so (structurally) different from the known crystal?

anomaly n°1: glass has a very different medium-range structure (boroxol rings)

anomaly n°2: glass has a low density (-30 %) compared to the known crystal

Why does B_2O_3 vitrify so easily and never crystallise from the melt?

anomaly n°3: poor polymorphism (despite very high aptitude to vitrify)

anomaly n°4: crystallisation from the melt at ambient pressure never observed unless pressure is applied (***crystallisation anomaly***).



The origin of these anomalies is to be found in the existence of yet ***unknown*** polymorphs

nature
materials

LETTERS

PUBLISHED ONLINE: 2 SEPTEMBER 2012 | DOI:10.1038/NMAT3416

Hidden polymorphs drive vitrification in B_2O_3

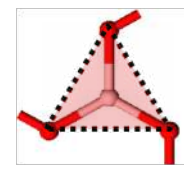
Guillaume Ferlat^{1*}, Ari Paavo Seitsonen^{1,2}, Michele Lazzeri¹ and Francesco Mauri^{1*}

Systematic construction of polymorphs

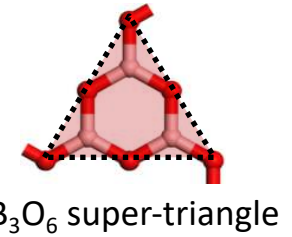
→ Using decoration of topological networks

- ✓ Relevant **building units** (for ambient polymorphs):

[Constraints to be fulfilled: every boron is three-fold coordinated
every oxygen is two-fold coordinated]



BO₃ triangle



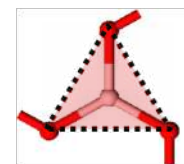
B₃O₆ super-triangle

N.B.: the boroxol units are **self-similar** to the BO₃ units.

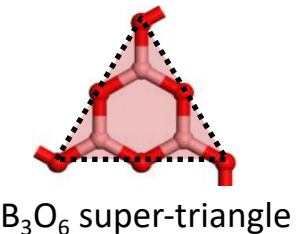
Systematic construction of polymorphs

→ Using decoration of topological networks

- ✓ Relevant **building units** (for ambient polymorphs):



BO₃ triangle

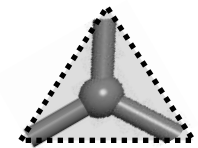


B₃O₆ super-triangle

- ✓ Use of topological databases of **three-fold coordinated networks**

Winkler *et al.* (CPL, 2001): from **graph theory**, prediction of all possible **three-coordinated 3D** frameworks with up to 6 atoms in the primitive cell:
12 networks (originally applied to sp^2 -carbon structures)

+ **2D** network of graphite: **13 networks**

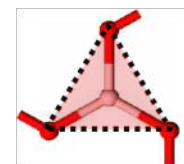


- ✓ **Decoration** of the networks vertices by the relevant **building units**:

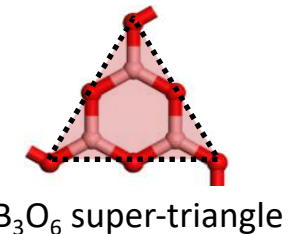
Systematic construction of polymorphs

→ Using decoration of topological networks

- ✓ Relevant **building units** (for ambient polymorphs):



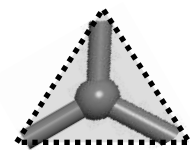
BO₃ triangle



B₃O₆ super-triangle

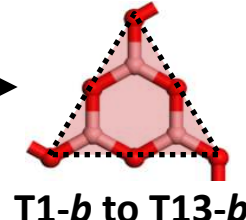
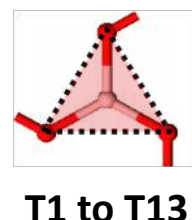
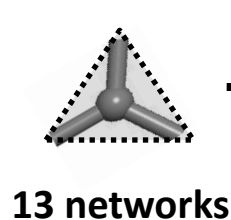
- ✓ Use of topological databases of **three-fold coordinated networks**

Winkler *et al.* (CPL, 2001): from **graph theory**, prediction of all possible **three-coordinated 3D** frameworks with up to 6 atoms in the primitive cell:
12 networks (originally applied to *sp*²-carbon structures)



+ **2D** network of graphite: **13 networks**

- ✓ **Decoration** of the networks vertices by the relevant **building units**:

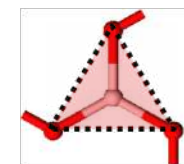


$2 * 13 - 1 = 25$ new B₂O₃ crystals
(with 10 to 135 atoms per unit cell)
N.B.: T13 is the known B₂O₃-I crystal

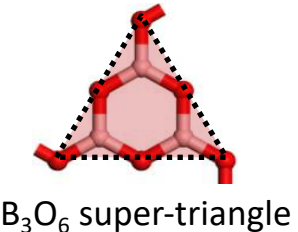
Systematic construction of polymorphs

→ Using decoration of topological networks

- ✓ Relevant **building units** (for ambient polymorphs):



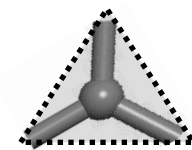
BO₃ triangle



B₃O₆ super-triangle

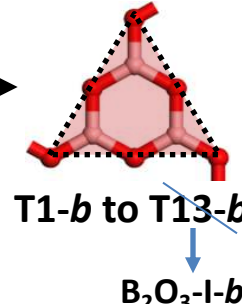
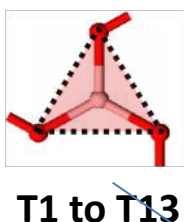
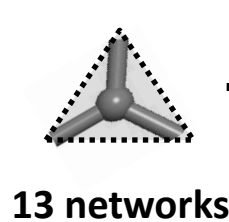
- ✓ Use of topological databases of **three-fold coordinated networks**

Winkler *et al.* (CPL, 2001): from **graph theory**, prediction of all possible **three-coordinated 3D** frameworks with up to 6 atoms in the primitive cell:
12 networks (originally applied to *sp*²-carbon structures)



+ **2D** network of graphite: **13 networks**

- ✓ **Decoration** of the networks vertices by the relevant **building units**:



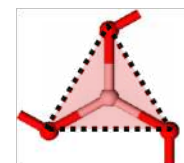
$2 * 13 - 1 = 25$ new B₂O₃ crystals
(with 10 to 135 atoms per unit cell)

N.B.: T13 is the known B₂O₃-I crystal
T8 and T10: some nodes belong to 3-fold rings

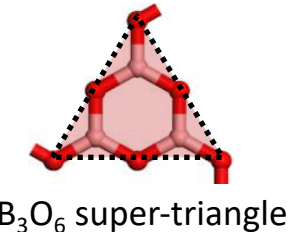
Systematic construction of polymorphs

→ Using decoration of topological networks

- ✓ Relevant **building units** (for ambient polymorphs):



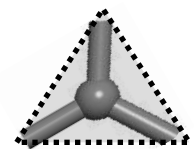
BO₃ triangle



B₃O₆ super-triangle

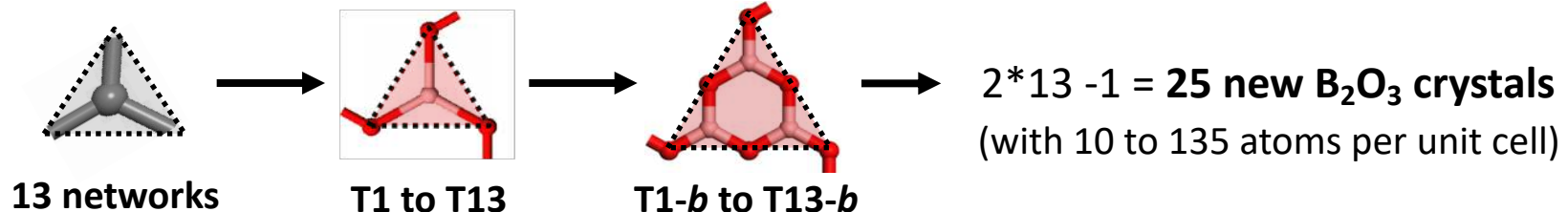
- ✓ Use of topological databases of **three-fold coordinated networks**

Winkler *et al.* (CPL, 2001): from **graph theory**, prediction of all possible **three-coordinated 3D** frameworks with up to 6 atoms in the primitive cell:
12 networks (originally applied to *sp*²-carbon structures)



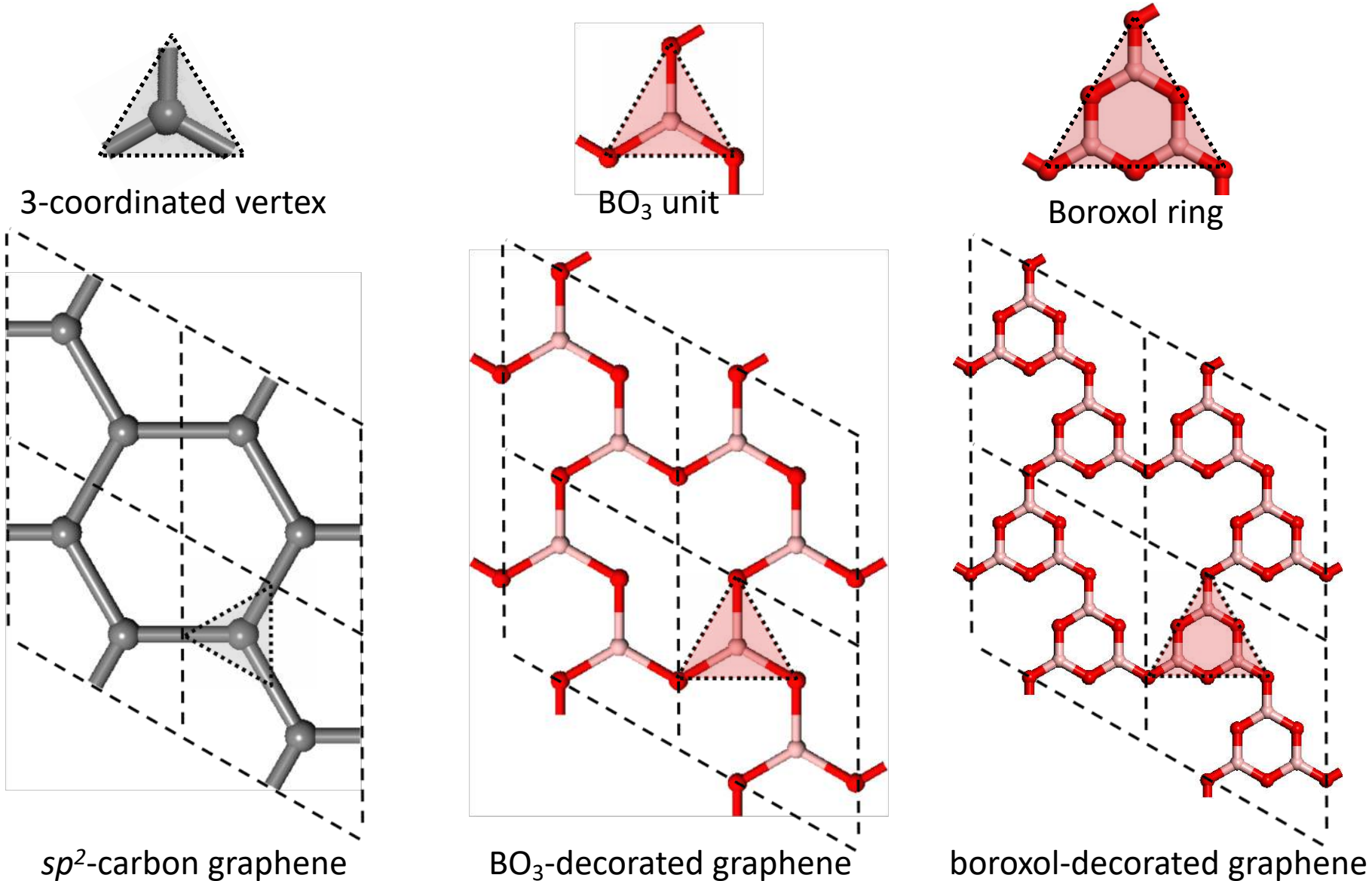
+ **2D** network of graphite: **13 networks**

- ✓ **Decoration** of the networks vertices by the relevant **building units**:

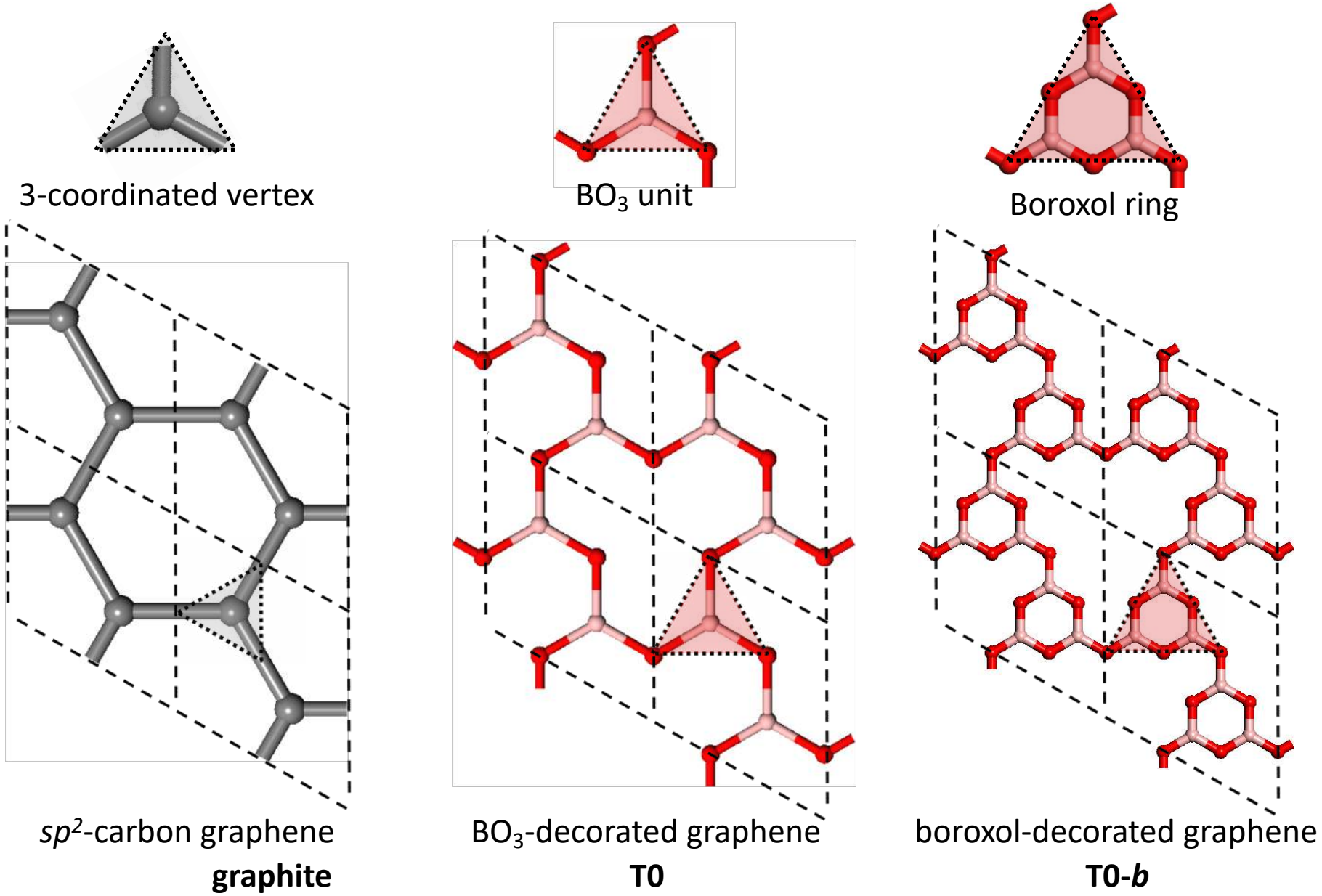


- ✓ **Relaxation** (positions and unit cell) of the structures by ***first-principles*** calculations within Density Functional Theory (GGA-PBE, ultra-soft pseudos, PW basis, CASTEP code)

Exploiting isomorphism: graphite-like

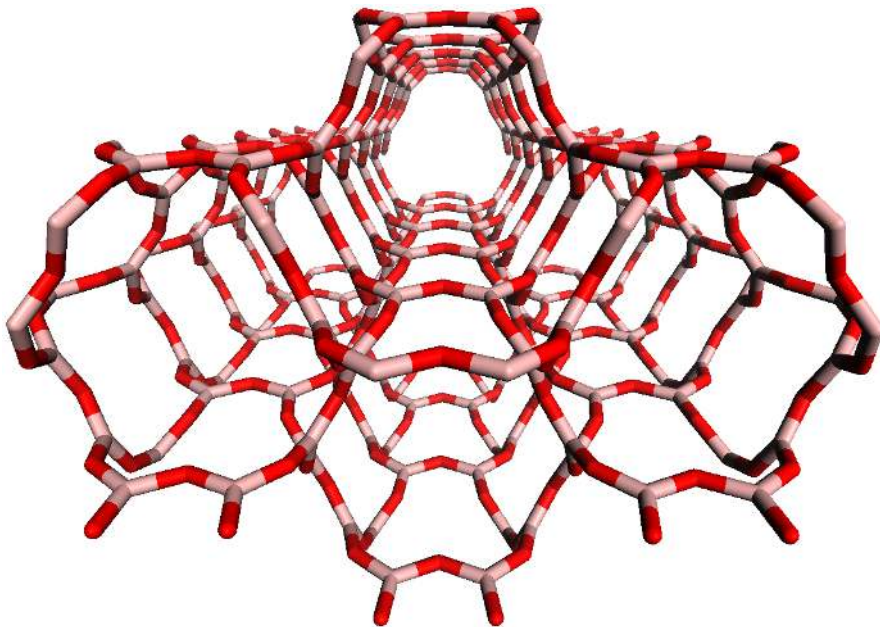


Exploiting isomorphism: graphite-like

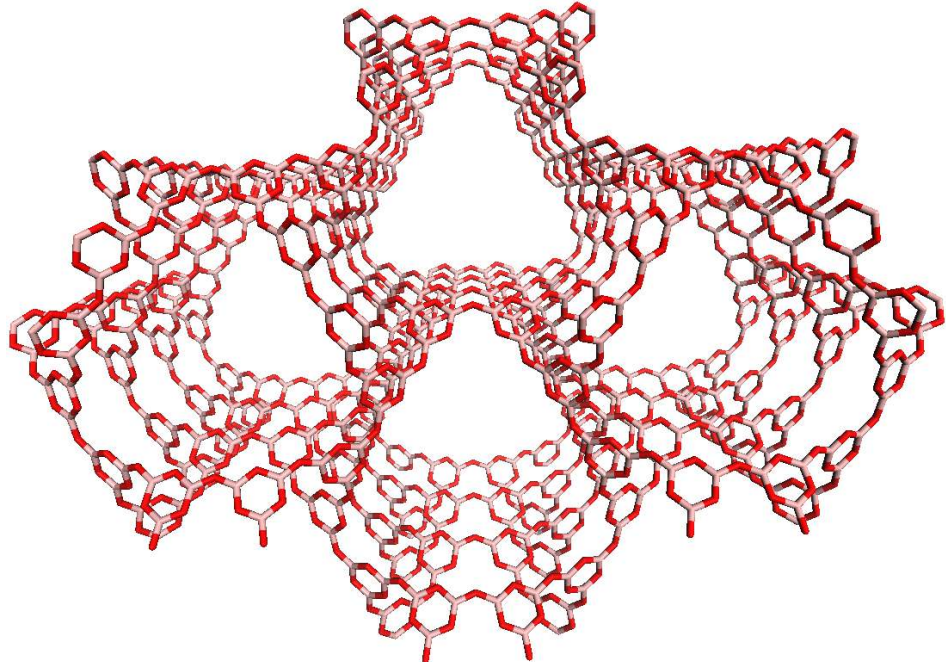


New B_2O_3 polymorphs

G. Ferlat *et al.*, Nature Materials (2012)



(BO₃-decorated) T7



(boroxol-decorated) T7-b

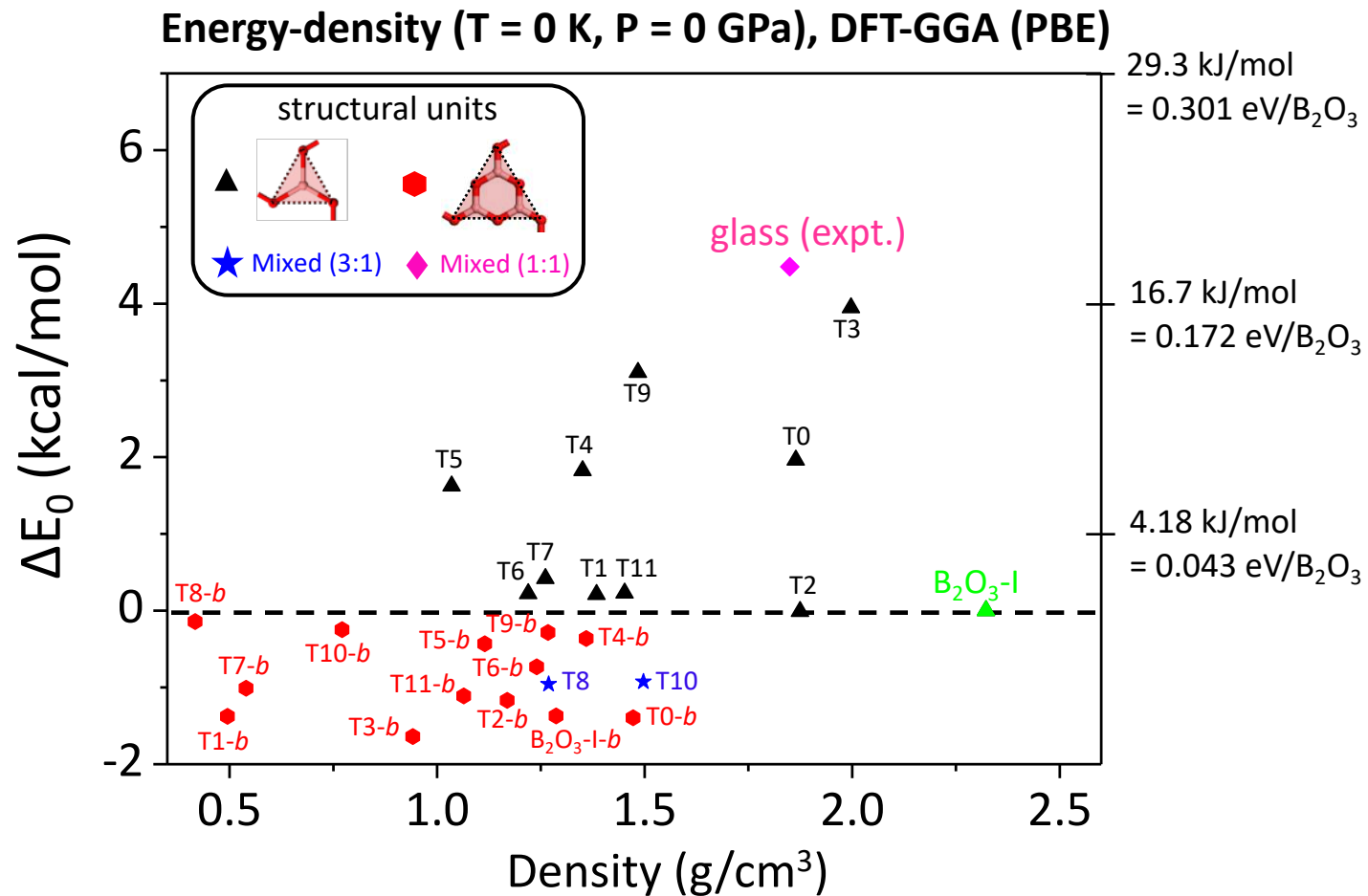
- ✓ Some crystals show *cage-* or *channel-like* structures

Light, crystalline and **porous**: possible applications as
e.g. molecular sieves, hydrogen storage matrices, ... ?

- ✓ Negative linear compressibility, auxeticity (negative poisson ratio) ...

New B_2O_3 polymorphs

G. Ferlat *et al.*, Nature Materials (2012)

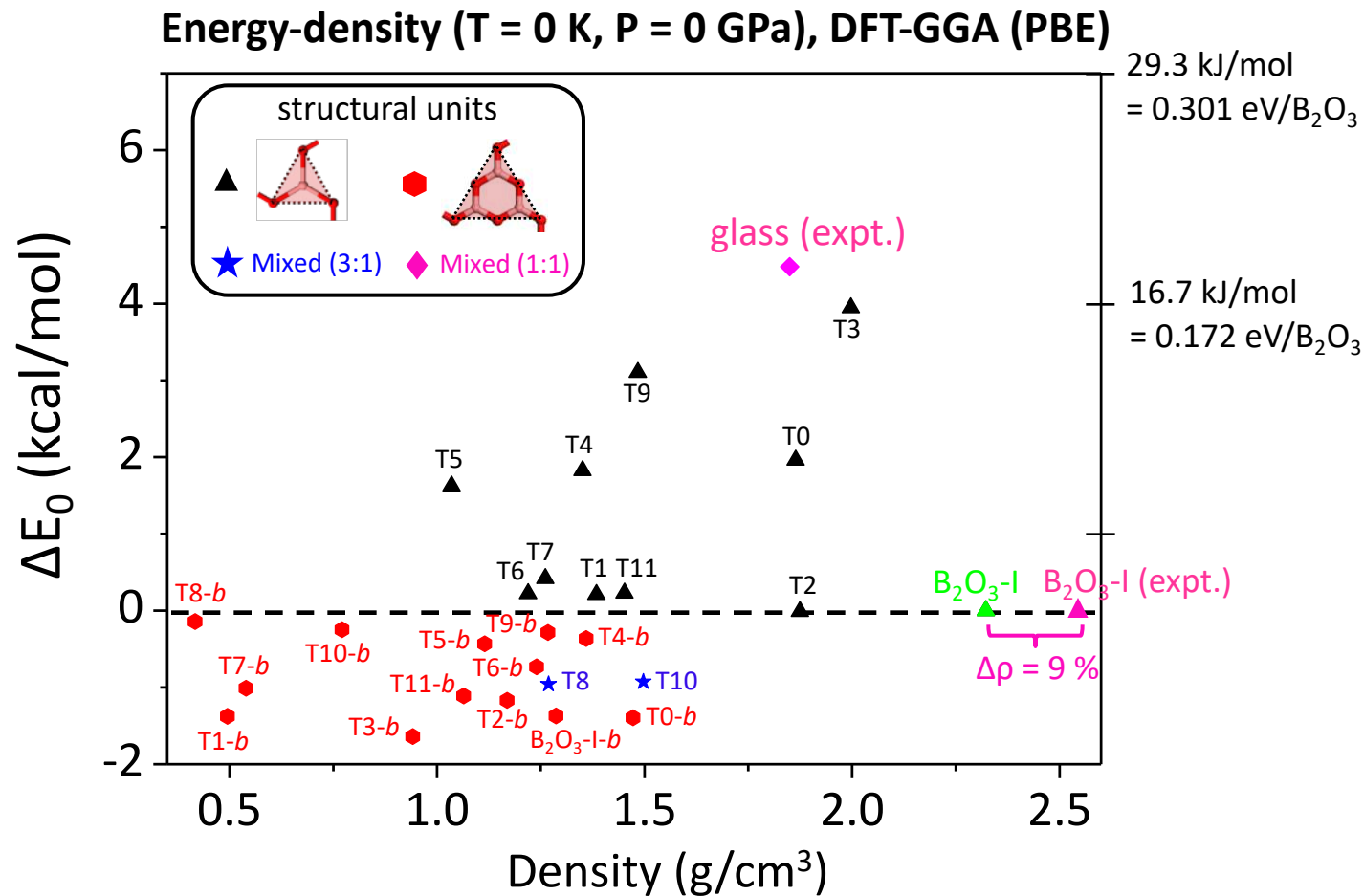


✓ Many low-energy crystals (lower than the glass, close to that of B_2O_3 -I)

Are these predictions experimentally realisable? Is B_2O_3 -I the true ground state?

New B_2O_3 polymorphs

G. Ferlat *et al.*, Nature Materials (2012)

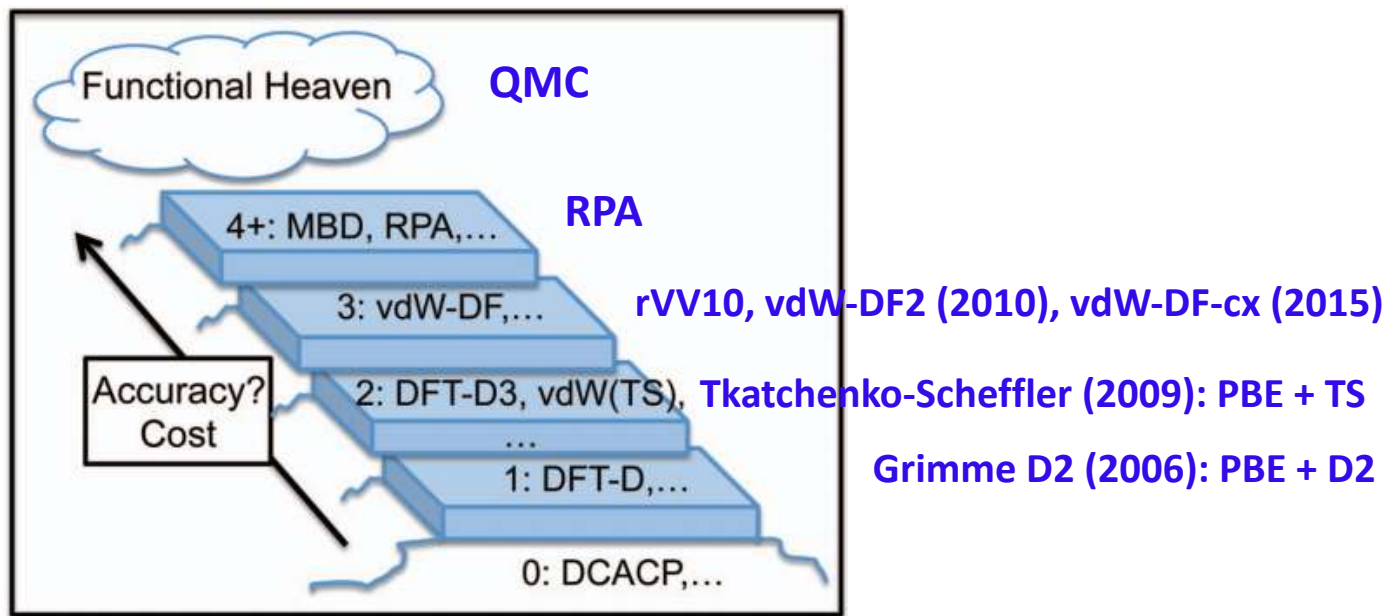


- ✓ Many low-energy crystals (lower than the glass, close to that of B_2O_3-I)

Are these predictions experimentally realisable? Is B_2O_3-I the true ground state ?
How robust are these predictions (DFT-GGA errors)?

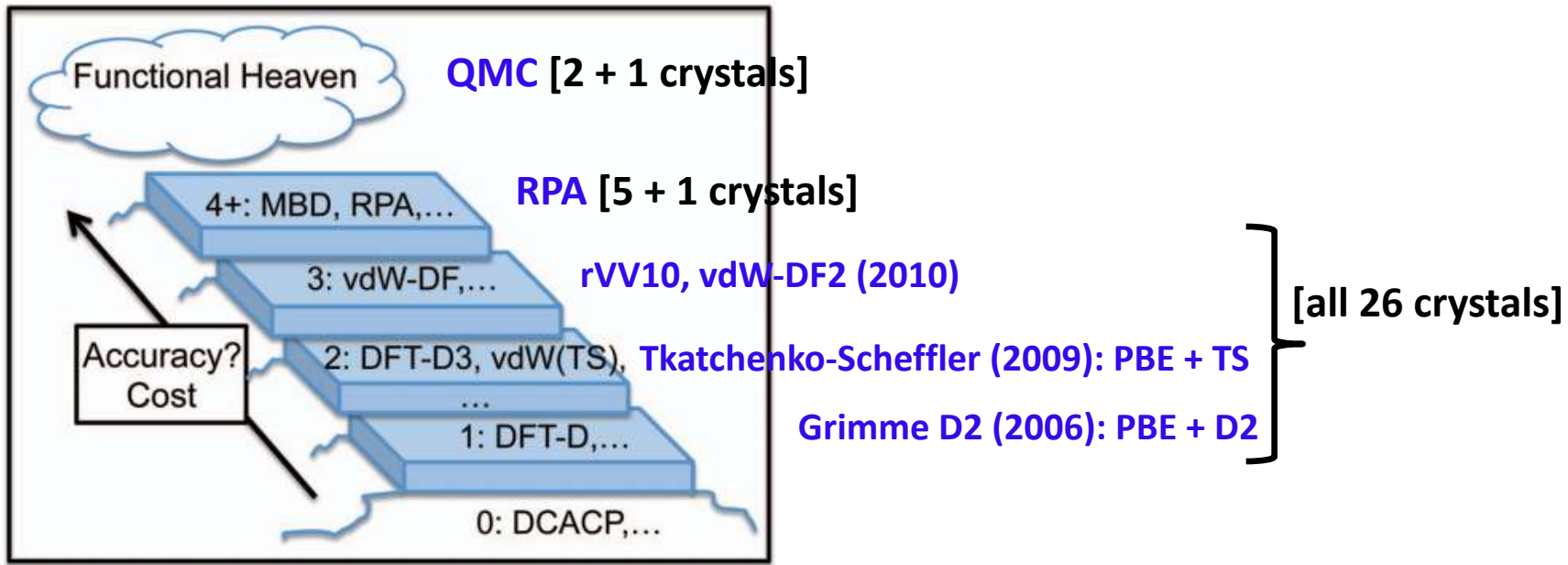
New B_2O_3 polymorphs: vdW and many-body contributions

- Assessing the van der Waals contributions (using DFT-vdW schemes)
- Beyond DFT: RPA (*collab. M. Hellgren*), Quantum Monte-Carlo (*M. Casula*)



New B_2O_3 polymorphs: vdW and many-body contributions

- Assessing the van der Waals contributions (using DFT-vdW schemes)
- Beyond DFT: RPA (*collab. M. Hellgren*), Quantum Monte-Carlo (*M. Casula*)



Classification of DFT-based dispersion correction schemes.

From Klimeš & Michaelides, J. Chem. Phys. (2012)

step 0: no account of long range asymptotics;

step 1: simple C_6 correction;

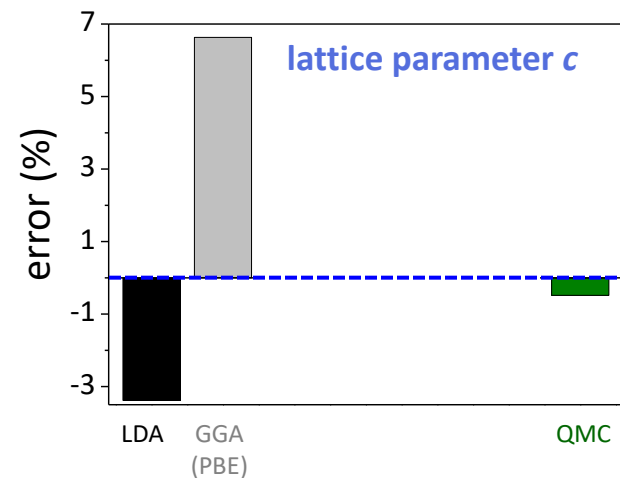
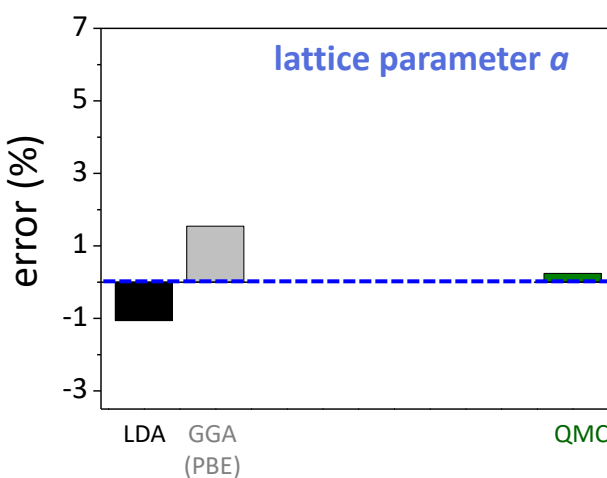
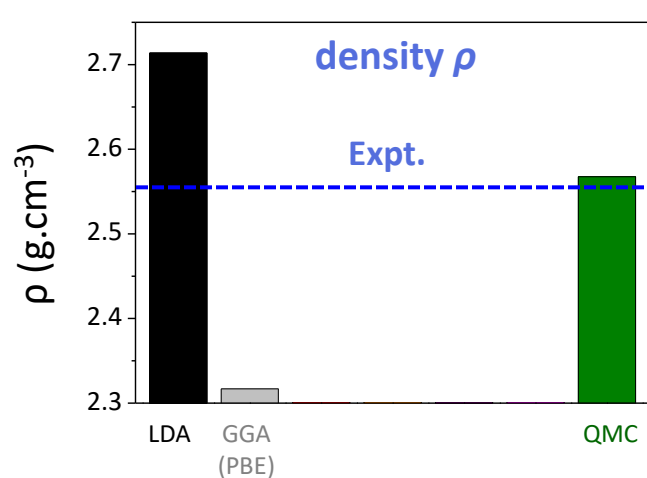
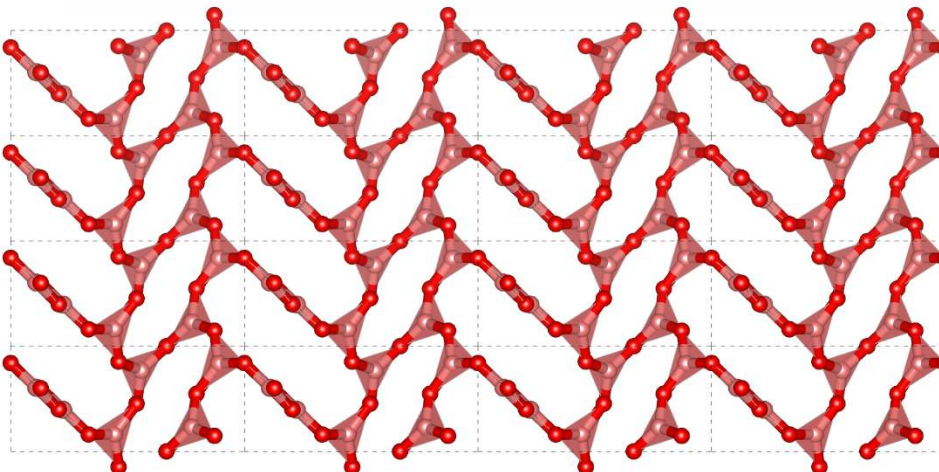
step 2: environment-dependent C_6 corrections;

step 3: long range density functionals.

Above: beyond pairwise additive determinations.

Benchmarking DFT: structure

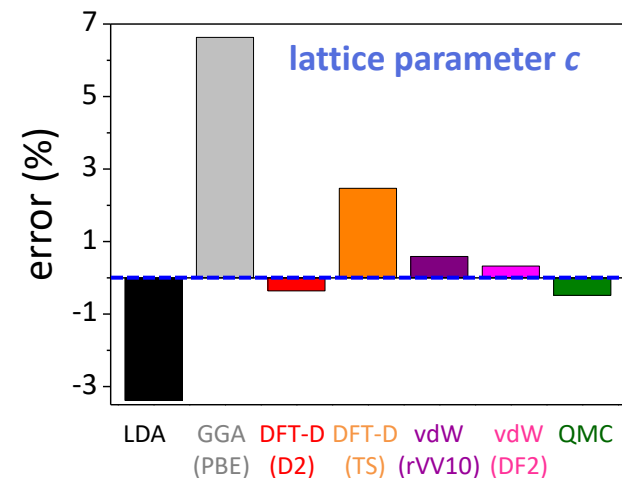
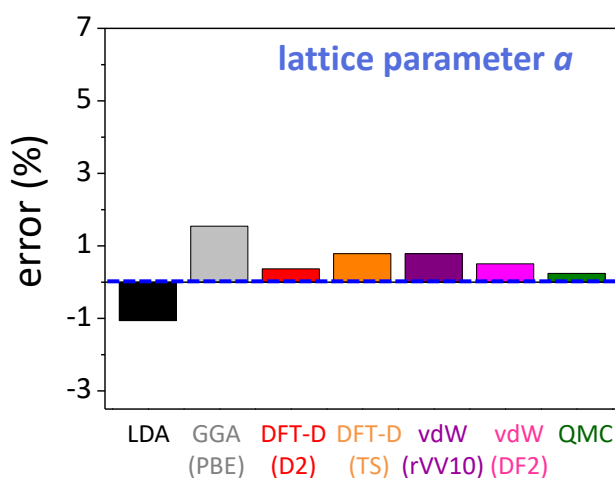
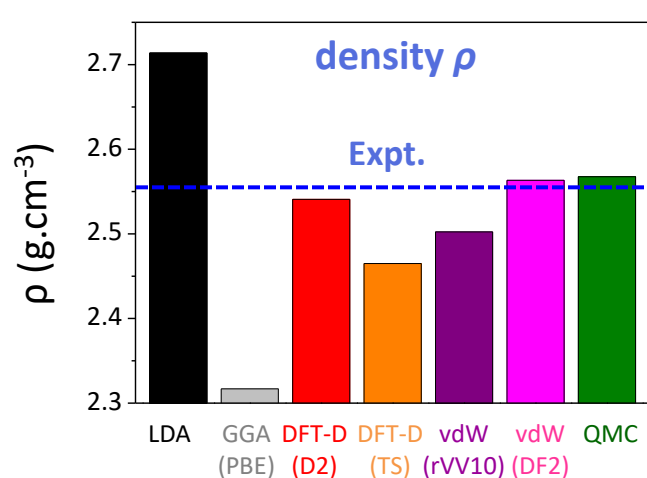
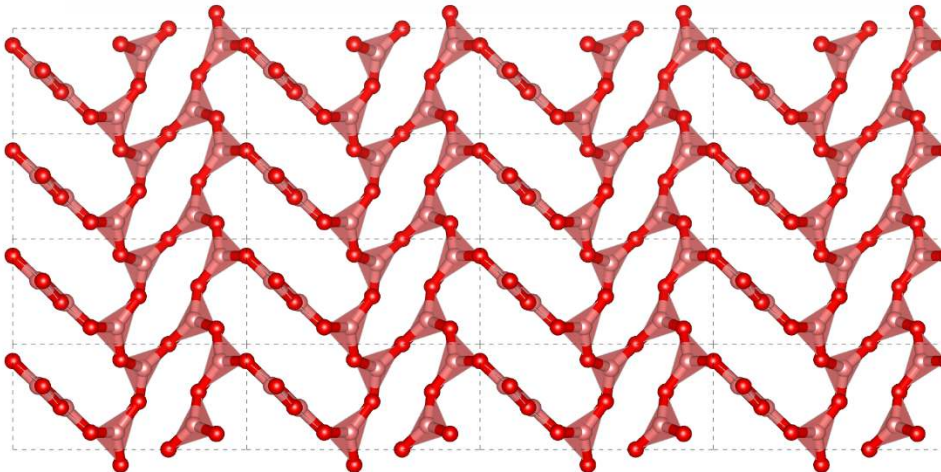
$\text{B}_2\text{O}_3\text{-I}$
(known polymorph)



- ✓ PBE: very significant underbinding (and overbinding with LDA)
- ✓ very anisotropic variation (there is a “soft” direction)

Benchmarking DFT: structure

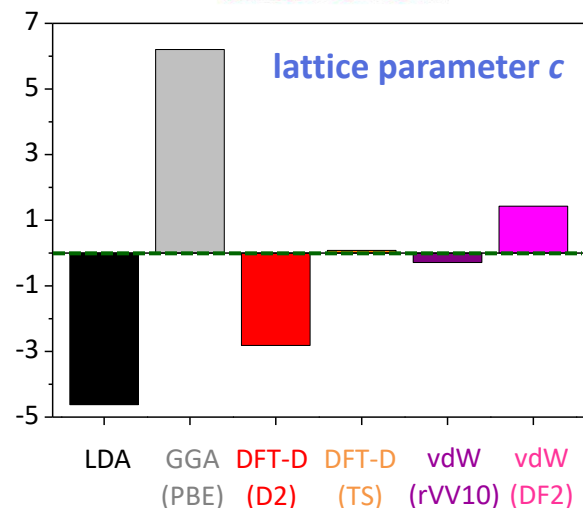
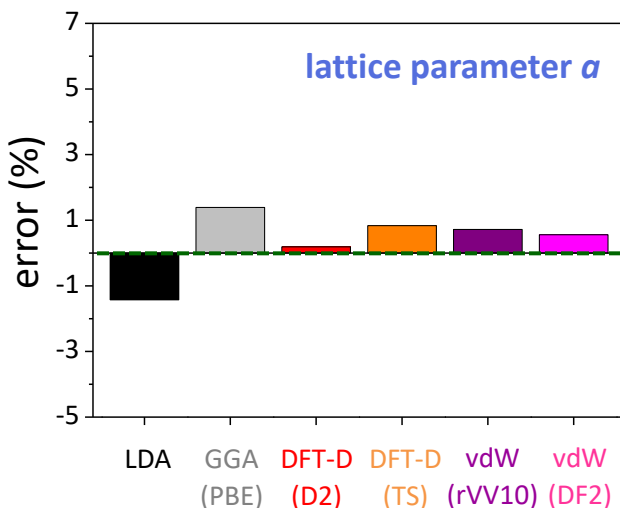
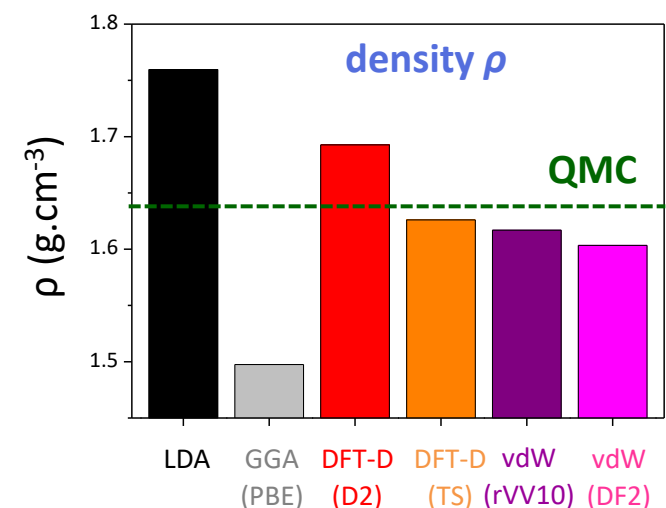
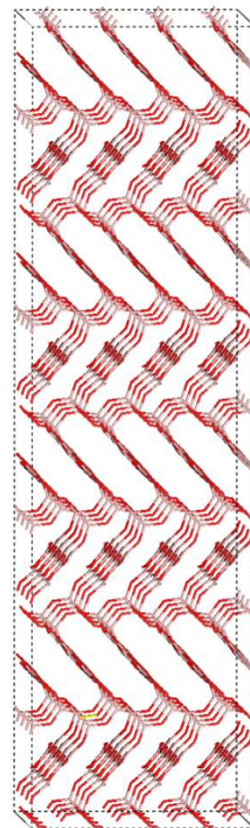
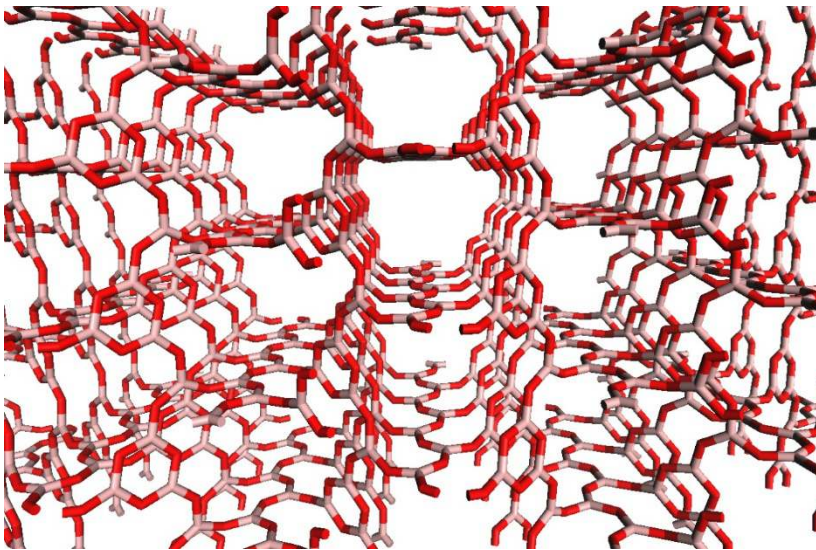
$\text{B}_2\text{O}_3\text{-I}$
(known polymorph)



✓ All DFT-vdW schemes perform quite well
(and bring significant improvements)

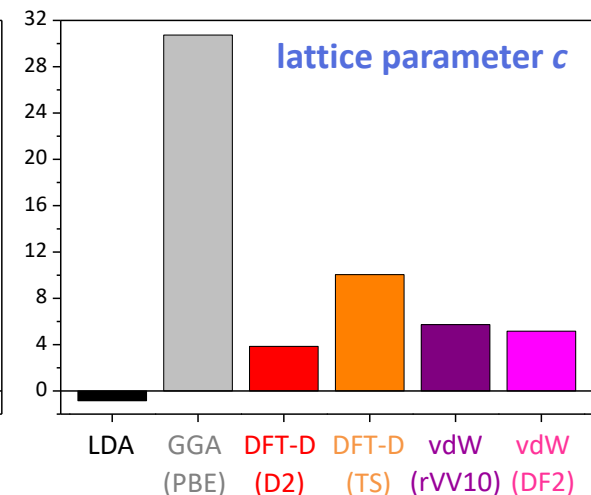
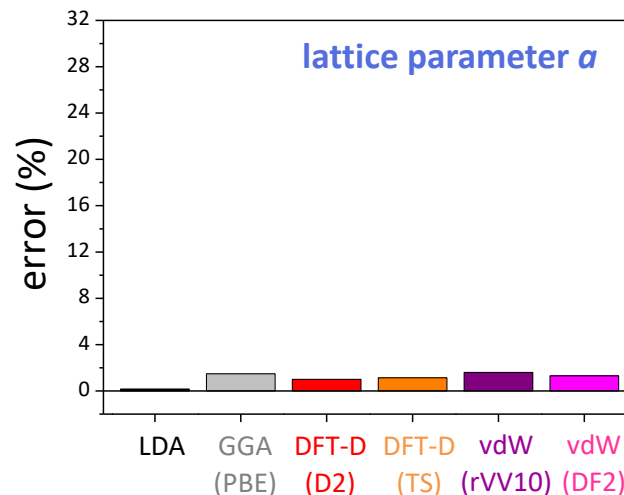
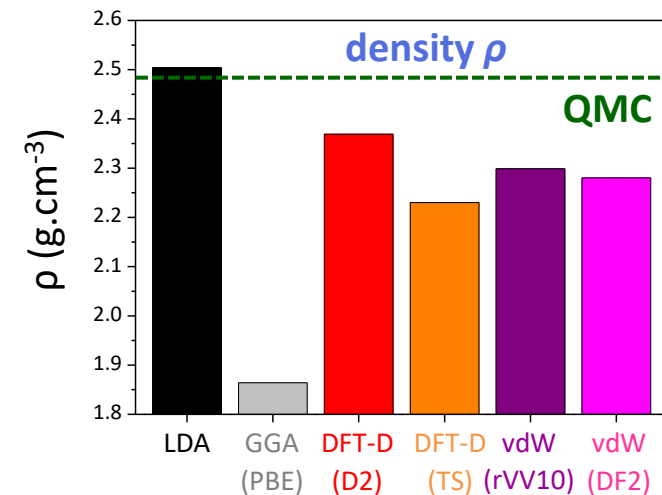
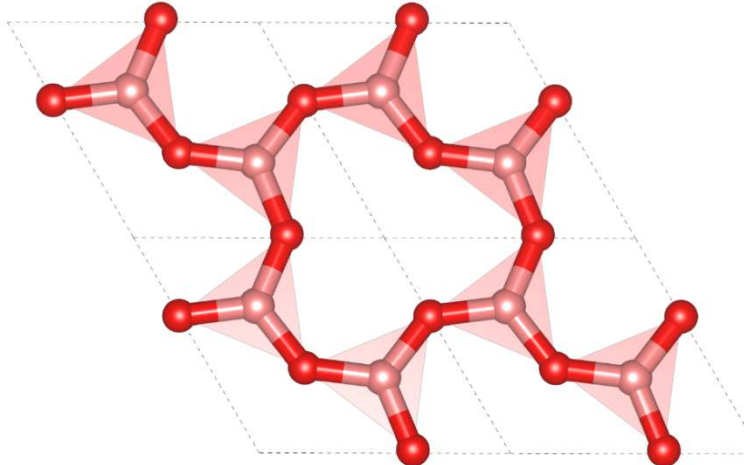
Benchmarking DFT: structure

T10 (new polymorph)



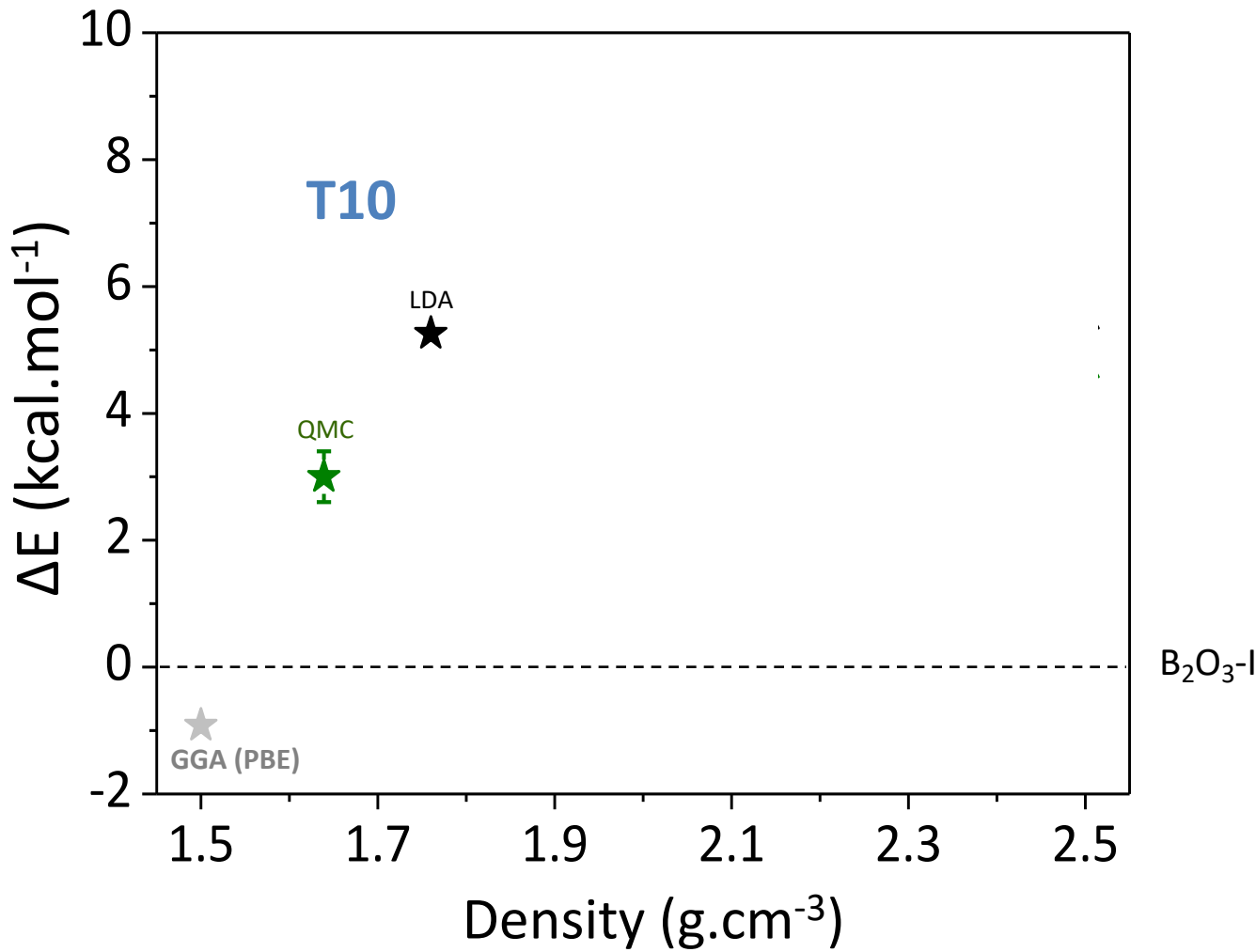
Benchmarking DFT: structure

T0 (new polymorph)

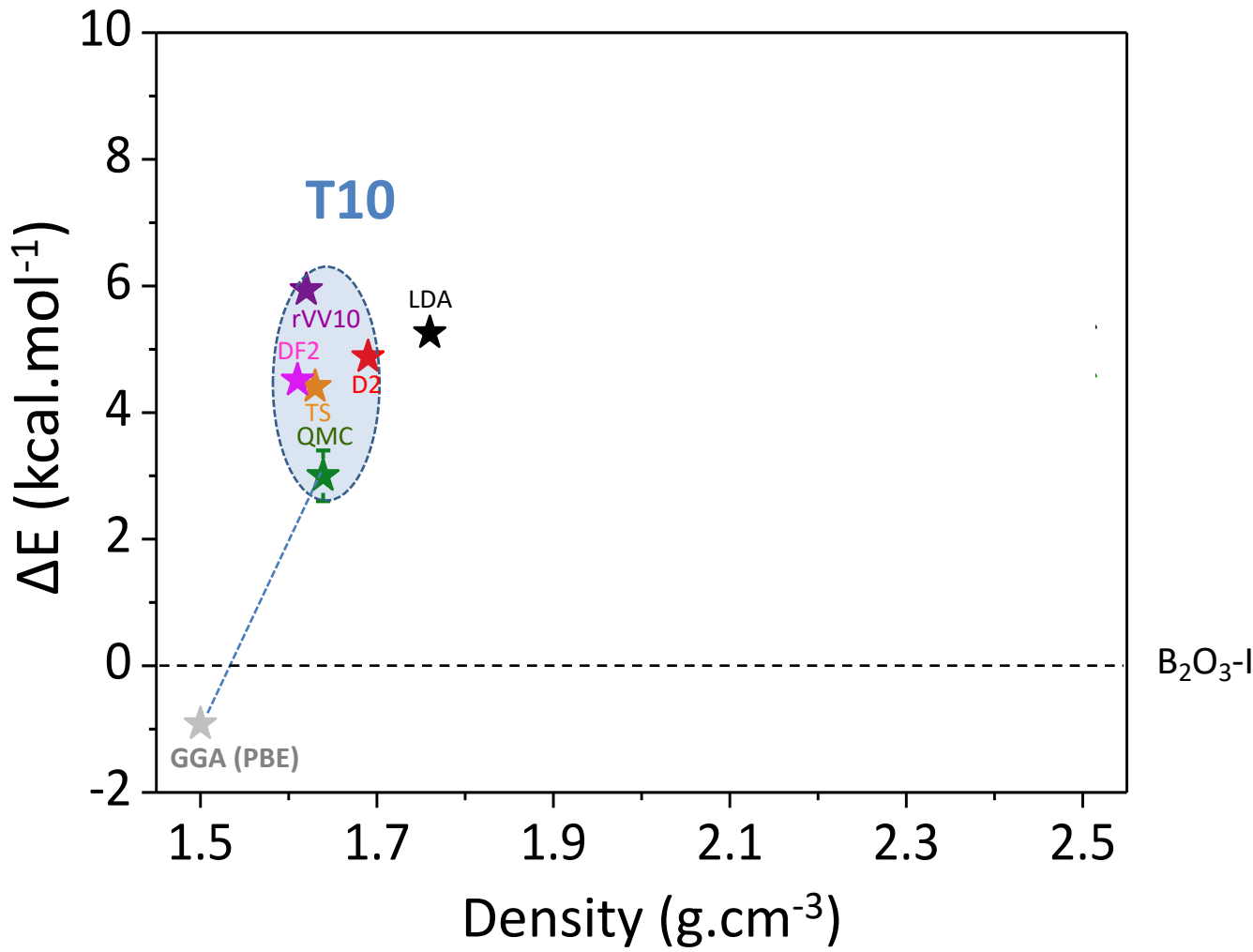


✓ Large GGA error (best result with LDA). Situation reminiscent of $h\text{-BN}$.

Benchmarking DFT: energy

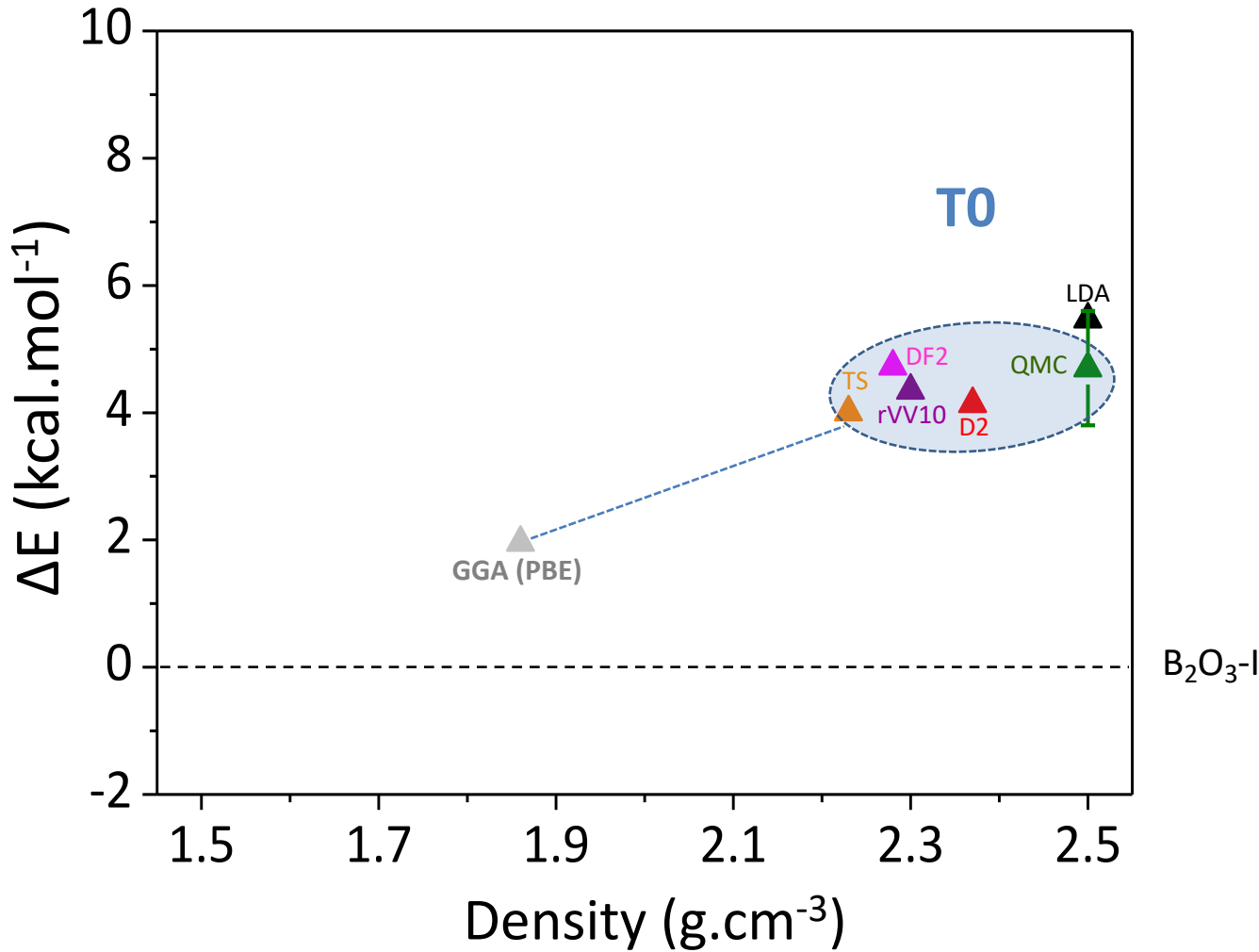


Benchmarking DFT: energy



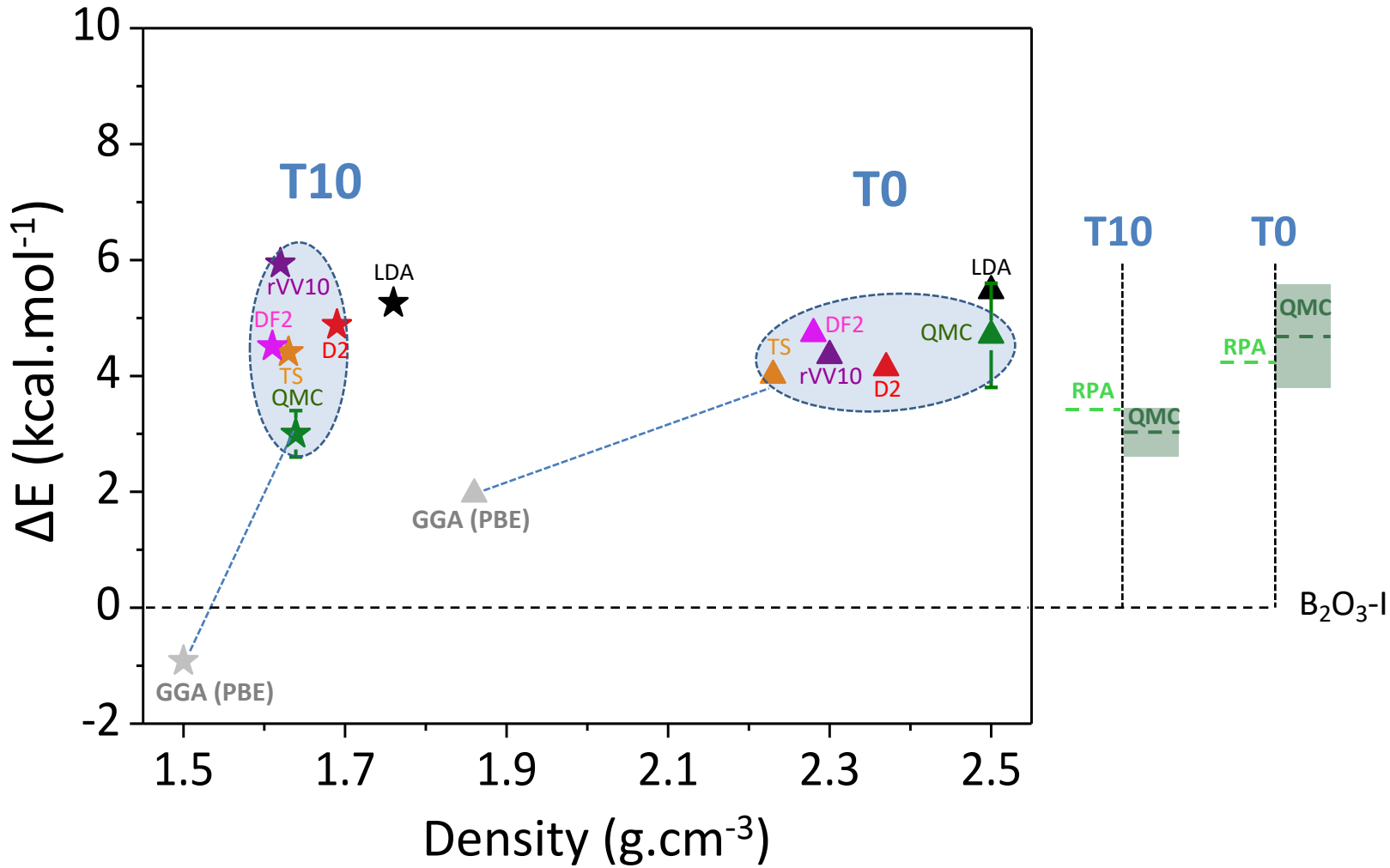
✓ Large GGA error. DFT + vdW reasonably well

Benchmarking DFT: energy

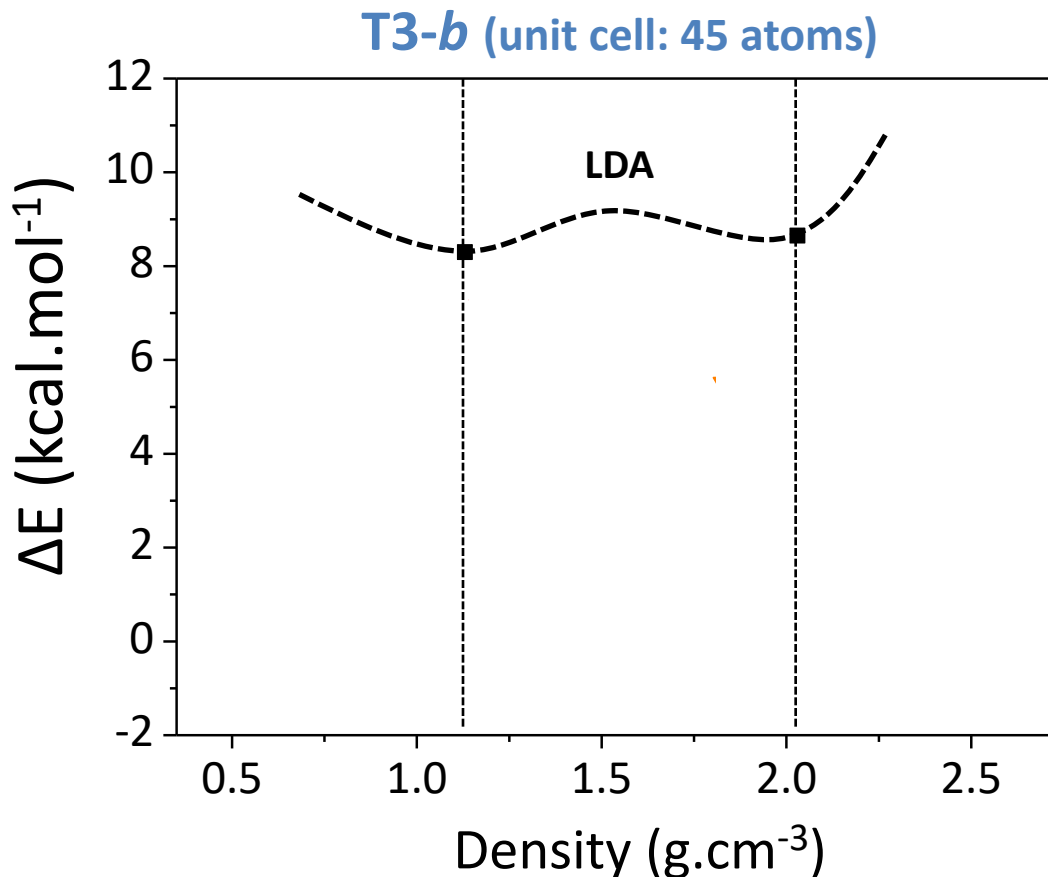


✓ Large GGA error (best result with LDA). Situation reminiscent of $h\text{-BN}$.

Benchmarking DFT: energy

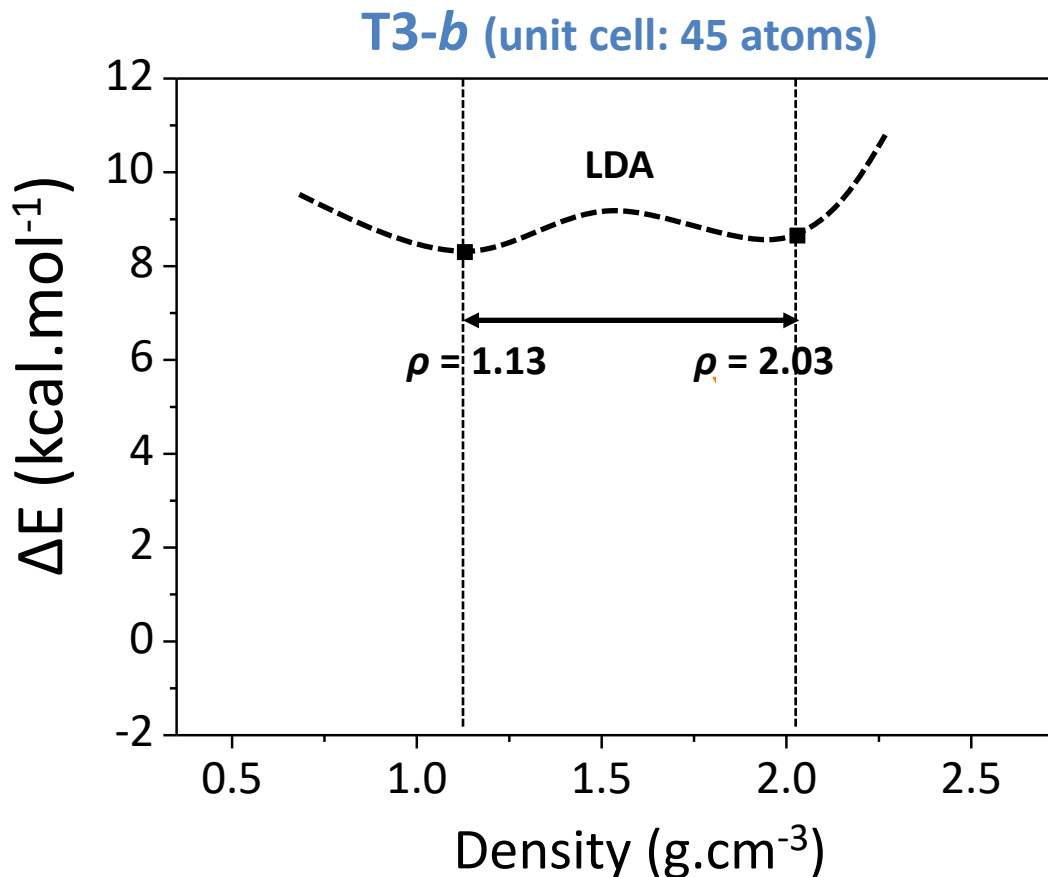


DFT energy landscape



- ✓ For a given topology (and a given XC), existence of **several minima (i.e. stable geometries)**
→ *Rugged* energy landscape

DFT energy landscape

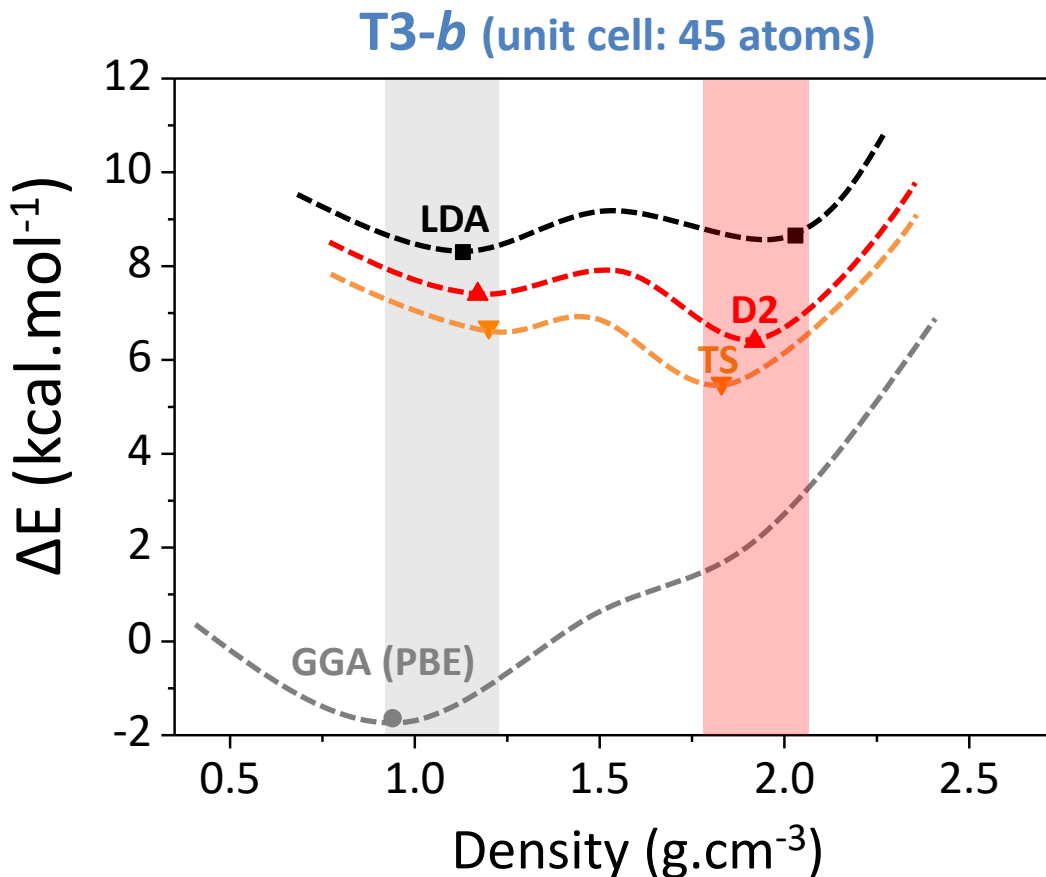


- ✓ For a given topology (and a given XC), existence of **several minima (i.e. stable geometries)**

→ **Rugged** energy landscape

[small energy differences while huge density differences → hard to « converge »]

DFT energy landscape



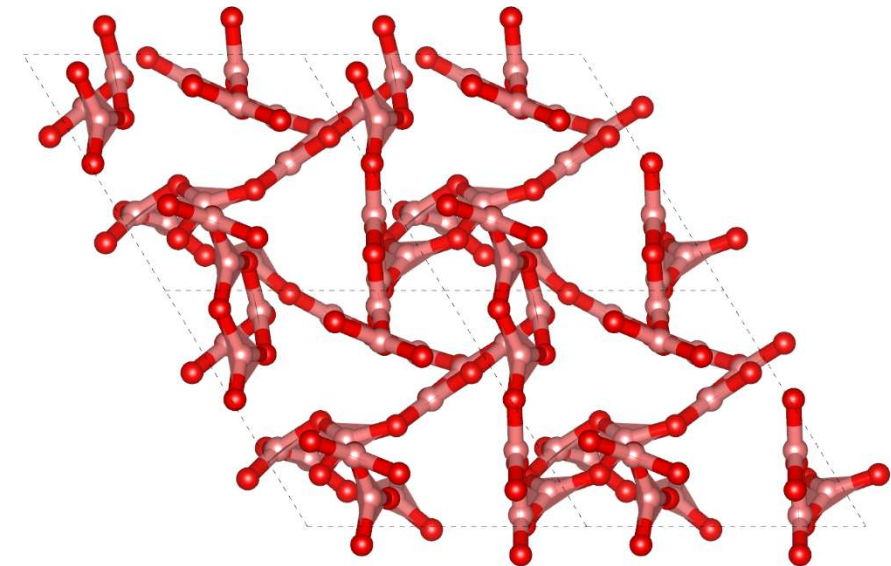
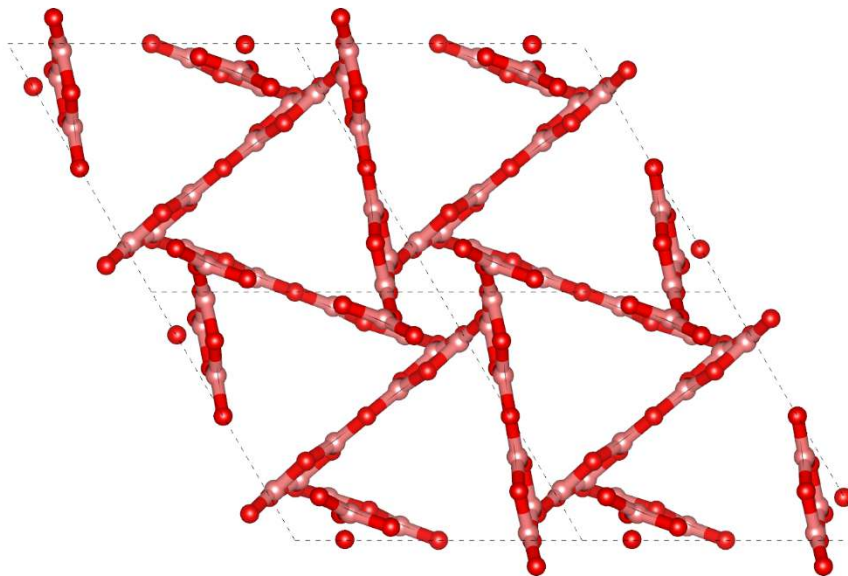
- ✓ For a given topology (and a given XC), existence of **several minima (i.e. stable geometries)**

PBE tends to favour low-density geometry

vdW high-density geometry

DFT energy landscape

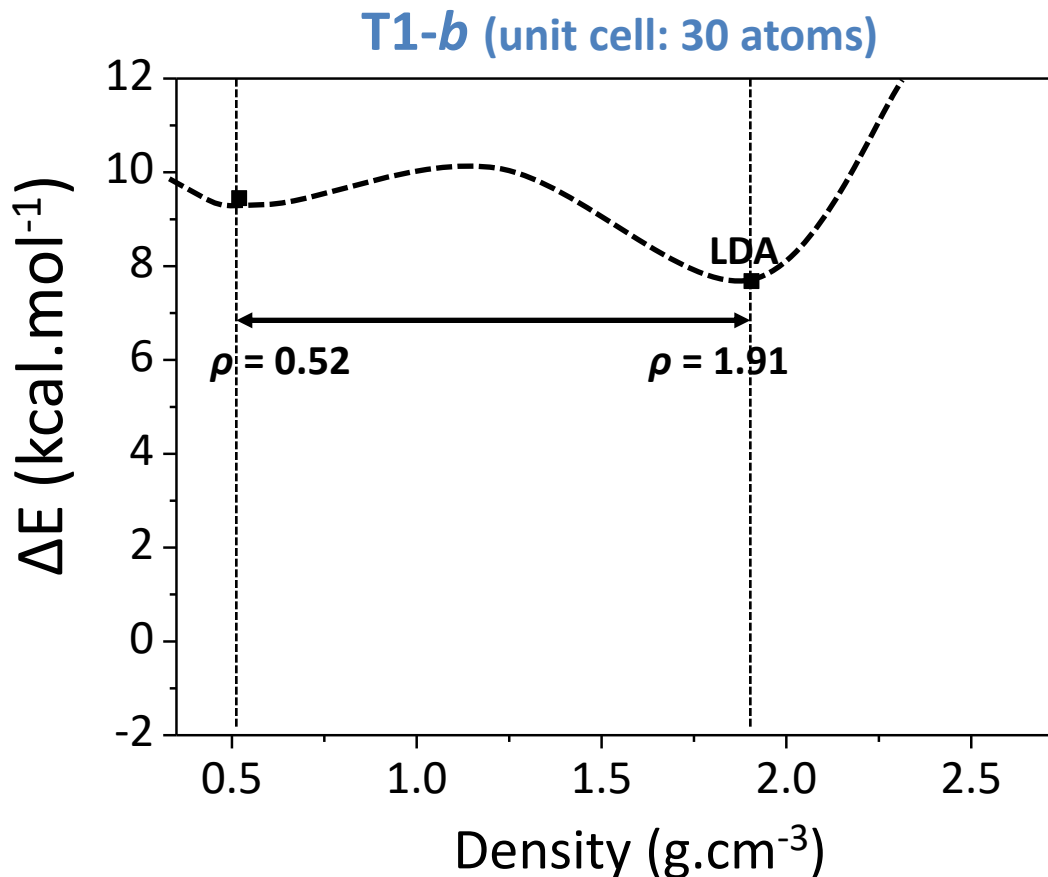
T3-*b* (unit cell: 45 atoms)



Low-density: highly symmetric, « puffed » rings
(as in SiO_2 β -cristobalite)

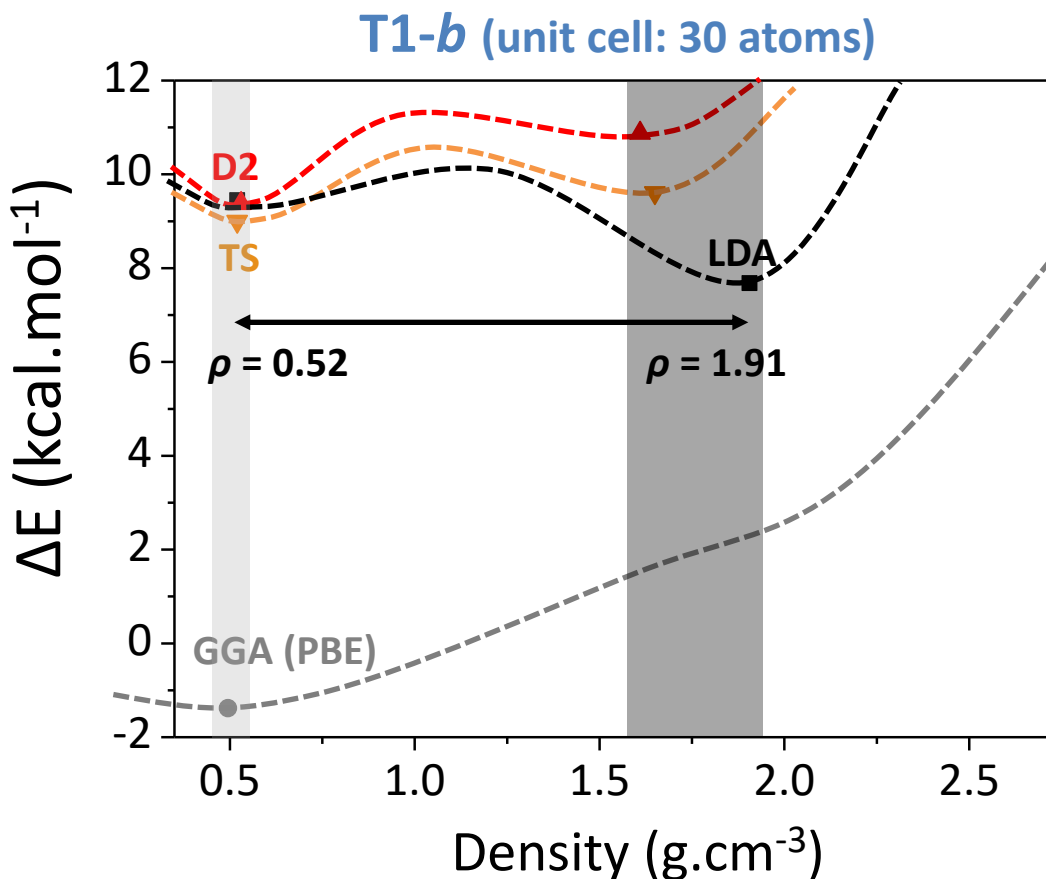
High-density: less symmetric, « puckered » rings
(as in SiO_2 α -cristobalite)

DFT energy landscape



- ✓ For a given topology (and a given XC), existence of **several minima (i.e. stable geometries)**

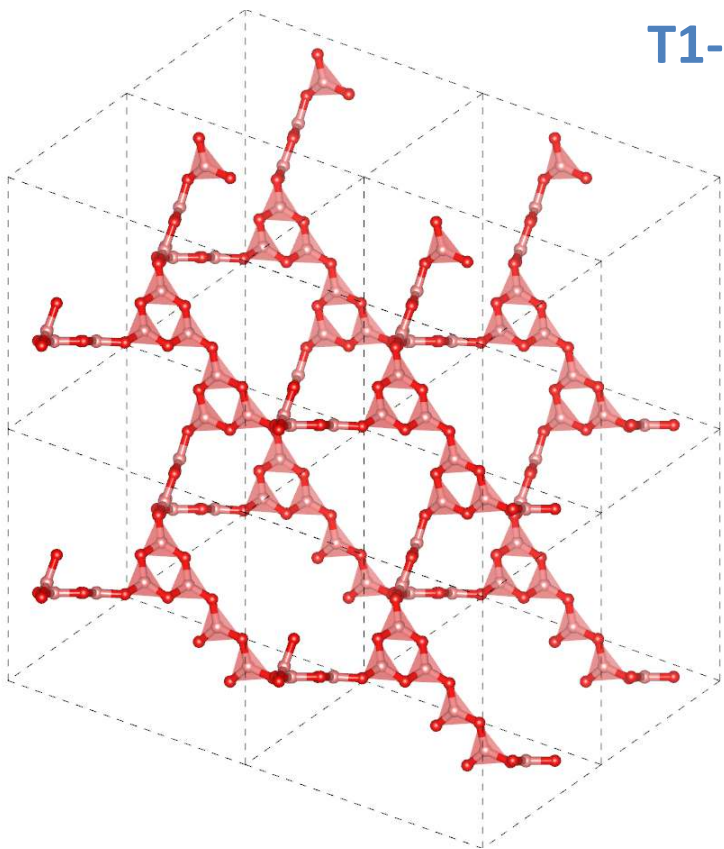
DFT energy landscape



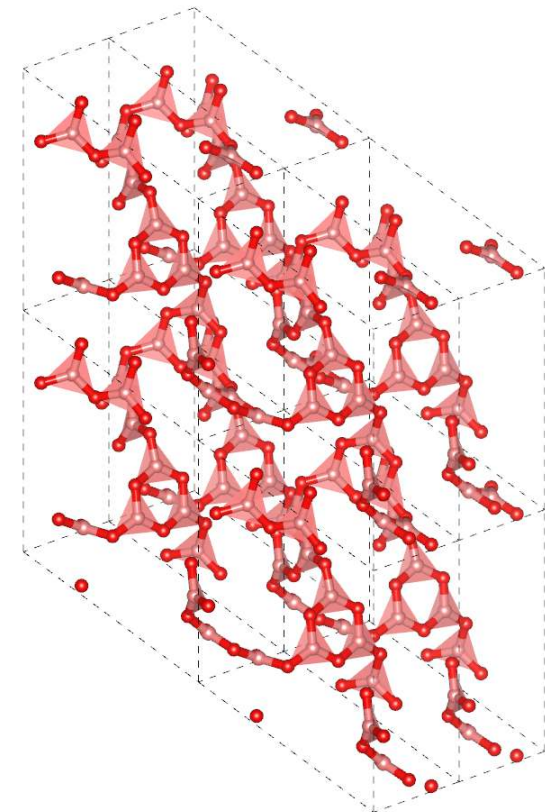
- ✓ For a given topology (and a given XC), existence of **several minima (i.e. stable geometries)**

DFT energy landscape

T1-*b* (unit cell: 30 atoms)

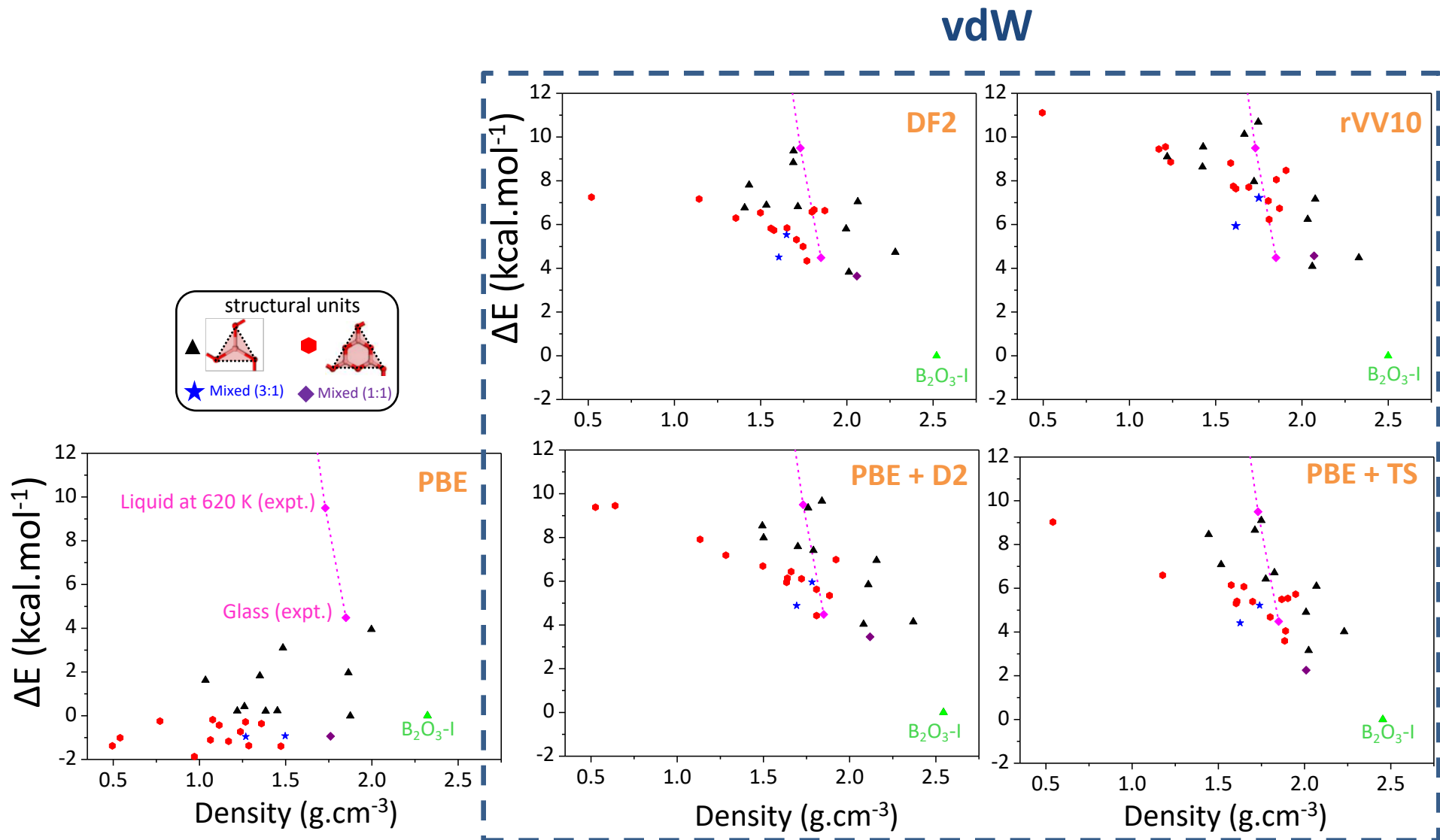


Low-density: highly symmetric, « puffed » rings
(as in $\text{SiO}_2 \beta$ -cristobalite)



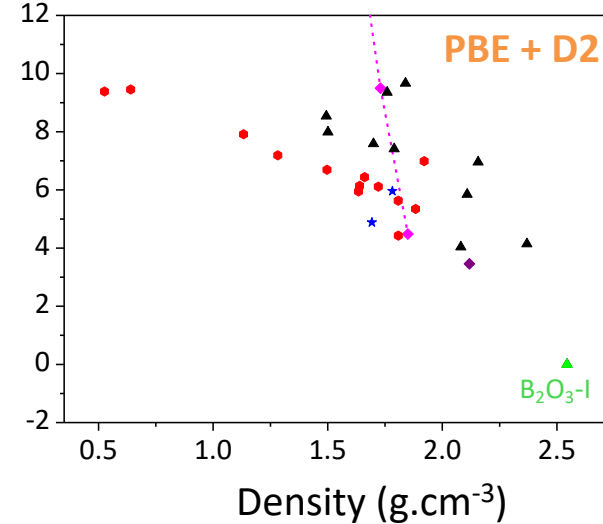
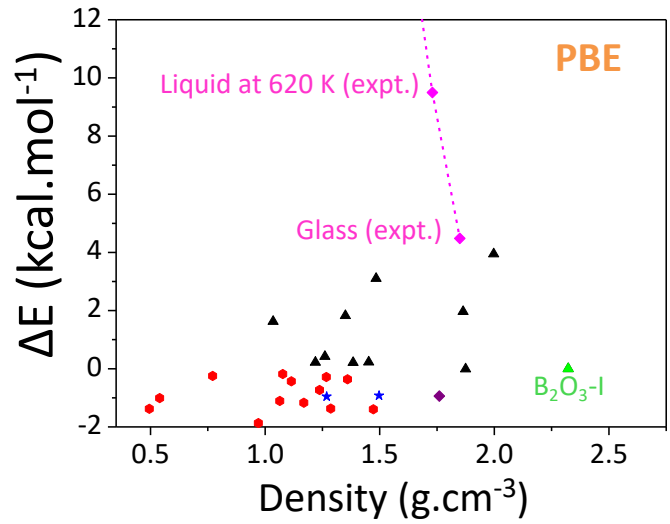
High-density: less symmetric, « puckered » rings
(as in $\text{SiO}_2 \alpha$ -cristobalite)

DFT (full set)



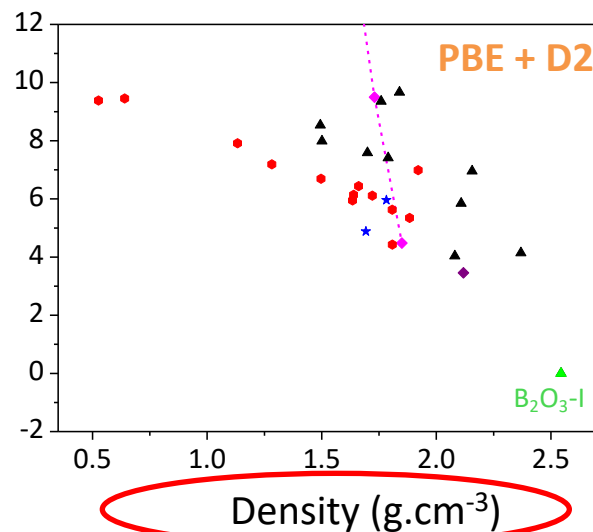
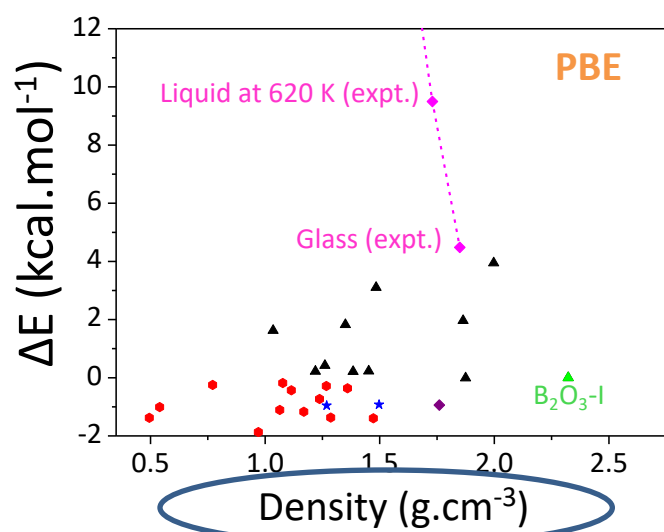
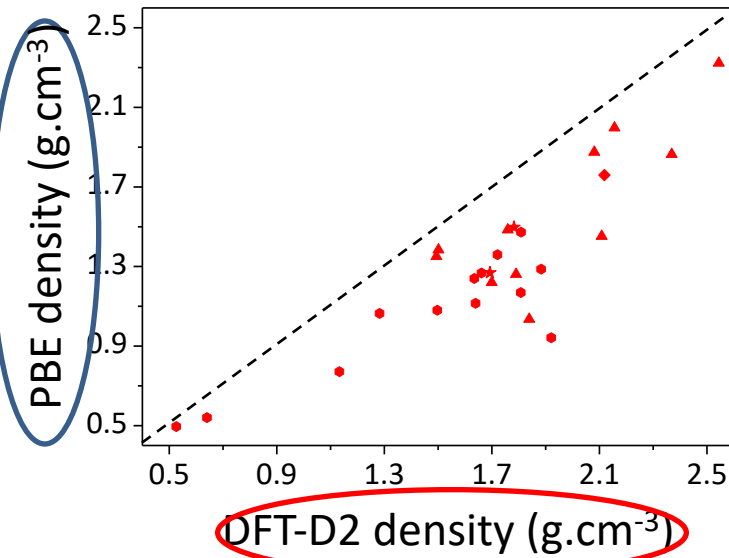
- ✓ Significant changes from PBE to “vdW”
- ✓ Good agreement between the various DFT-vdW schemes [$\text{B}_2\text{O}_3\text{-I}$ consistently found as ground state]

PBE versus DFT-D

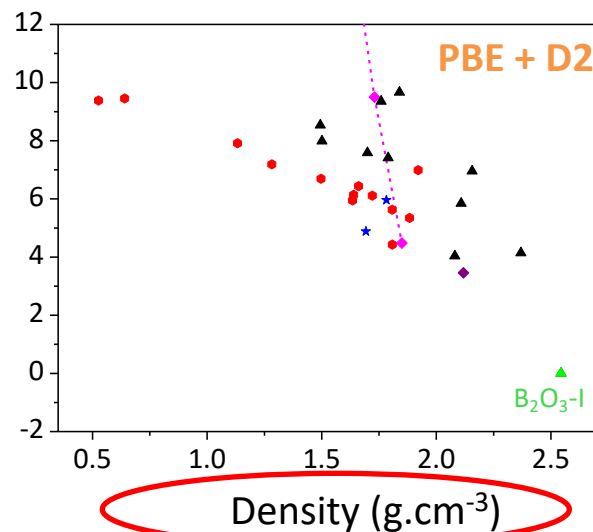
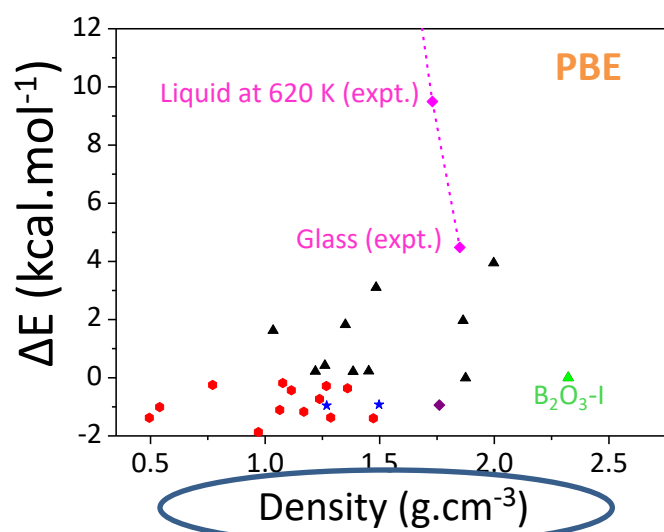
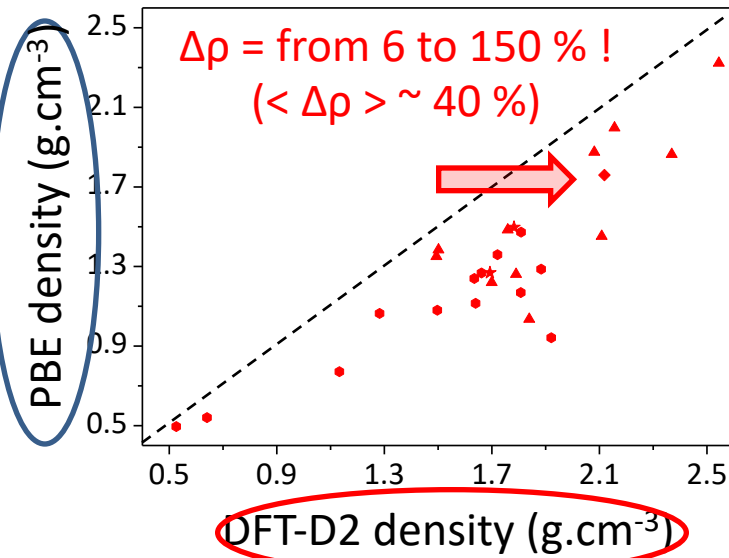


- ✓ Significant changes from PBE to “vdW”
- ✓ Good agreement between the various DFT-vdW schemes [B_2O_3-I consistently found as ground state]

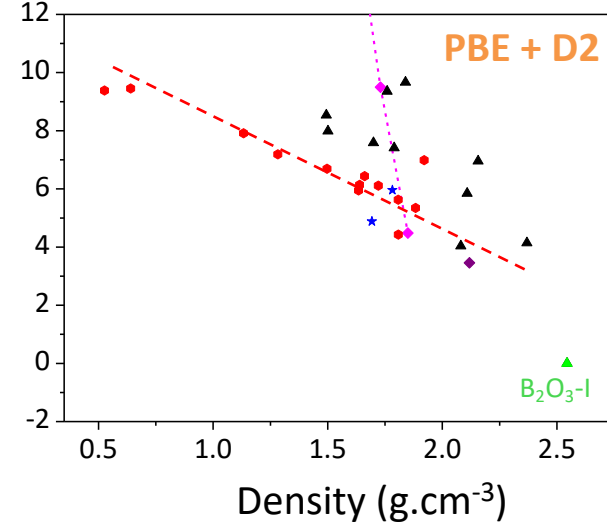
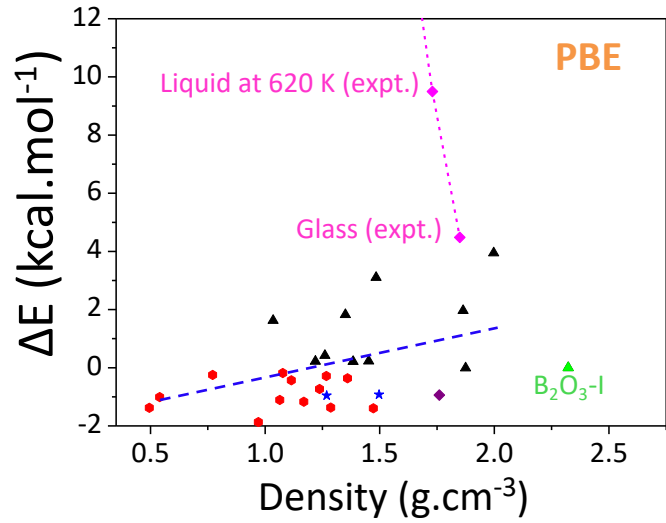
PBE versus DFT-D: density corrections



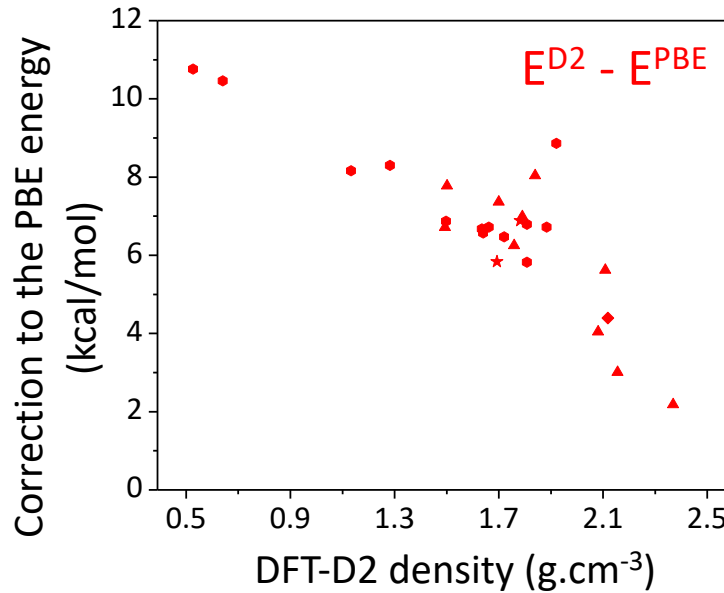
PBE versus DFT-D: density corrections



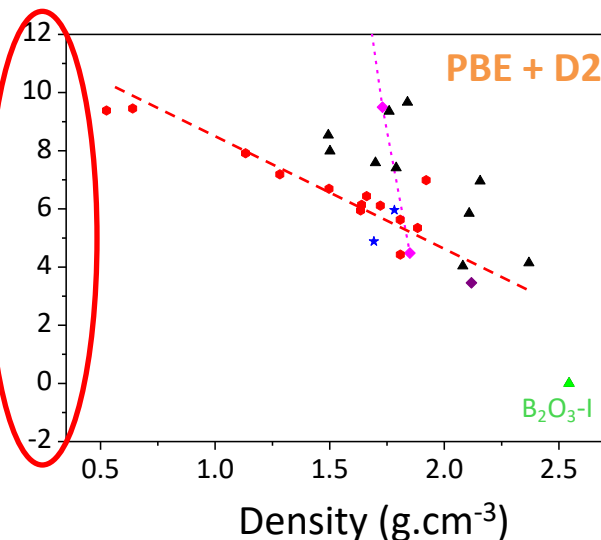
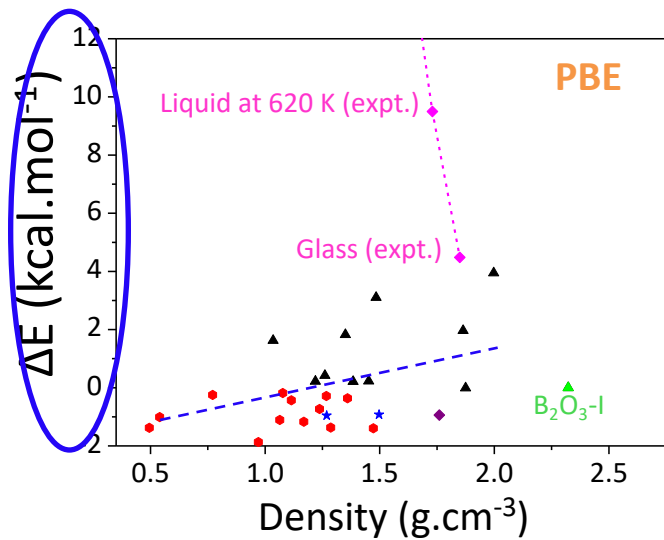
PBE versus DFT-D: energy corrections



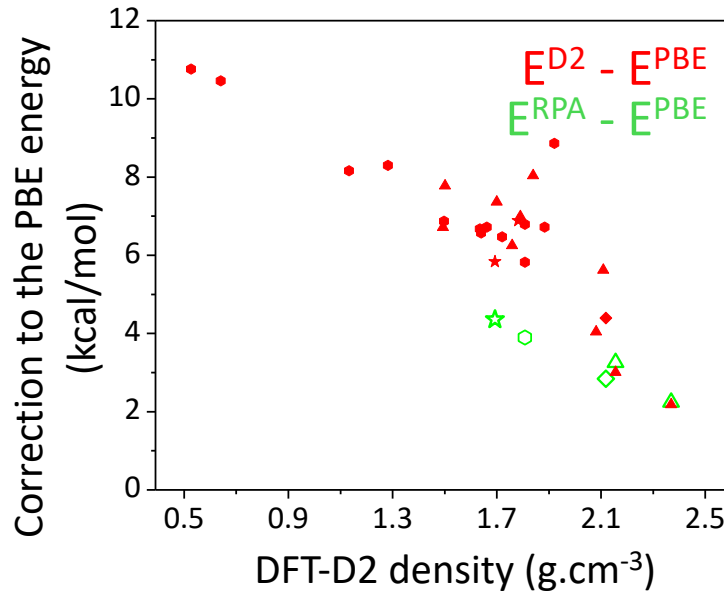
PBE versus DFT-D: energy corrections



vdW: increasing energy penalty
with decreasing density

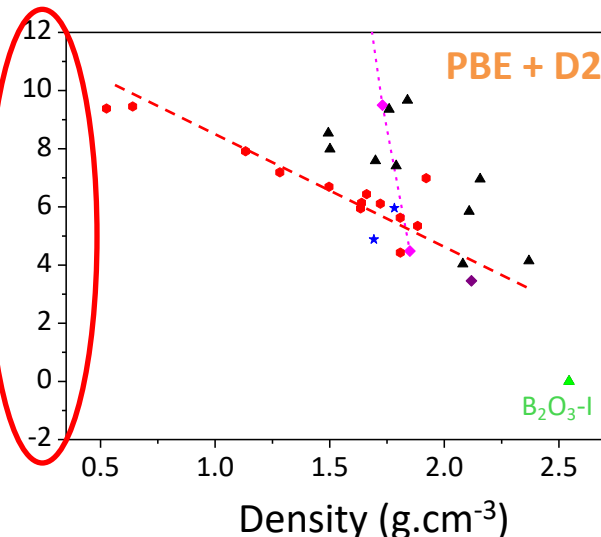
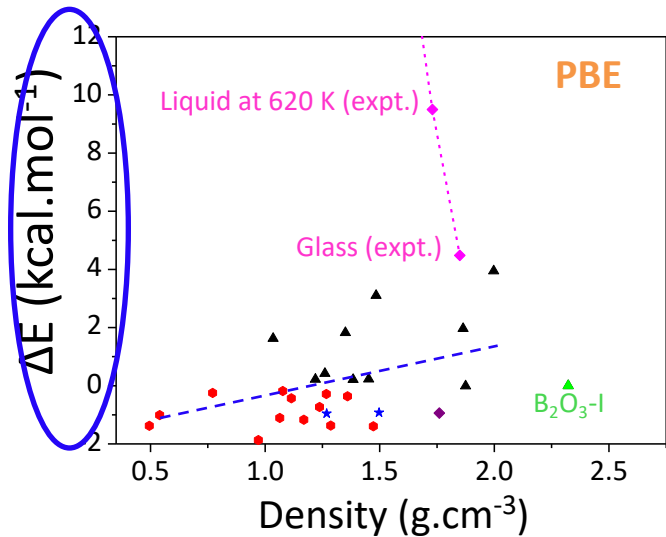


PBE versus DFT-D: energy corrections

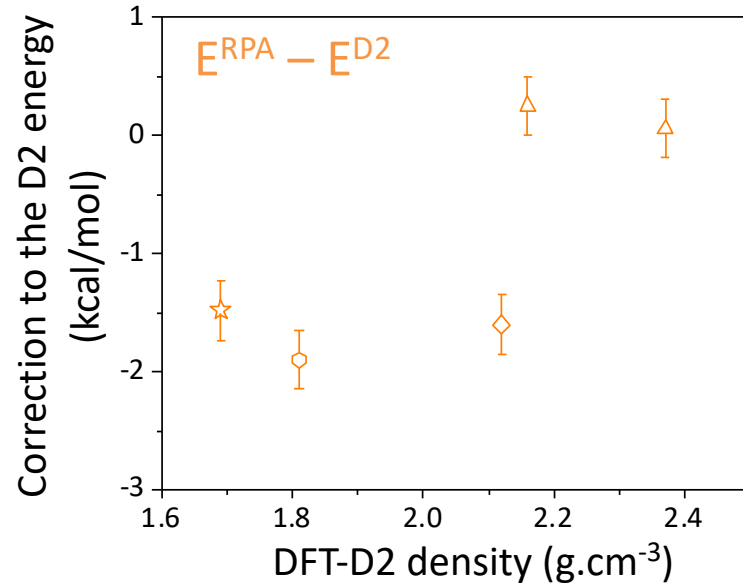


vdW: increasing energy penalty with decreasing density

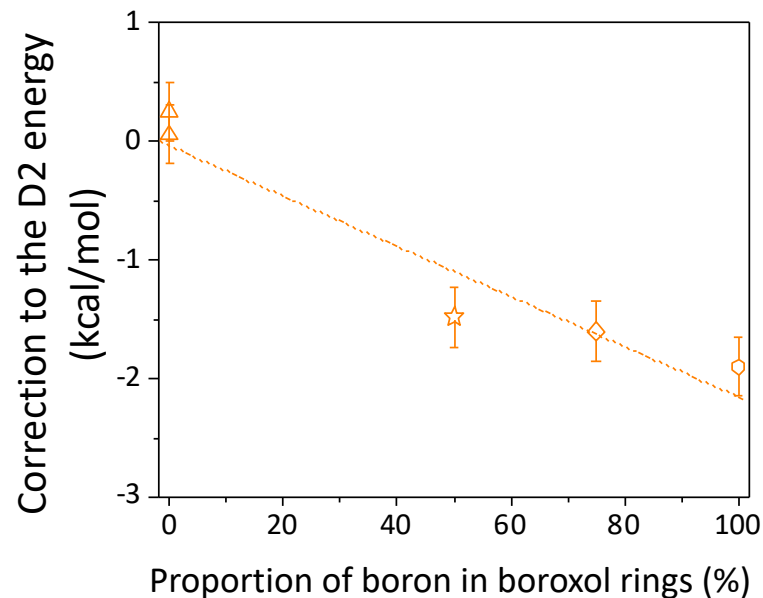
Trend confirmed by RPA



Many-body beyond vdW ?



$E^{\text{RPA}} - E^{\text{D2}}$ ≡
Many-body contribution ?
(on top of vdW, not captured by DFT)

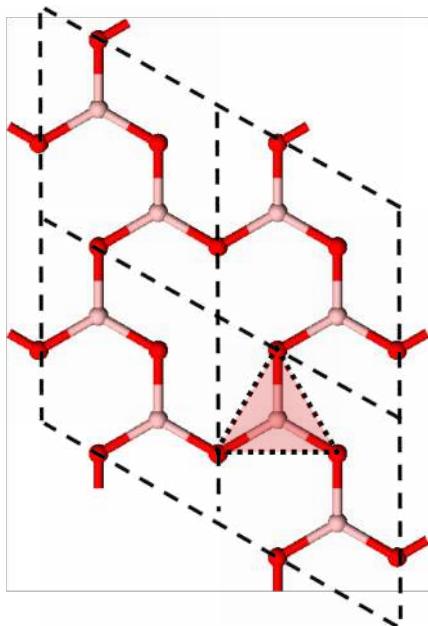


Related to the boroxol-ring
stabilisation energy?

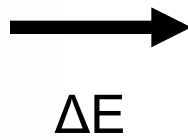
Work in progress ...

Boroxol stabilisation energy

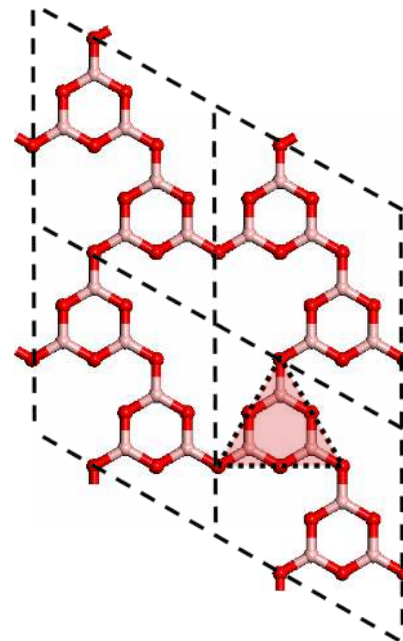
- « graphite » iso-structural crystals



100 % triangles “graphite”: T0



ΔE



100 % boroxols “graphite”: T0-b

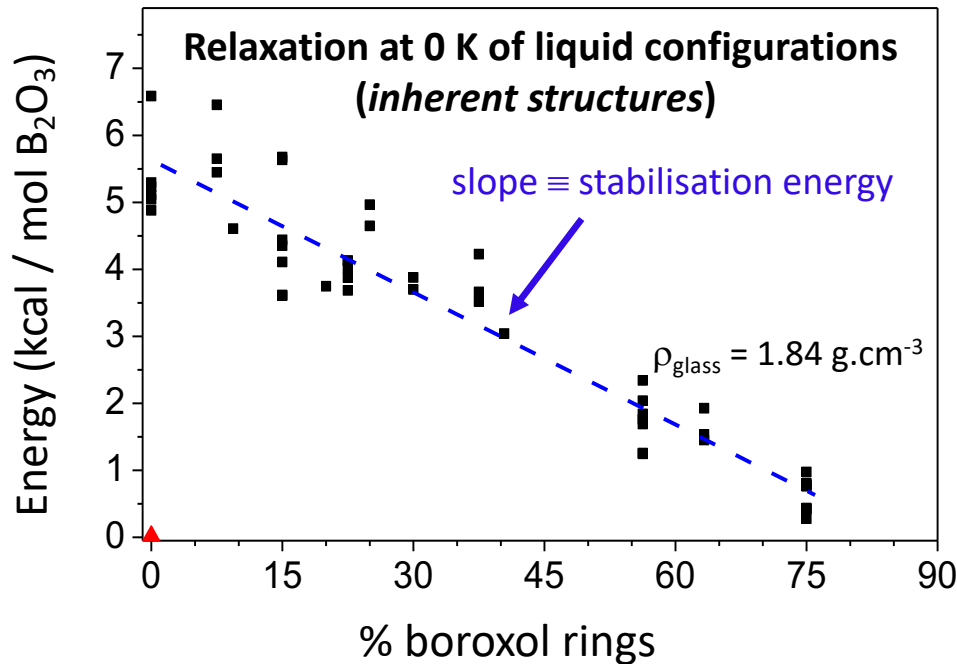
No relaxation (B-O-B angles fixed to 120°): $\Delta E^{\text{DFT}} \sim -10 \text{ kcal/mol}$

After relaxation: $\Delta E^{\text{DFT}} \sim 0 \text{ kcal/mol}$

$\Delta E^{\text{RPA}} \sim -2 \text{ kcal/mol}$

Boroxol stabilisation energy

G. Ferlat, T. Charpentier, A.P. Seitsonen, A. Takada, M. Lazzeri, L. Cormier, G. Calas, F. Mauri,
Phys. Rev. Lett., **101**, 065504 (2008)

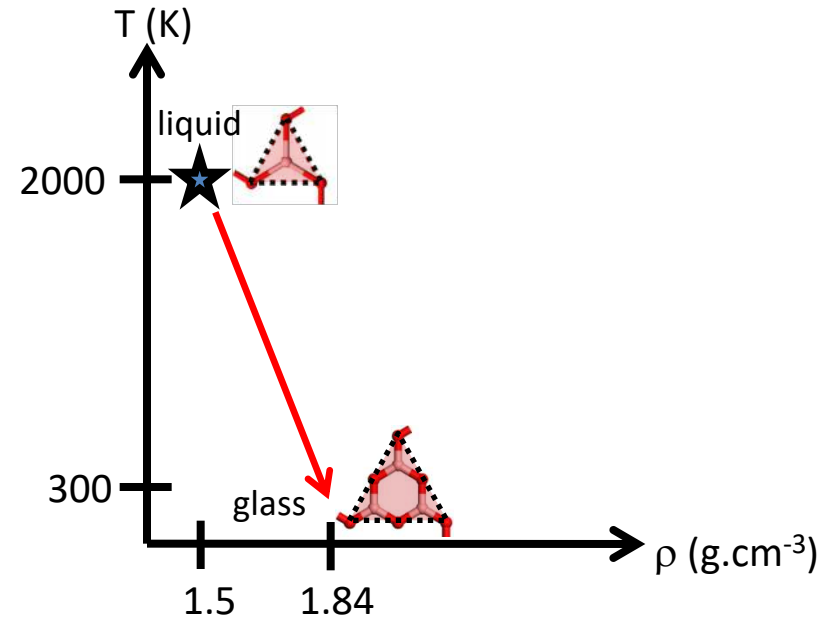
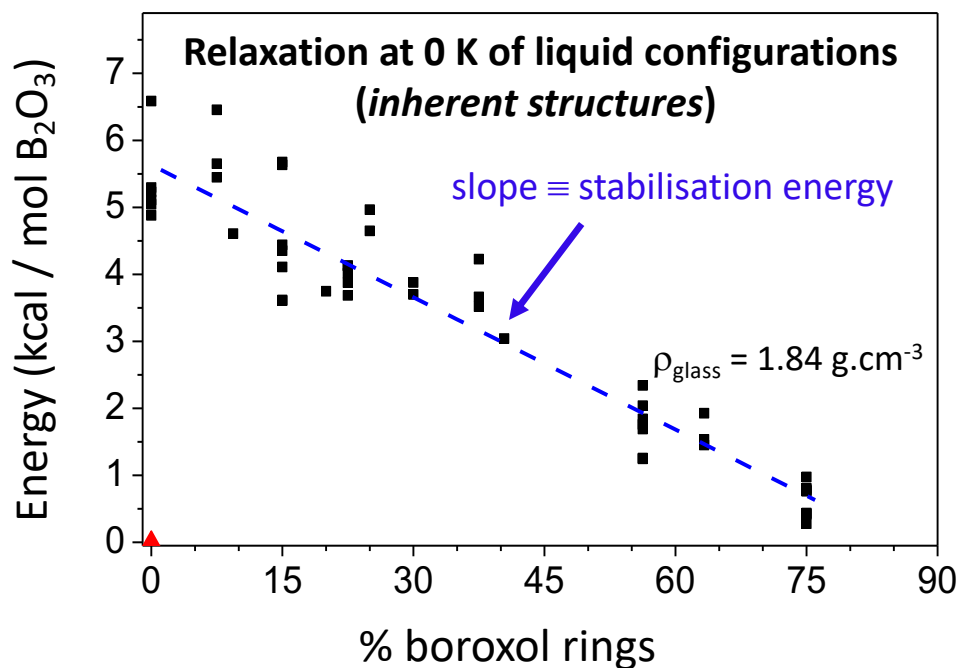


- ✓ At the glass density, *boroxol*-rich are more stable than *triangle*-rich structures
- ✓ Numerical evidence of a boroxol stabilisation-energy (in \sim good agreement with expt.)

PBE + D2: $E_{\text{stab}} = -9 \pm 2 \text{ kcal}/(\text{mol boroxol})$ for
a glass with $f = 75\%$ boroxol rings

Boroxol stabilisation energy

G. Ferlat, T. Charpentier, A.P. Seitsonen, A. Takada, M. Lazzeri, L. Cormier, G. Calas, F. Mauri,
Phys. Rev. Lett., **101**, 065504 (2008)



- ✓ At the glass density, *boroxol-rich* are more stable than *triangle-rich* structures
- ✓ Numerical evidence of a boroxol stabilisation-energy (in ~ good agreement with expt.)

PBE + D2: $E_{\text{stab}} = -9 \pm 2 \text{ kcal}/(\text{mol boroxol})$ for a glass with $f = 75\%$ boroxol rings

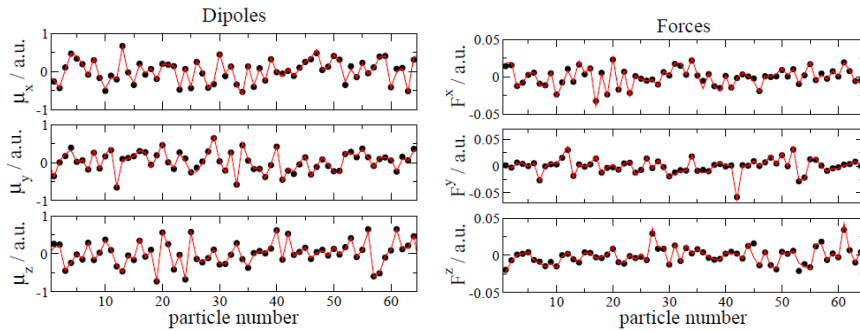
Expt.: $E_{\text{stab}} \sim -6 \pm 1 \text{ kcal}/(\text{mol boroxol})$

Polarisable force-fields from *first-principles*

Collab. M. Salanne (PHENIX, Sorbonne Univ.)

Phys. Rev. B (2014), *J. Phys. Condens. Matter* (2015), *J. Chem. Phys.* (2019)

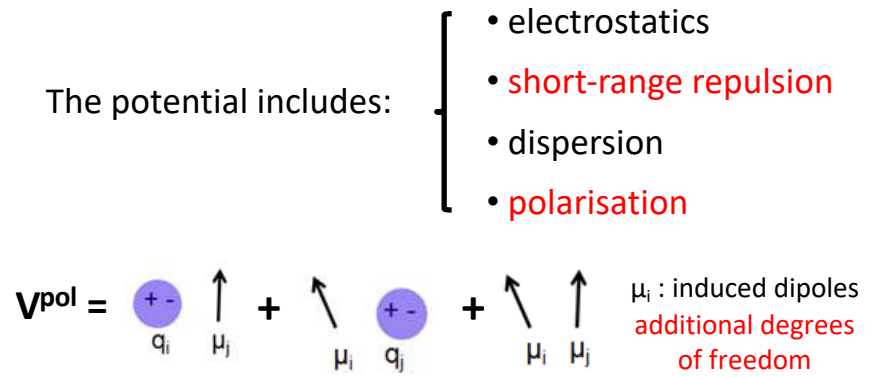
- *first-principles* (CPMD) simulations used as benchmarks
- Force- and dipole-matching to calibrate the parameters



CPMD – *Fitted polarisable ion model*

Rotenberg, Salanne, Simon, Vuilleumier, *Phys. Rev. Lett.* (2010)

The potential includes:

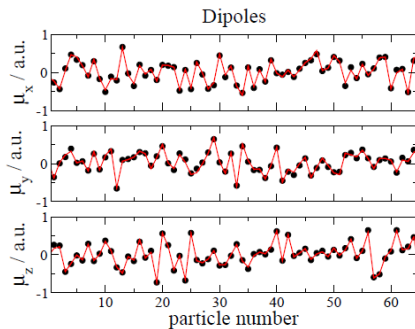


Polarisable force-fields from *first-principles*

Collab. M. Salanne (PHENIX, Sorbonne Univ.)

Phys. Rev. B (2014), *J. Phys. Condens. Matter* (2015), *J. Chem. Phys.* (2019)

- *first-principles* (CPMD) simulations used as benchmarks
- Force- and dipole-matching to calibrate the parameters



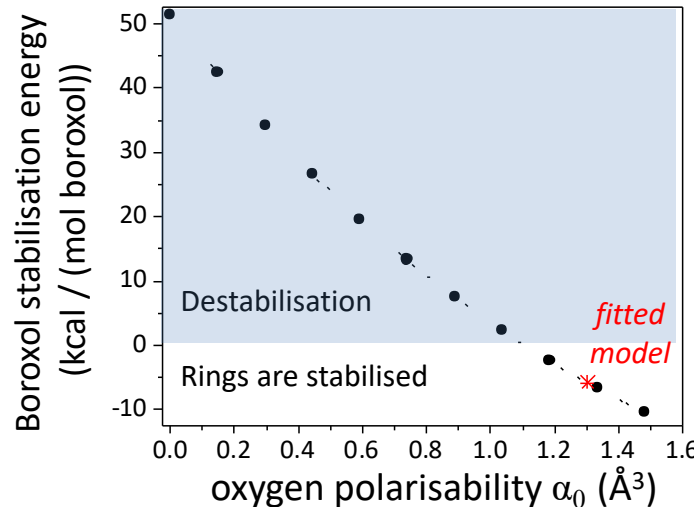
CPMD – *Fitted polarisable ion model*

Rotenberg, Salanne, Simon, Vuilleumier, *Phys. Rev. Lett.* (2010)

- The potential includes:
- electrostatics
 - short-range repulsion
 - dispersion
 - polarisation

$$V^{\text{pol}} = \frac{q_i q_j}{r} + \frac{\mu_i \cdot \mu_j}{r^3} + \frac{\mu_i \cdot \mu_j}{r^6}$$

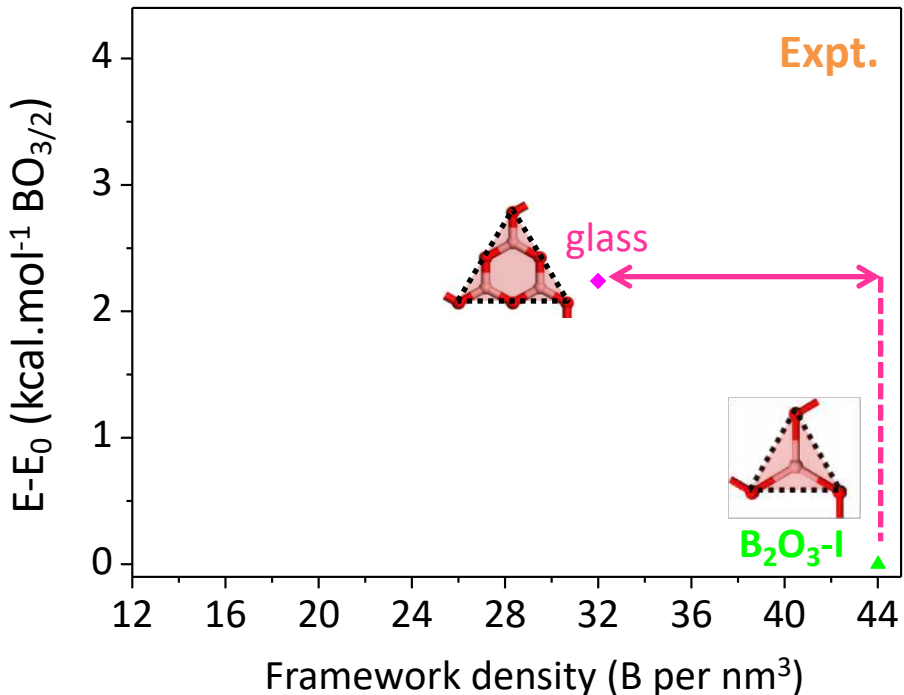
μ_i : induced dipoles
additional degrees of freedom



✓ strong dependence of the boroxols' stabilisation energy upon the **oxygen polarisability**

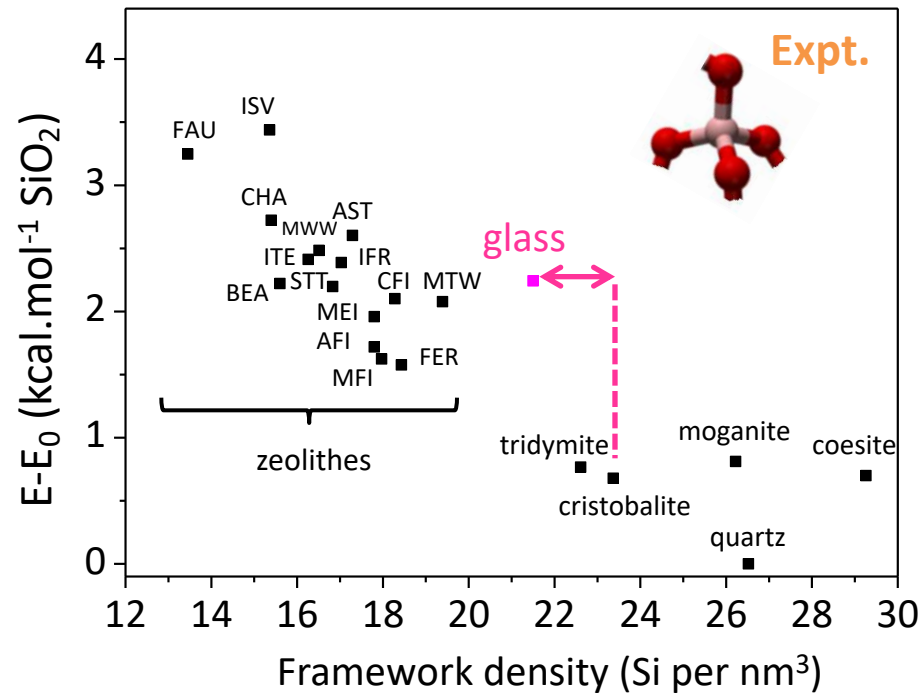
Back to the B_2O_3 anomalies

B_2O_3



- ✓ B_2O_3 : - glass structure \neq crystal
 - $\rho_{\text{glass}} \sim 0.71 \rho_{\text{crystal}}$
 - poor polymorphism

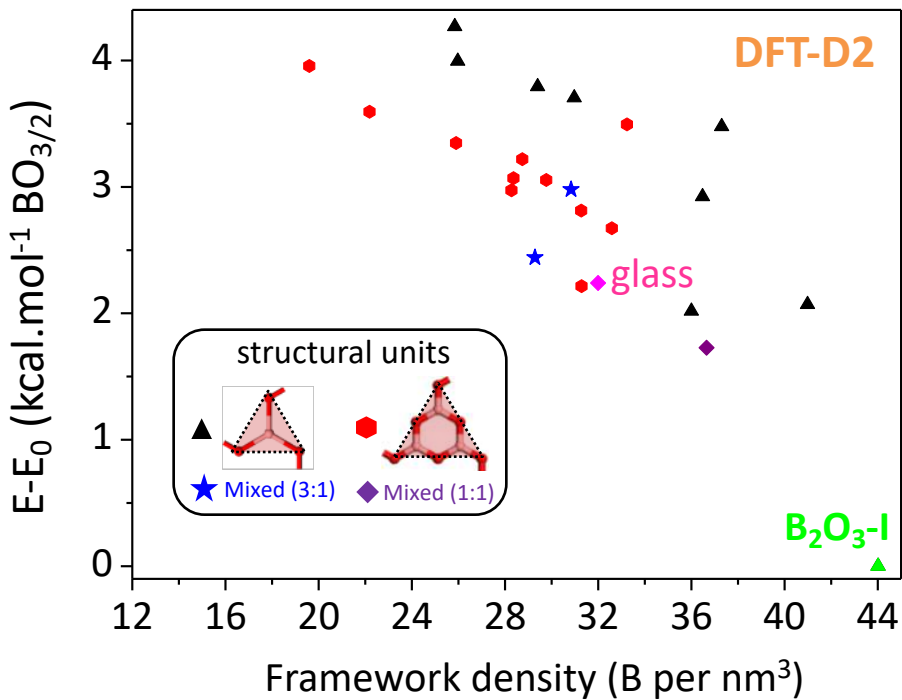
SiO_2



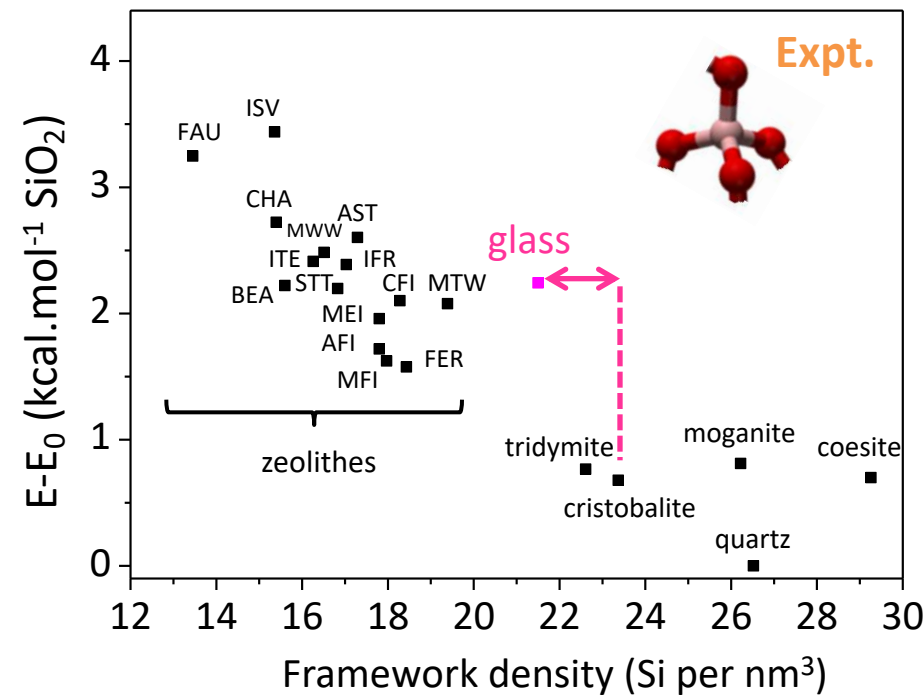
- ✓ SiO_2 : - glass \sim cristobalite
 - $\rho_{\text{glass}} \sim 0.92 \rho_{\text{cristobalite}}$
 - rich polymorphism

Back to the B_2O_3 anomalies

B_2O_3



SiO_2



✓ B_2O_3 : - glass structure ~ crystals

$$\cancel{- \rho_{\text{glass}} \sim 0.71 \rho_{\text{crystal}}} \quad \rho_{\text{glass}} \sim \rho_{\text{crystal}}$$

- poor rich polymorphism

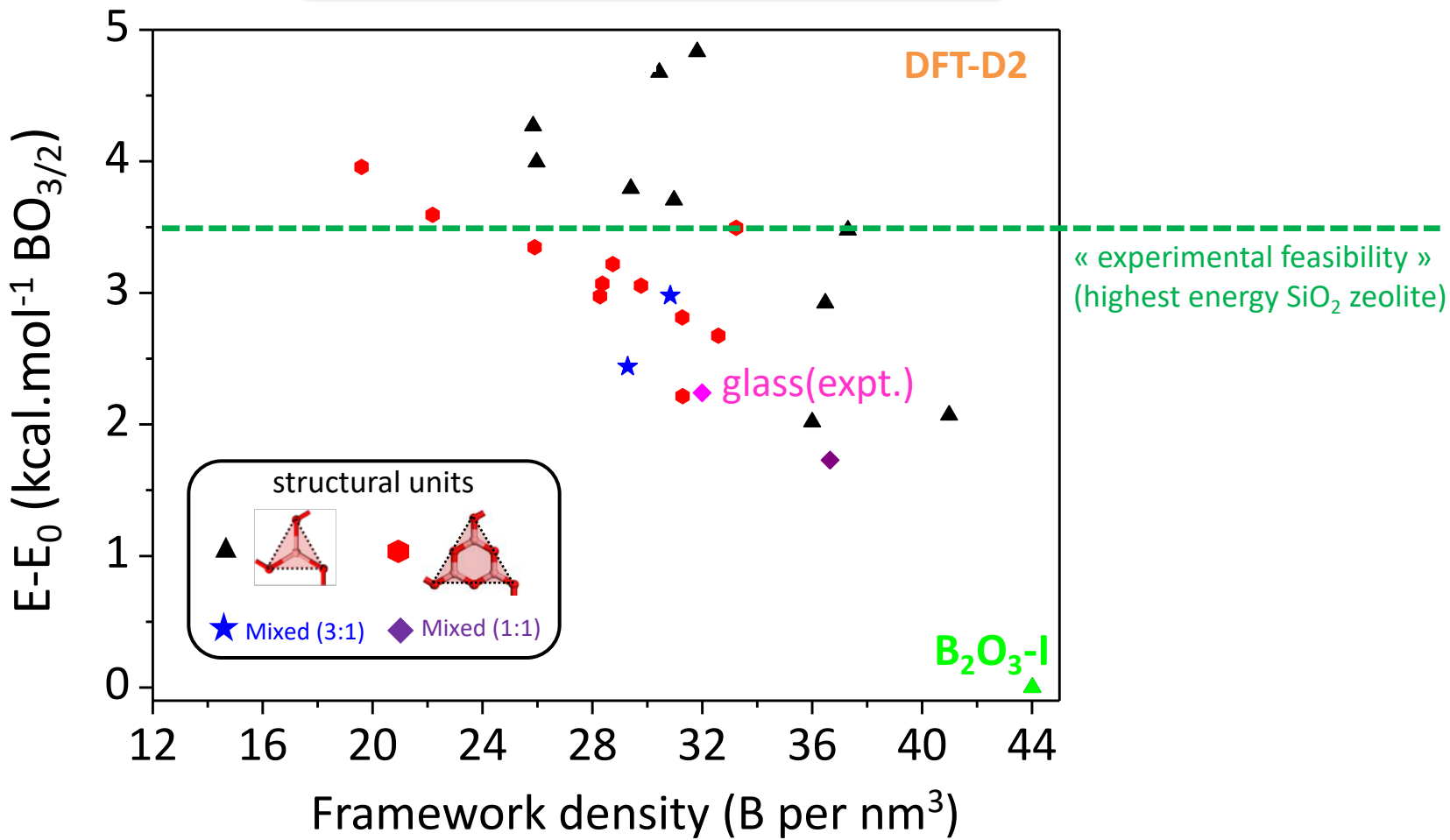
✓ SiO_2 : - glass ~ cristobalite

$$- \rho_{\text{glass}} \sim 0.92 \rho_{\text{cristobalite}}$$

- rich polymorphism

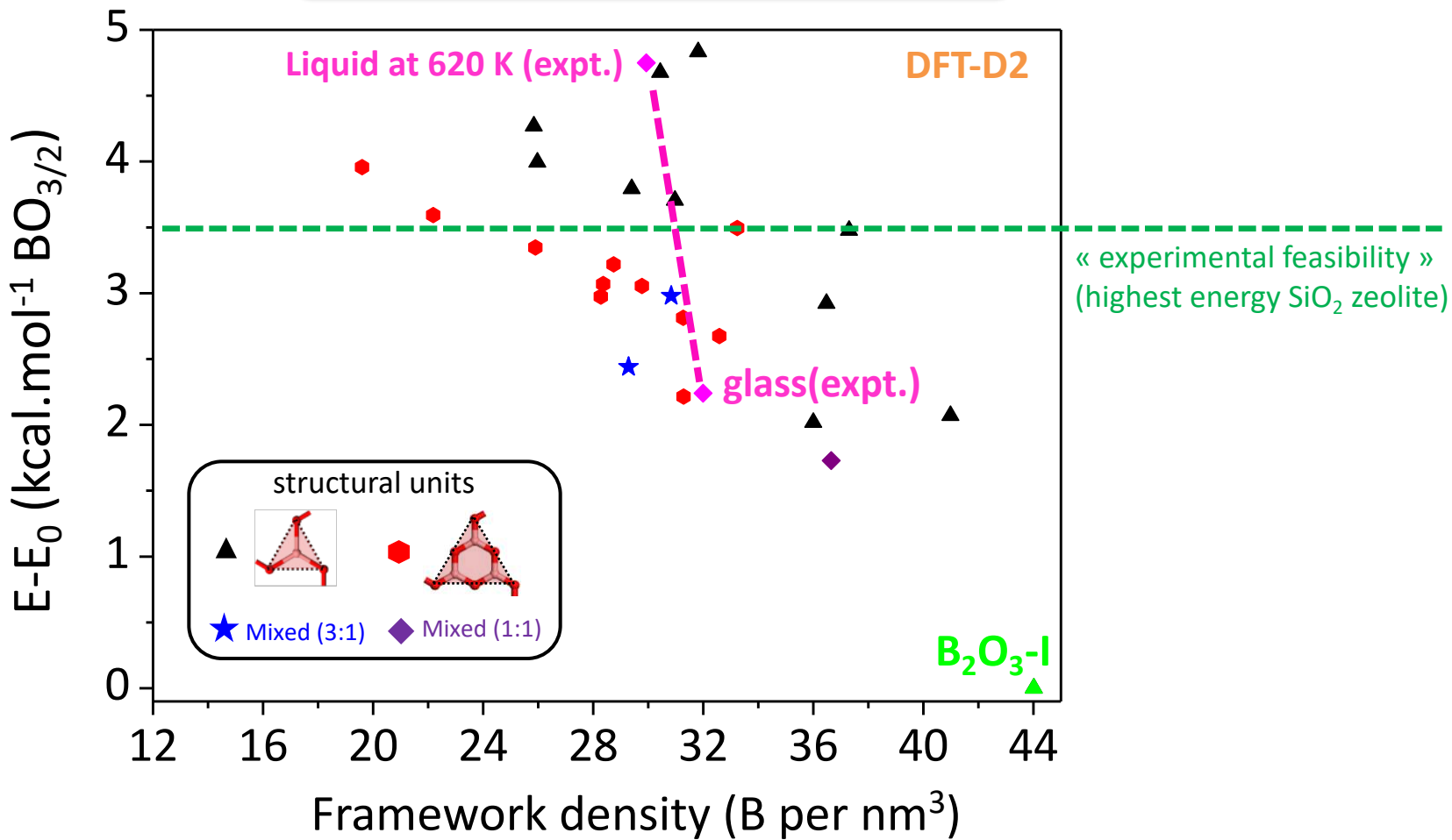
✓ New polymorphs more relevant (than B_2O_3 -I) for understanding the glass properties

B₂O₃ polymorphism: energy



- ✓ Most polymorphs in **thermodynamically accessible energy range**. Why not yet observed?

B₂O₃ polymorphism: energy



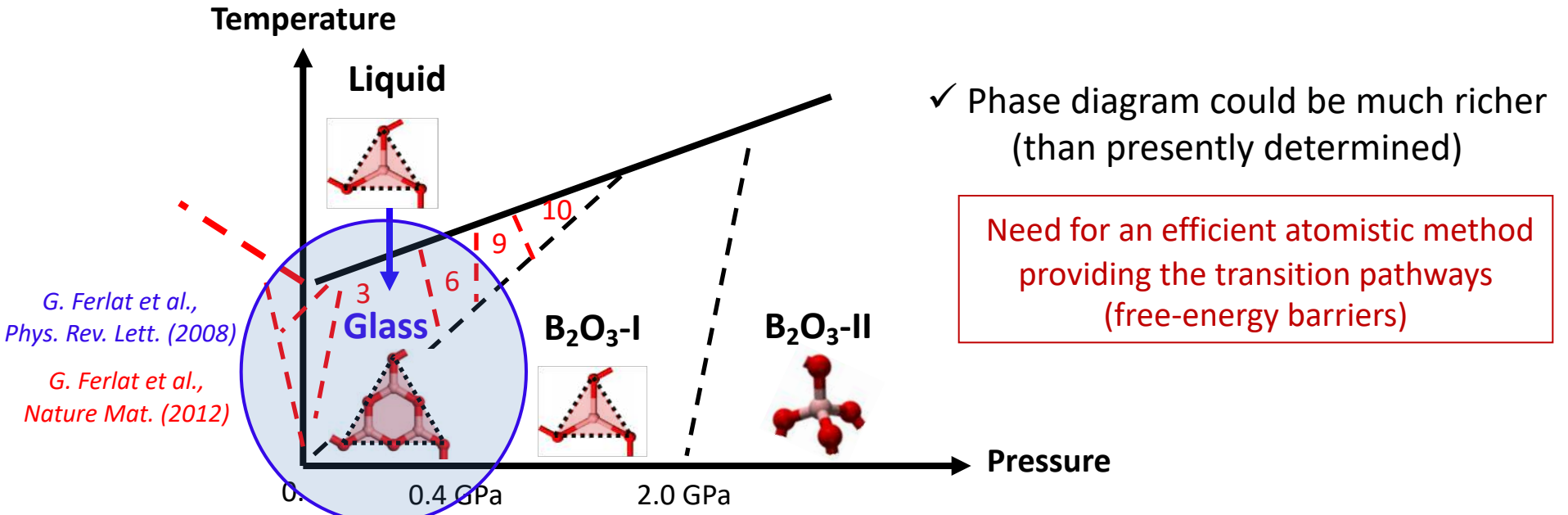
- ✓ Most polymorphs in **thermodynamically accessible energy range**. **Why not yet observed?**
- ✓ Spontaneous vitrification (***crystallisation anomaly***) likely results from 2 factors:
 - 1) rich degeneracy of competing polymorphs (*rugged energy landscape*)
 - 2) poor mechanical strength [not shown in this talk]

Take-home messages

- Prediction of 26 new B_2O_3 crystalline polymorphs of low-energy
Ferlat *et al.*, Nature Materials (2012)
Ferlat, Hellgren, Coudert, Hay, Mauri, Casula, Phys. Rev. Materials (2019)

→ Data set used here to **benchmark DFT against RPA and QMC**
- B_2O_3 : strong (iono-covalent) bonds, fully connected 3D networks.
Yet, very significant effects of **vdW interactions**: qualitative (not only quantitative) changes. This is related to the flexibility of the bonds between units and to the existence of « soft » directions.
- **Challenging system** for DFT.

Perspectives



- parametrisation of B_2O_3 accurate force-fields from *ab-initio*:

Phys. Rev. B (2014), *J. Phys. Condens. Matter* (2015), *J. Chem. Phys.* (2019)

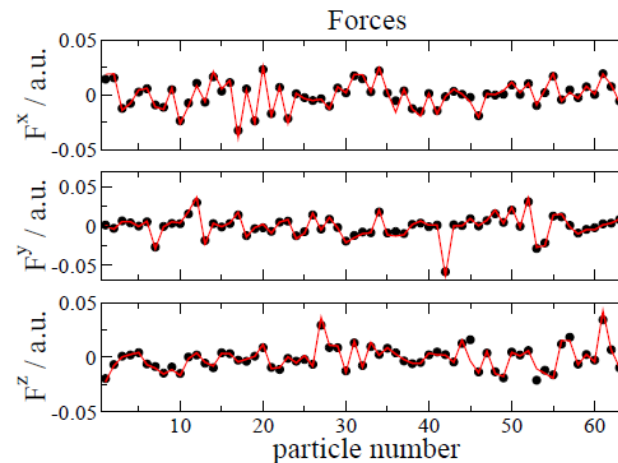
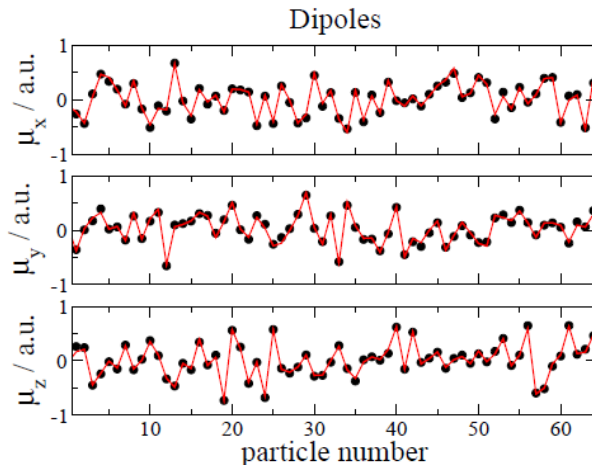
- enhanced sampling:***

Navigating at will on the water phase diagram, Phys. Rev. Lett (2017)

Collaboration: M. Salanne, F. Pietrucci (Sorbonne Université)

Polarisable force-fields from *first-principles*

- *First-principles* MD simulations (CPMD) used as benchmark trajectories
- Force- and dipole-matching approach to calibrate the force-field parameters



CPMD – *Fitted polarisable ion model*

V is an analytical function of the positions. It includes:

- electrostatics
- short-range repulsion
- dispersion
- polarisation

- ✓ Transferable parameters for a family of compounds

B. Rothenberg, M. Salanne, C. Simon, R. Vuilleumier “From Localized Orbitals to Material Properties: Building Classical Force Fields for Nonmetallic Condensed Matter Systems”, Phys. Rev. Lett. **104**, 138301 (2010)

Polarisable Ion Model (PIM)

✓ Pairwise additive components:

- Charge-charge interactions:

$$V_{\text{charge-charge}} = \sum_{i,j>i} \frac{q^i q^j}{r^{ij}}$$

- Short-range repulsion:

$$V_{\text{repulsion}} = \sum_{i,j>i} B^{ij} \exp(-a^{ij} r^{ij})$$

- Dispersion interactions:

$$V_{\text{dispersion}} = - \sum_{i,j>i} \left[f_6^{ij}(r^{ij}) \frac{C_6^{ij}}{(r^{ij})^6} + f_8^{ij}(r^{ij}) \frac{C_8^{ij}}{(r^{ij})^8} \right]$$

✓ Polarisation component:

- Charge-dipole and dipole-dipole interactions

$$\begin{aligned} V_{\text{polarization}} &= \sum_{i,j>i} \left(q^i \mu_\alpha^j g_D^{ij}(r^{ij}) - q^j \mu_\alpha^i g_D^{ji}(r^{ij}) \right) \nabla_\alpha \frac{1}{r^{ij}} \\ &\quad \sum_{i,j>i} -\mu_\alpha^i \mu_\beta^j \nabla_\alpha \nabla_\beta \frac{1}{r^{ij}} \\ &\quad + \sum_i \frac{1}{2\alpha^i} |\vec{\mu}^i|^2 \end{aligned}$$

$\vec{\mu}^i$ are the induced dipoles → Additional degrees of freedom

- Self-consistent calculation of $\vec{\mu}^i$ by conjugate gradients

Aspherical Ion Model (AIM)

Modified repulsion term:

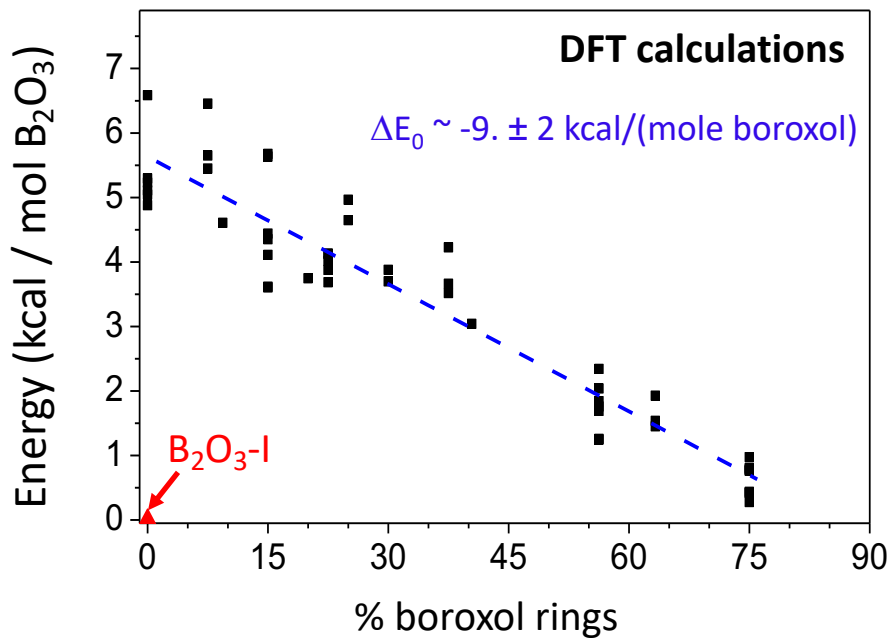
$$\begin{aligned} V^{\text{rep}} &= \sum_{j>i} \left(A^{ij} e^{-a^{ij}\rho^{ij}} + B^{ij} e^{-b^{ij}\rho^{ij}} + C^{ij} e^{-c^{ij}r^{ij}} \right) \\ &\quad + \sum_{i \in O} \left[D^i (e^{\beta^i \delta\sigma^i} + e^{-\beta^i \delta\sigma^i}) + (e^{\zeta^i |\nu^i|^2} - 1) + (e^{\eta^i |\kappa^i|^2} - 1) \right] \\ \rho^{ij} &= r^{ij} - \delta\sigma^i - S_{\alpha}^{(1)} \nu_{\alpha}^i - S_{\alpha\beta}^{(2)} \kappa_{\alpha\beta}^i \end{aligned} \quad (1) \quad (2)$$

Additional degrees of freedom (SCF calculation):

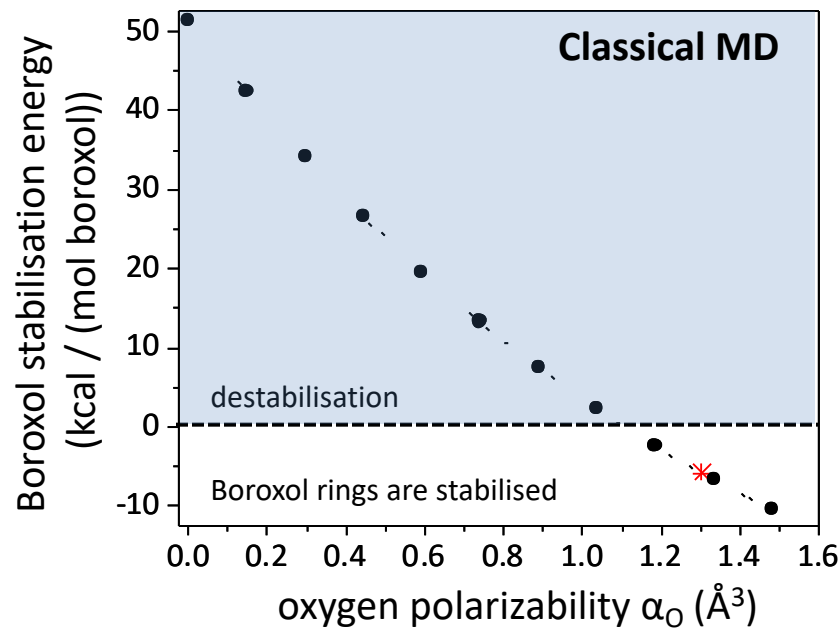
- $\delta\sigma^i$: “Breathing” of the ion
- ν_{α}^i : Dipolar distortion of the ion
- $\kappa_{\alpha\beta}^i$: Quadrupolar distortion of the ion

Boroxol stabilisation energy

Relaxation at 0 K of *glassy* configurations

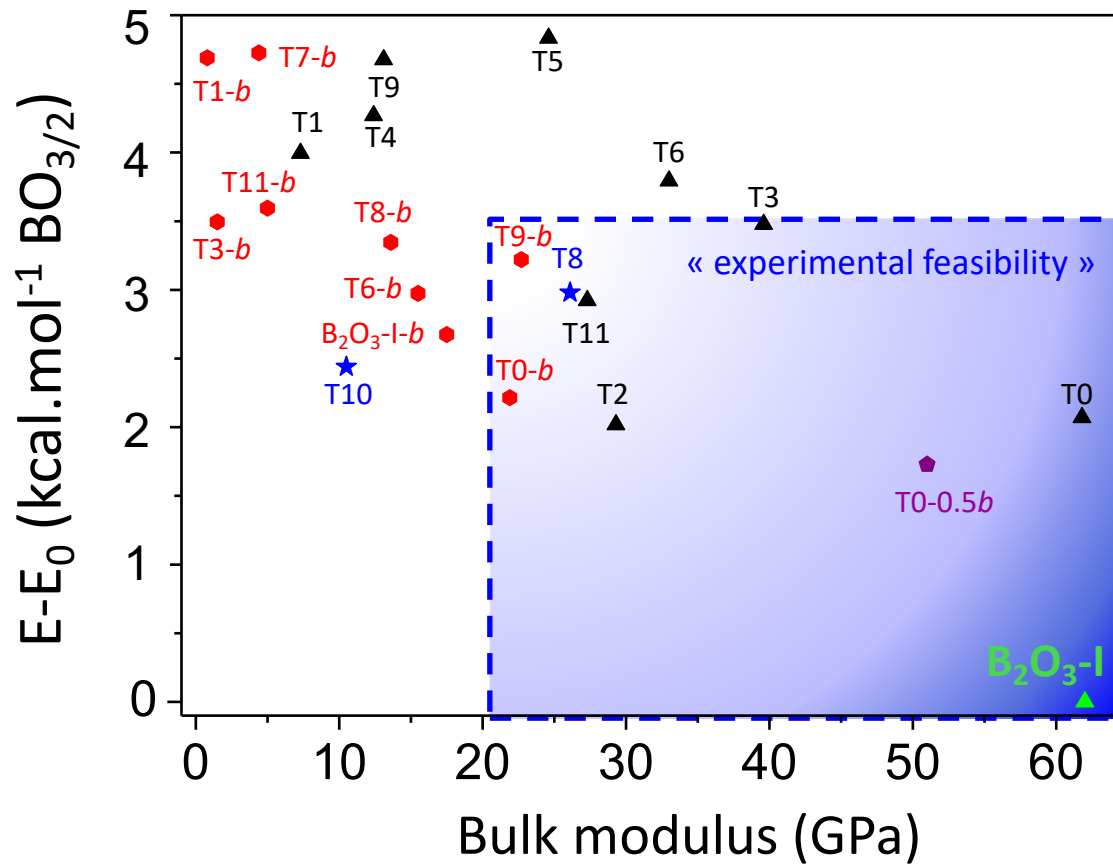


Polarizability in classical force-fields



B_2O_3 polymorphism: mechanical properties

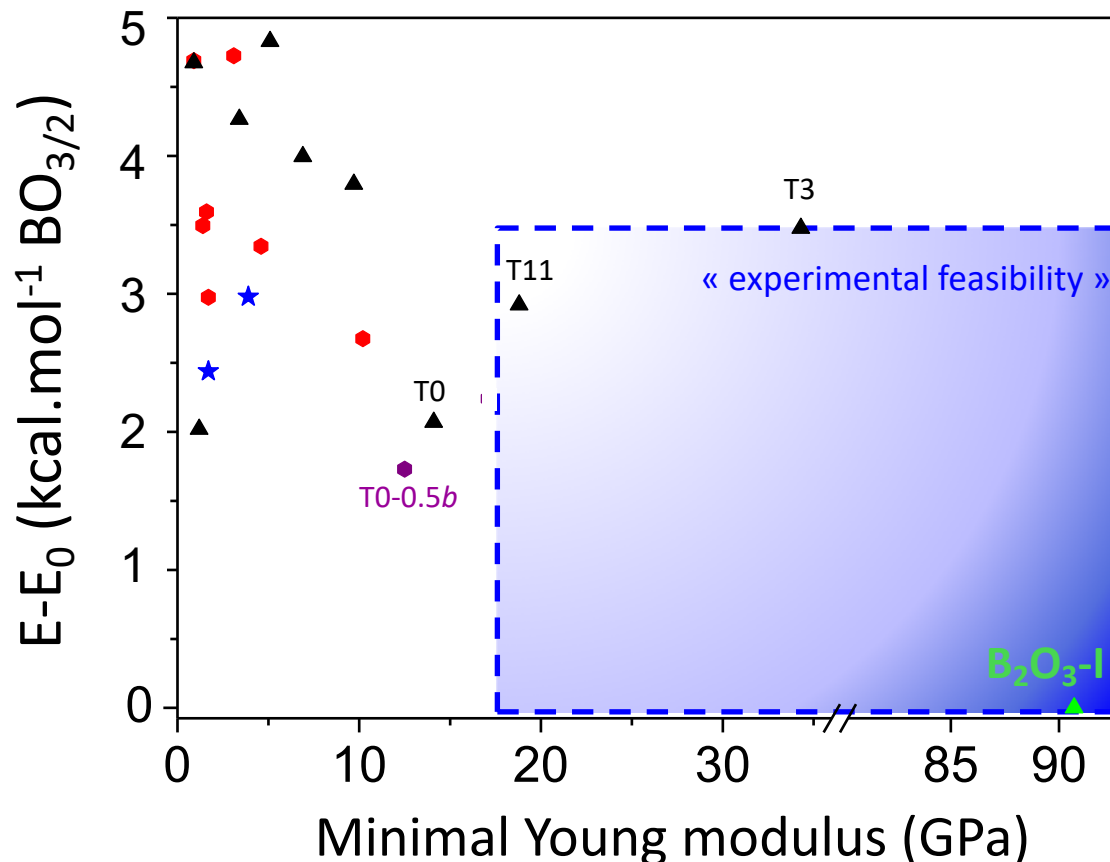
Computation of bulk (B), shear (E) and Young (Y) moduli



- ✓ New polymorphs are mechanically much “weaker” than $\text{B}_2\text{O}_3\text{-I}$
- ✓ Prone to “collapse”. Reason for not being observed ?
Part of the *crystallisation anomaly* explanation ?
[applying pressure favours higher density and stiffer structures → $\text{B}_2\text{O}_3\text{-I}$]

B_2O_3 polymorphism: mechanical properties

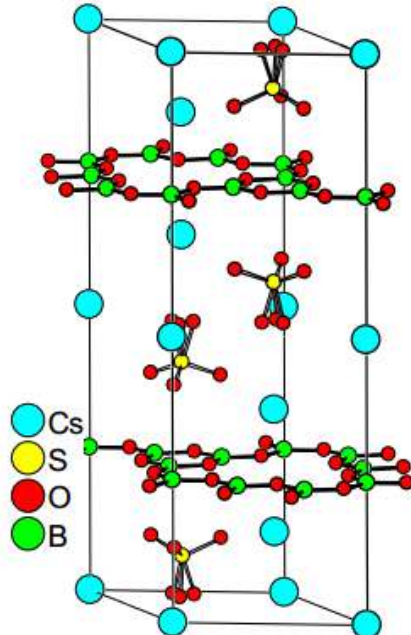
Computation of bulk (B), shear (E) and Young (Y) moduli



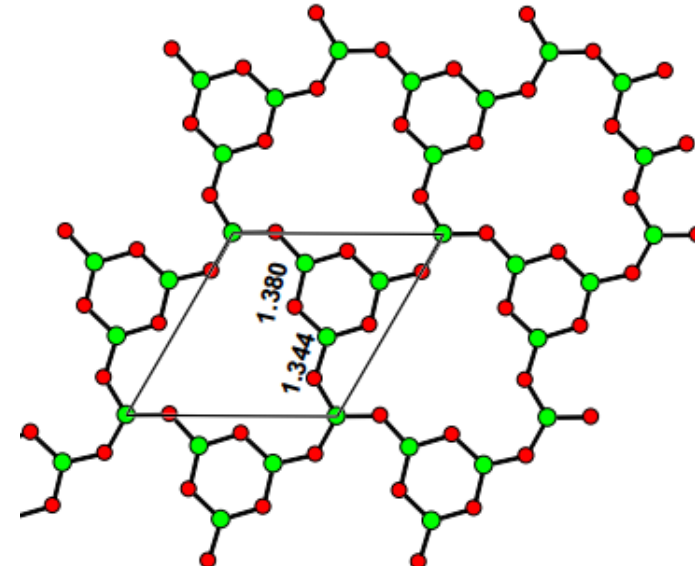
- ✓ New polymorphs are mechanically much “weaker” than B_2O_3 -I
- ✓ Prone to “collapse”. Reason for not being observed ?
Part of the *crystallisation anomaly* explanation ?
[applying pressure favours higher density and stiffer structures → B_2O_3 -I]

Hints for synthesis? B_2O_3 layers in borates

Experiment from H. Hillebrecht *et al.* (Eur. J. Inorg. Chem. 2015)



$\text{Cs}_3\text{H}(\text{SO}_4)_2 \cdot 2\text{B}_2\text{O}_3$

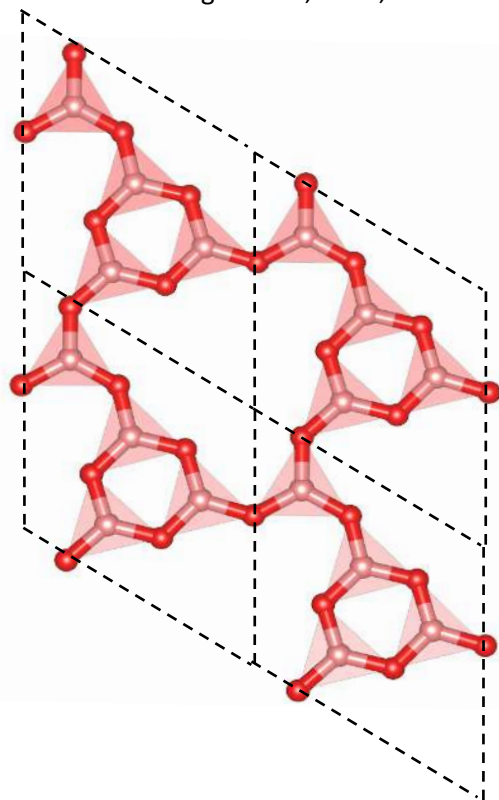


The B_2O_3 layer in $\text{Cs}_3\text{H}(\text{SO}_4)_2 \cdot 2\text{B}_2\text{O}_3$

Could a pure B_2O_3 phase obtained from deintercalation?

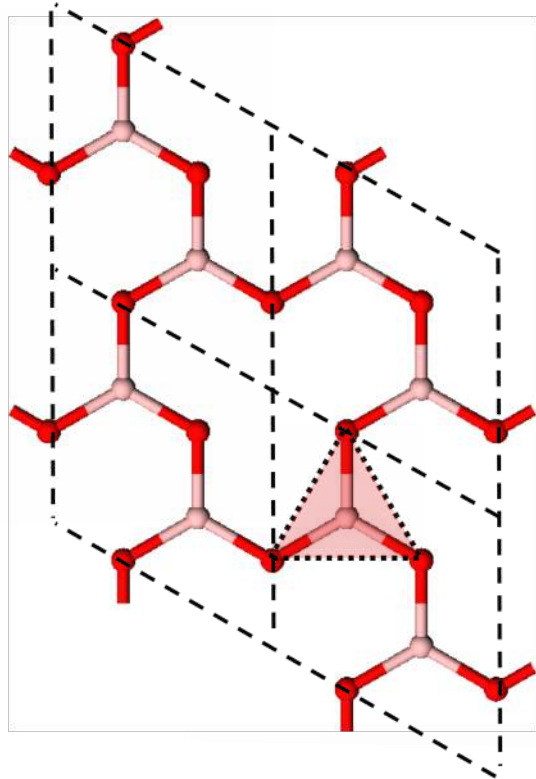
B₂O₃ layered polymorphs

Built upon M. Daub, H. Hillebrecht,
Eur. J. Inorg. Chem., **2015**, 4176



B₂O₃ layered polymorphs

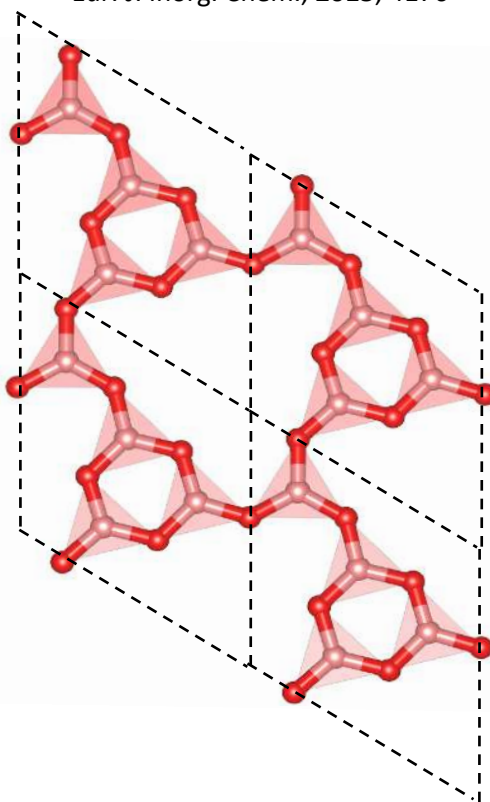
T0



Motif: triangle

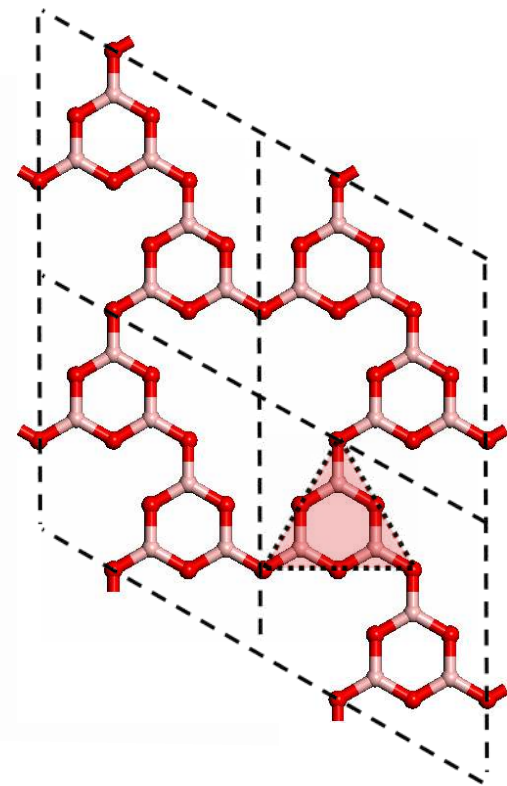
T0-0.5*b*

Built upon M. Daub, H. Hillebrecht,
Eur. J. Inorg. Chem., 2015, 4176



Motif: triangle and boroxol

T0-*b*



Motif: boroxol

Calculations: lowest energy !

Experimental realisations of other B₂O₃ polymorphs?

- There are at least two reports of low-density crystals (incorrectly assigned as B₂O₃-I):

✓ S. S. Cole, N. W. Taylor, J. Am. Ceram. Soc., **18**, 55 (1935) : $\rho = 1.805 \text{ g.cm}^{-3}$

✓ S. Kocakusak *et al.*, Chem. Eng. Proc. **35**, 311 (1996) : $\rho = 0.69 \text{ g.cm}^{-3}$!



Chemical Engineering and Processing 35 (1996) 311–317

Chemical
Engineering
Processing

Production of anhydrous, crystalline boron oxide in fluidized bed reactor

S. Kocakusak, K. Akçay, T. Ayok, H.J. Köroğlu, M. Koral, Ö.T. Savaşçı, R. Tolun
Tibitak-Marmara Research Center, Chemical Engineering Department, P.O. Box 21, 41470, Gebze/Kocaeli, Turkey

Received 21 September 1995; accepted 25 November 1995

Abstract

Industrial production of boron oxide is via fusion of boric acid at 550–1000 °C. The glassy melt thus obtained is then cooled until solid; crushed, ground and then sieved to allow classification according to particle size and distribution. The melting of boric acid is both the most critical and costly stage of all these operations, because boron oxide is highly corrosive to refractories and steel.

Our study allows the production of commercial quality anhydrous and crystalline boron oxide without the melting and other processes mentioned above. This is achieved by dehydrating boric acid in a fluidized bed with a gradual increase in the bed temperature up to 250 °C. During this process as the bed temperature is increased gradually, particular attention is paid to keep the dehydration rate below a certain value to prevent melting or sticking, and to secure the desired bulk density value of the product.

- Chemical synthesis, using Chemical Vapor Deposition (CVD) techniques: MOCVD, Atomic Layer Deposition (ALD) , ...



Available online at www.sciencedirect.com

SCIENCE @ DIRECT®

Physica E 27 (2005) 319–324

PHYSICA E

www.elsevier.com/locate/physce

Crystalline boron oxide nanowires on silicon substrate

Qing Yang^a, Jian Sha^b, Lei Wang^a, Yu Zou^a, Junjie Niu^a,
Can Cui^a, Deren Yang^{a,*}

*State Key Laboratory of Silicon Materials, Zhejiang University, 20 Yu Gu Road, Hangzhou 310027, People's Republic of China

^bDepartment of Physics, Zhejiang University, 20 Yu Gu Road, Hangzhou 310027, People's Republic of China

Received 26 November 2004; accepted 20 December 2004

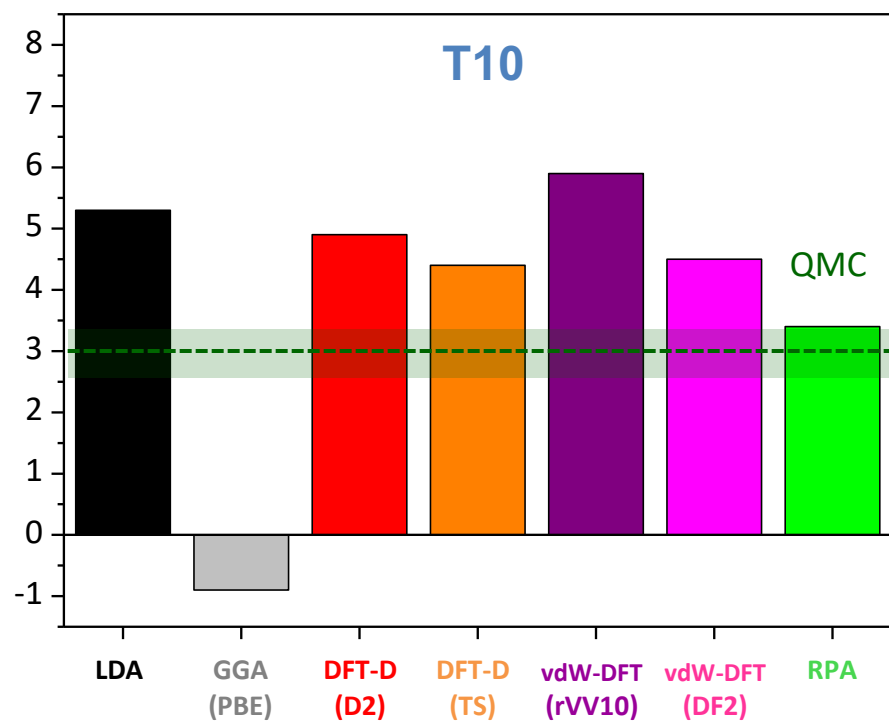
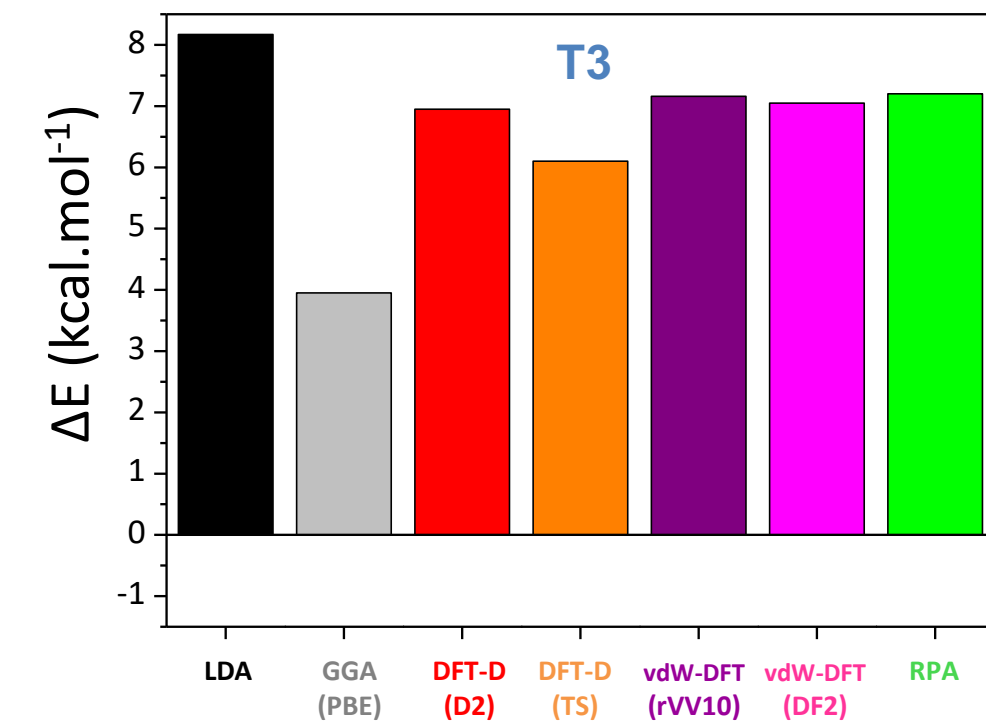
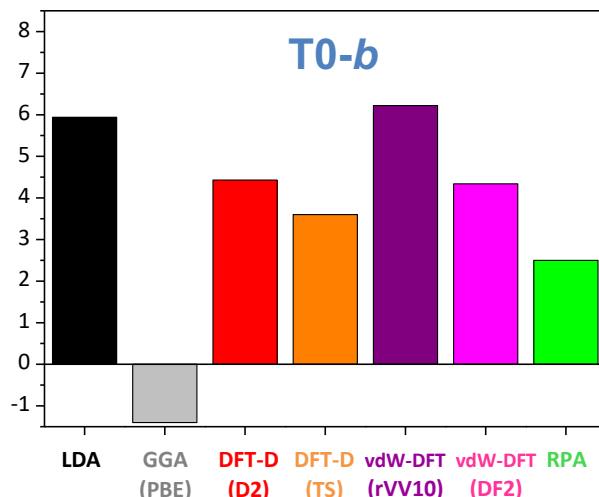
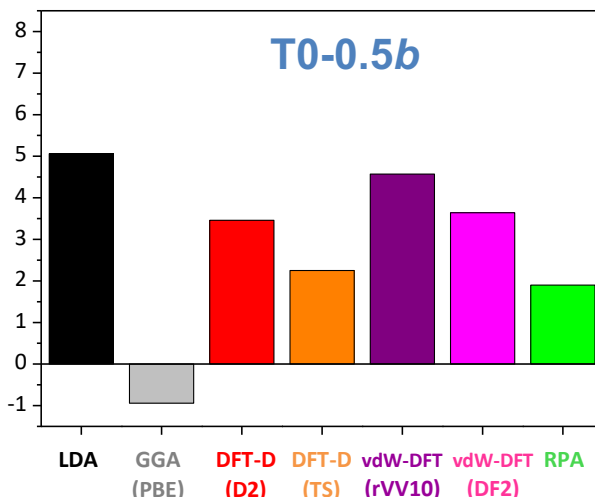
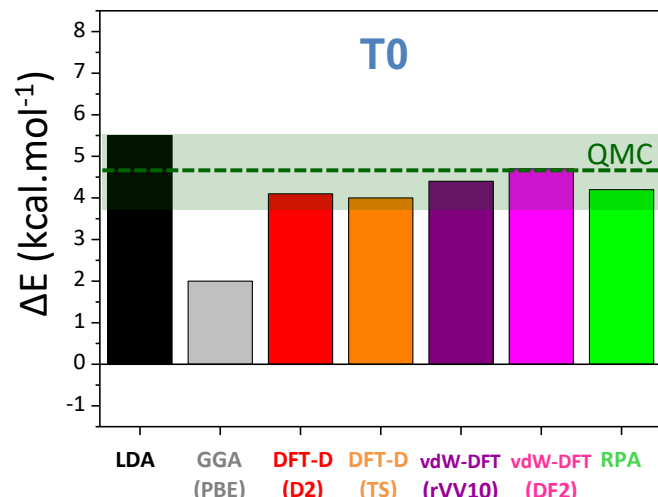
Abstract

Crystalline boron oxide nanowires have been synthesized on silicon substrates by chemical vapor deposition (CVD) process without the use of catalysts or templates. It is pointed out that the boron oxide nanowires are cubic and single crystalline, and the diameter of the nanowires is in the range of 20–80 nm. Some of the nanowires branched, and the diameters of the branches and stems of the branched boron oxide nanowires are in the range of 20–80 and 100–200 nm, respectively. The crystallinity, morphology, and structure features of the as-prepared boron oxide nanowires were investigated by field emission scanning electron microscopy, X-ray diffraction, transmission electron microscopy, and selected area electron diffraction. Furthermore, Raman spectrum and Fourier transform infrared spectroscopy of the nanowires were also investigated.

✓ cubic phase? That originally seen in J. Am. Ceram. Soc., **18**, 55 (1935)?

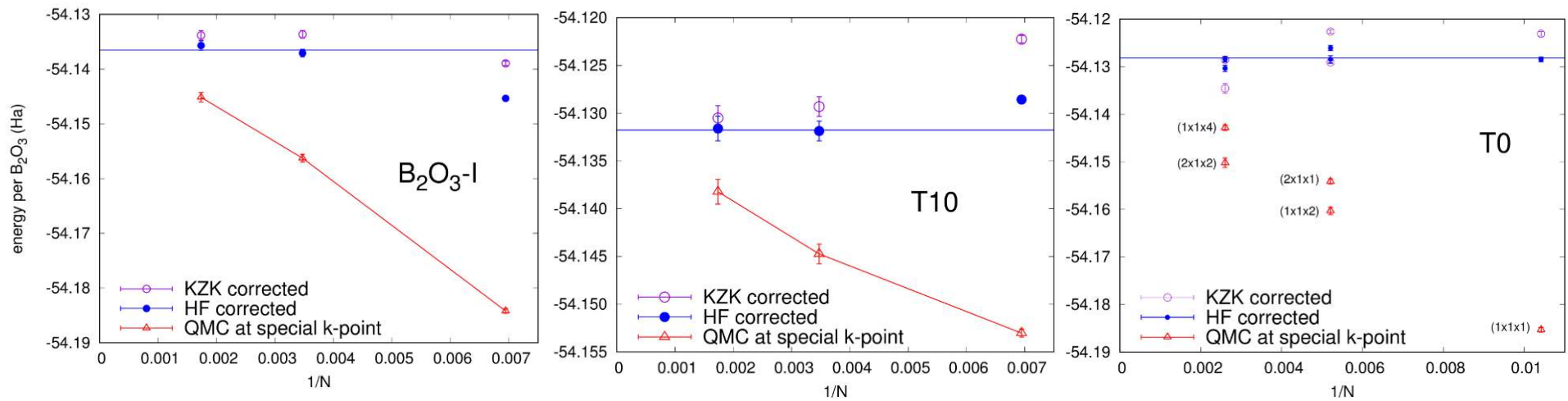
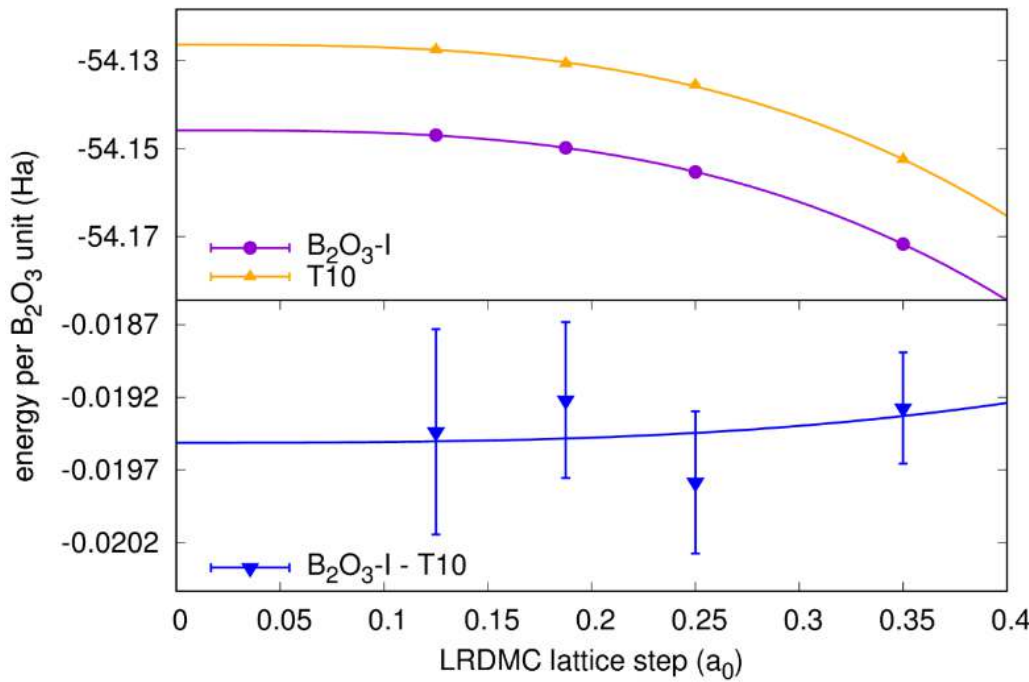
$\rho = 1.805 \text{ g.cm}^{-3}$

Benchmarking DFT: energy

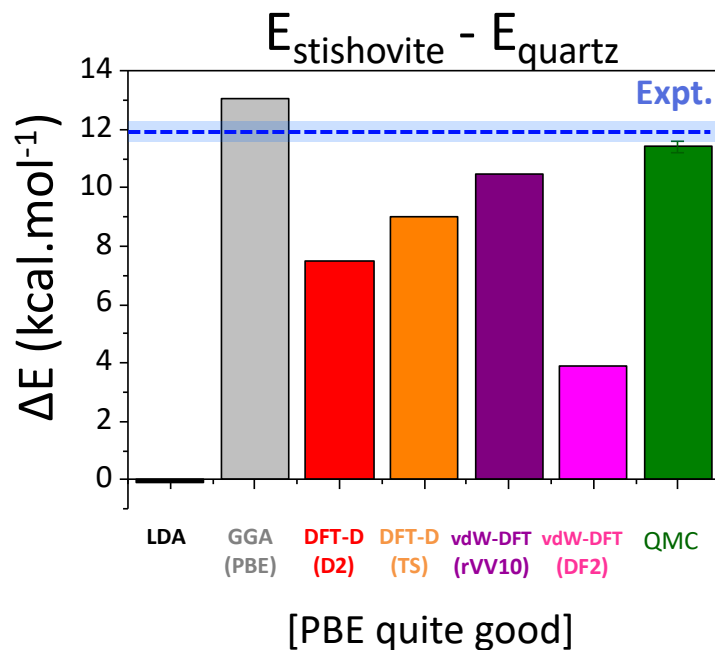
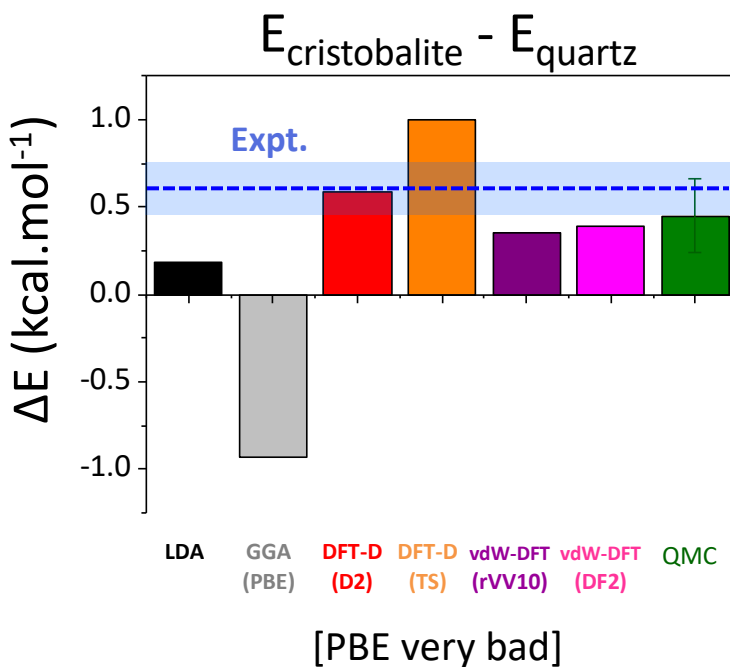
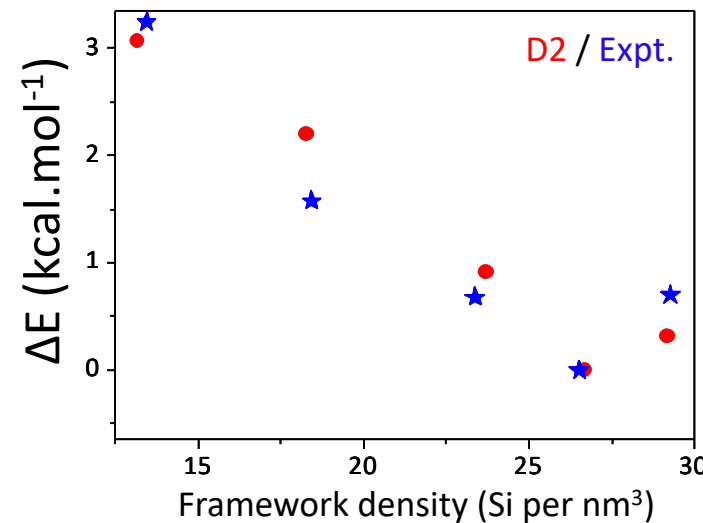
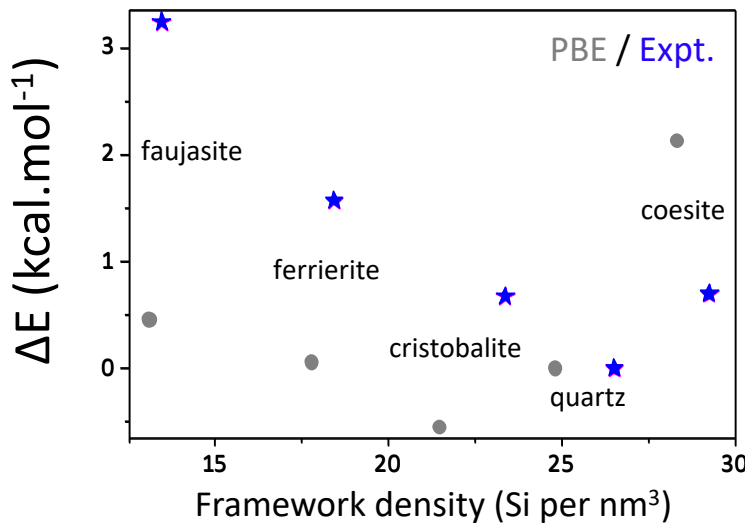


| | LDA | PBE | HSE06 | PBE+D2 | PBE+TS | rVV10 | DF2 | RPA | QMC |
|-----------------|-----|------|-------|--------|--------|-------|-----|-----|---------------|
| T0 | 5.5 | 2.0 | 2.1 | 4.1 | 4.0 | 4.5 | 4.7 | 4.2 | 4.7 ± 0.9 |
| T0-0.5 <i>b</i> | 5.1 | -0.9 | -1.4 | 3.5 | 2.2 | 4.6 | 3.6 | 1.9 | |
| T0- <i>b</i> | 5.9 | -1.4 | | 4.4 | 3.6 | 6.2 | 4.3 | 2.5 | |
| T3 | 8.2 | 3.9 | | 7.0 | 6.1 | 7.2 | 7.0 | 7.2 | |
| T10 | 5.3 | -0.9 | -0.9 | 4.9 | 4.4 | 5.9 | 4.5 | 3.4 | 3.0 ± 0.4 |

| | LDA | PBE | PBE+D2 | PBE+TS | DF2 | DF-cx | RPA | QMC |
|-----------------|-----|------|--------|--------|-----|-------|-----|---------------|
| T0 | 5.5 | 2.0 | 4.1 | 4.0 | 4.7 | 4.6 | 4.2 | 4.7 ± 0.9 |
| T0-0.5 <i>b</i> | 5.1 | -0.9 | 3.5 | 2.2 | 3.7 | 3.5 | 1.9 | - |
| T0- <i>b</i> | 5.9 | -1.4 | 4.4 | 3.6 | 4.3 | 4.4 | 2.5 | - |
| T3 | 8.2 | 3.9 | 7.0 | 6.1 | 7.0 | 6.9 | 7.2 | - |
| T10 | 5.3 | -0.9 | 4.9 | 4.4 | 4.5 | 4.9 | 3.4 | 3.0 ± 0.4 |

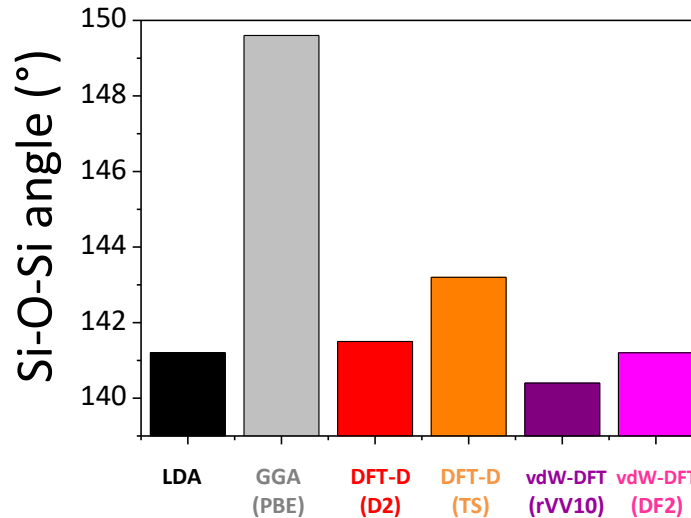
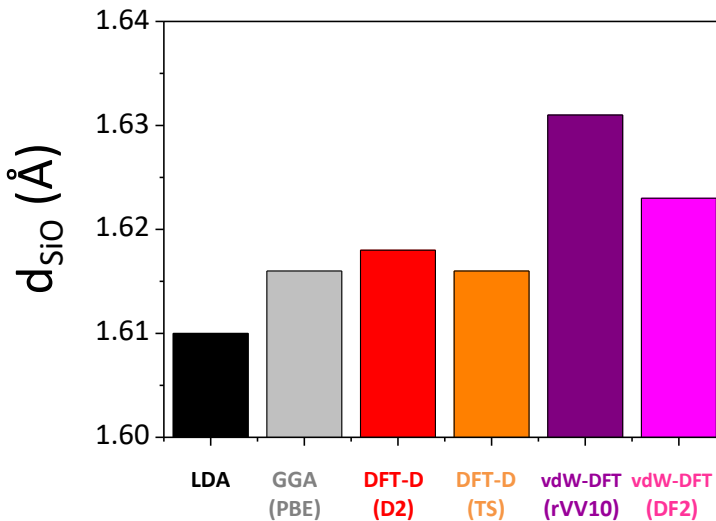


Energy of SiO_2 polymorphs

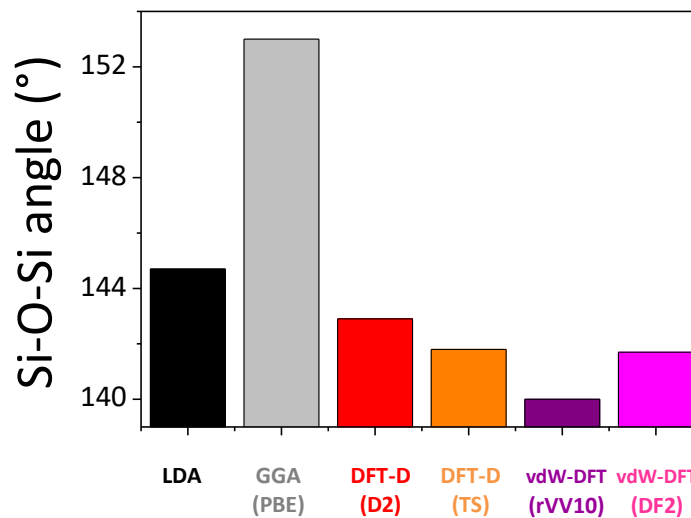
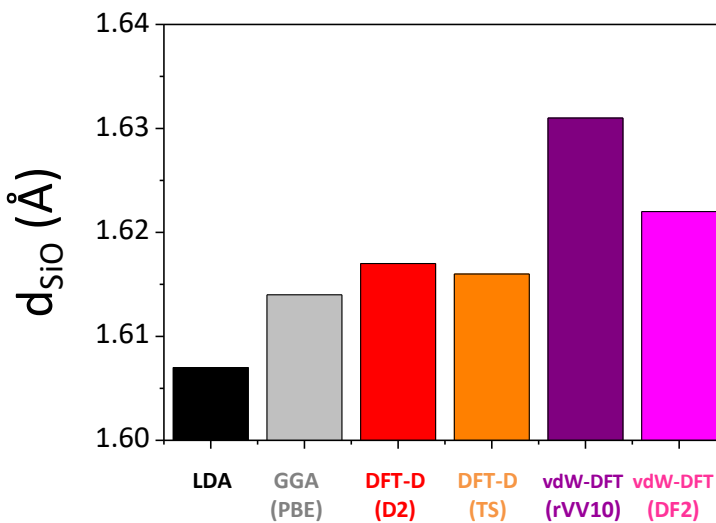


Structure of SiO₂ polymorphs

quartz



cristobalite



DFT relaxation: details

General framework

- Density Functional Theory (DFT)
- Exchange-correlation: GGA (PBE)
- Pseudo-potentials (PP)

Aim: for each topology, we want to determine the lowest-energy minimum

- Preliminary *first-principles Molecular Dynamics* at 500 K (*Siesta* code):
DZP basis, Born-Oppenheimer, Trouiller-Martins PP, real-space grid 600 Ry
- **Relaxations (T = 0 K)** of positions and unit cell (*CASTEP* code):
PW basis set: 60 Ry, Ultra-soft PP, k -points grid $\leq 0.05 \text{ \AA}^{-1}$
- For some networks, several local minima were observed
(compressing/decompressing the obtained structures helped to found better geometries)

- Vibrational contribution: $E_{vib} = \sum_i \frac{\hbar\omega_i}{2}$ Zero-point energy

$$F_{vib} = k_B T \sum_i \ln \left[2 \sinh \left(\frac{\hbar\omega_i}{k_B T} \right) \right] \quad \text{Free-energy}$$

Vibrational contribution negligible at $T = 0 \text{ K}$ ($< 0.5 \text{ kcal/mol}$), small at $T \sim T_g$ ($\sim 1 \text{ kcal/mol}$)
→ contribution not included in the following

There is no crystallization anomaly !

Review:

Phys. Chem. Glasses: Eur. J. Glass Sci. Technol. B, April 2018, 59 (2), 65–87

The structural chemistry of B_2O_3

Adrian C. Wright*

J.J. Thomson Physical Laboratory, University of Reading, Whiteknights, Reading, RG6 6AF, UK

The structural chemistry of B_2O_3 has been the subject of considerable controversy in the literature, especially in the case of the vitreous phase. A brief review is presented as to the present state of knowledge concerning the structures of crystalline, liquid and vitreous B_2O_3 , and it is demonstrated that the key to the structural chemistry of B_2O_3 lies in understanding that of the liquid state, which is dominated by the equilibrium reaction between $B_3O_3\ddot{O}_3$ boroxol groups and independent $B\ddot{O}_3$ basic structural units (i.e. those not in boroxol groups): $B_3O_3\ddot{O}_3 \rightleftharpoons 3B\ddot{O}_3$. The failure of the low pressure polymorph, B_2O_3 -I, to form, either by crystallisation from the supercooled liquid at ambient pressure, or on devitrification of vitreous B_2O_3 , is due to the high activation energy involved both in the break-up of boroxol groups and as a result of the large difference in number density between the crystal and supercooled liquid/glass. SAXS studies of vitreous and supercooled liquid B_2O_3 by V. V. Golubkov indicate that, in addition to the scattering due to thermal density fluctuations, there is extra small-Q scattering, centred at $Q=0$, arising from regions of inhomogeneity $\sim 15 \text{ \AA}$ in size. These disappear for B_2O_3 equilibrated at temperatures below 240°C , and are interpreted as being linked with the above equilibrium reaction. The fact that the time scale for establishing the equilibrium boroxol fraction, x_B , in the supercooled liquid state is very much longer than that associated with the thermal density fluctuations means that the structural rearrangements during quenching to the vitreous state are more complex than for SiO_2 , thus explaining the wide range of glass transition temperatures, T_g , and number densities, ρ° , reported in the literature for vitreous B_2O_3 . Golubkov's SAXS data also mitigate against a two-phase nanoheterogeneous structure for vitreous B_2O_3 , based on nanodomains rich in either boroxol groups or independent $B\ddot{O}_3$ triangles. Contrary to conventional wisdom, it is indeed possible to crystallise B_2O_3 from the supercooled liquid just above T_g . However, this takes considerable time, and the resulting long forgotten polymorph is not B_2O_3 -I, but one that has an average number density within the range of that exhibited by the glass, and which almost certainly has a structure that includes boroxol groups.

There is no crystallization anomaly !

Review:

The structural chemistry of B_2O_3

Adrian C. Wright*

J.J. Thomson Physical Laboratory, University of Reading, Whiteknights, Reading, RG6 6AF, UK

✓ S. S. Cole, N. W. Taylor, J. Am. Ceram. Soc., **18**, 55 (1935)

$$\rho = 1.805 \text{ g.cm}^{-3}$$

crystal structure analysis. Even if their x-ray analysis is incorrect, the fact remains that they succeeded in preparing a crystalline B_2O_3 polymorph with an average number density within the range exhibited by vitreous B_2O_3 .

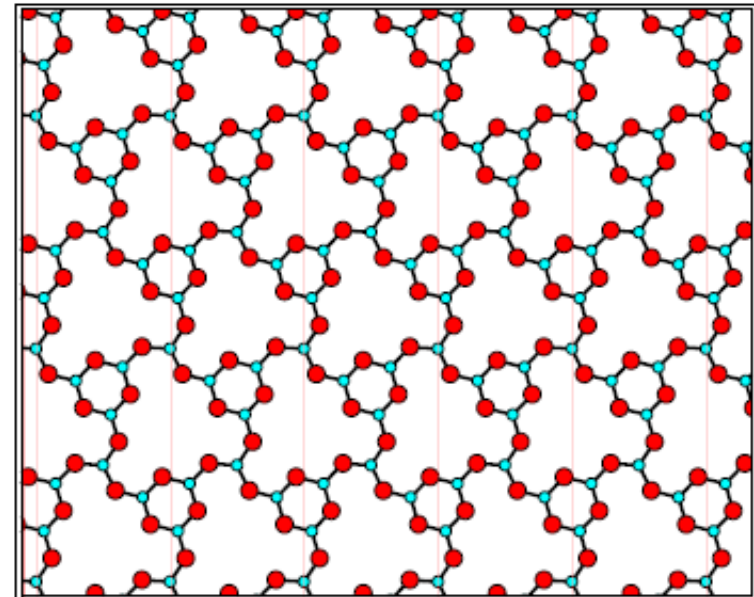
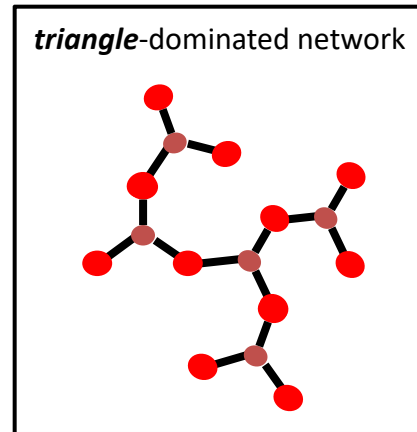
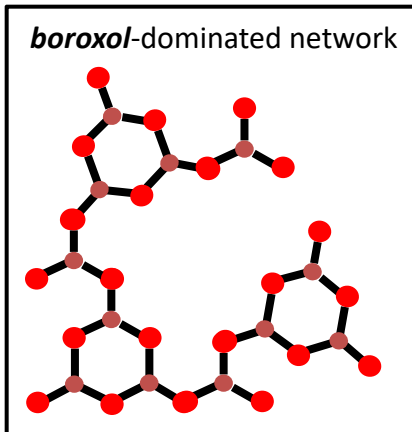


Figure 17. A two-dimensional crystalline layer formed from alternate boroxol groups and independent BO_3 triangles (Key as Figure 2) [Colour available online]

Medium-range order in v-B₂O₃

The *boroxol dispute* (30s to 2008)



Fraction of (boron atoms in) boroxol rings:

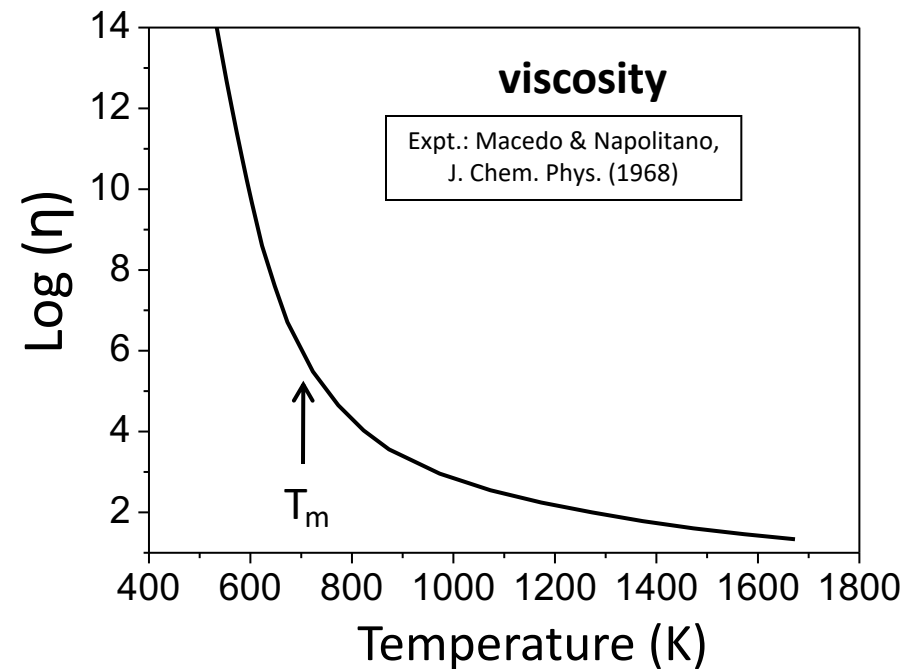
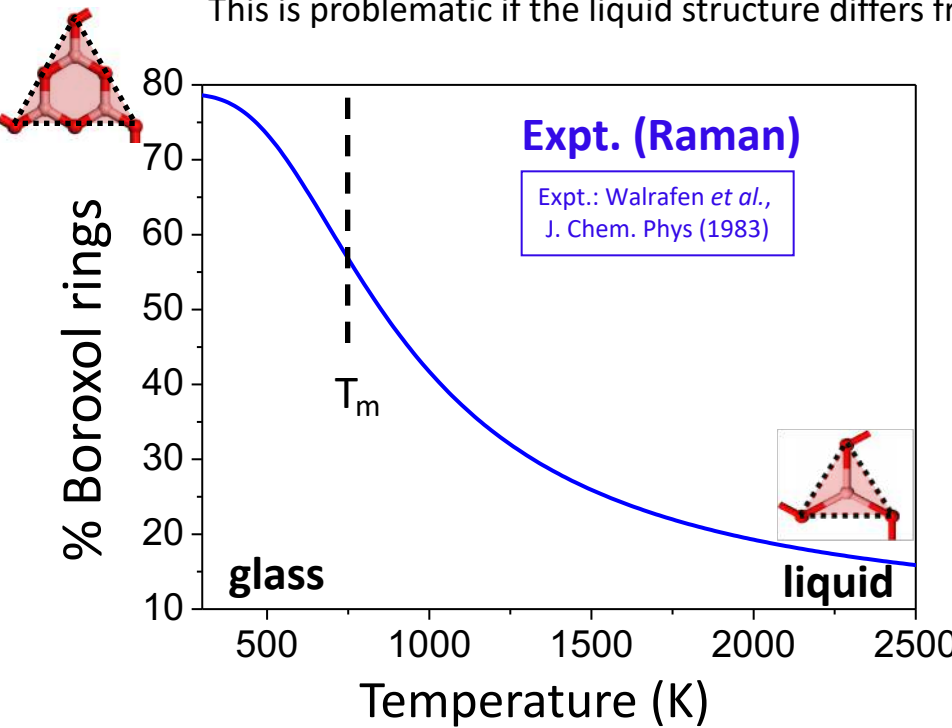
Some XRD/ND interpretations: 60-85 %
Raman: 64-79 %
NMR, NQR: ~ 75-85 %
INS: ~ 75 %
Statistical model: ~ 80 %

Some XRD/ND (or IR) interpretations: 0 %
RMC (XRD, ND): < 30 %
MD (2-body potentials): 0 %
MD (3-, 4-body or polarisable): < 30 %
FPMD (from quenched melts): 9 - 22%

Glass \leftrightarrow liquid B_2O_3

MD simulations: a timescale problem

(Brute-force) MD simulations produce glasses from liquid at a much **too fast** quenching rate ($> 10^{11}$ K/s). This is problematic if the liquid structure differs from that of the glass (B_2O_3 !).



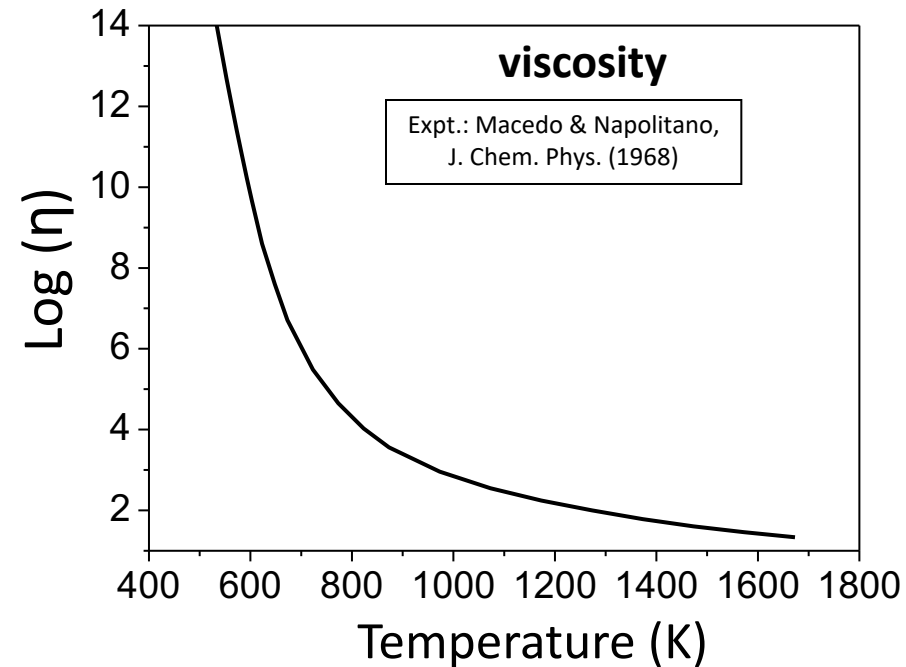
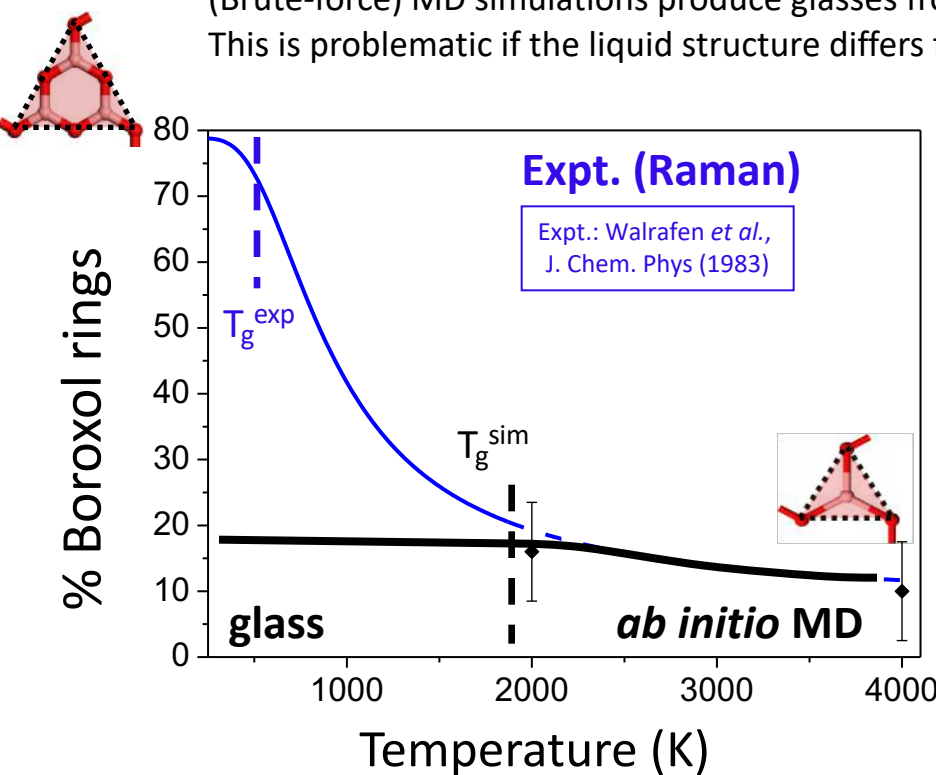
- ✓ Structural changes occur for $T < 1500$ K (concomitant with huge viscosity increase)
 - + small *driving force* (stabilisation energy of boroxol ring: $\Delta E \approx -4$ kcal/mol)

Numerically, these structural changes are extremely **challenging** to reproduce (dynamics much too slow given the available simulation time)

Glass \longleftrightarrow liquid B_2O_3

MD simulations: a timescale problem

(Brute-force) MD simulations produce glasses from liquid at a much **too fast** quenching rate ($> 10^{11}$ K/s). This is problematic if the liquid structure differs from that of the glass (B_2O_3 !).



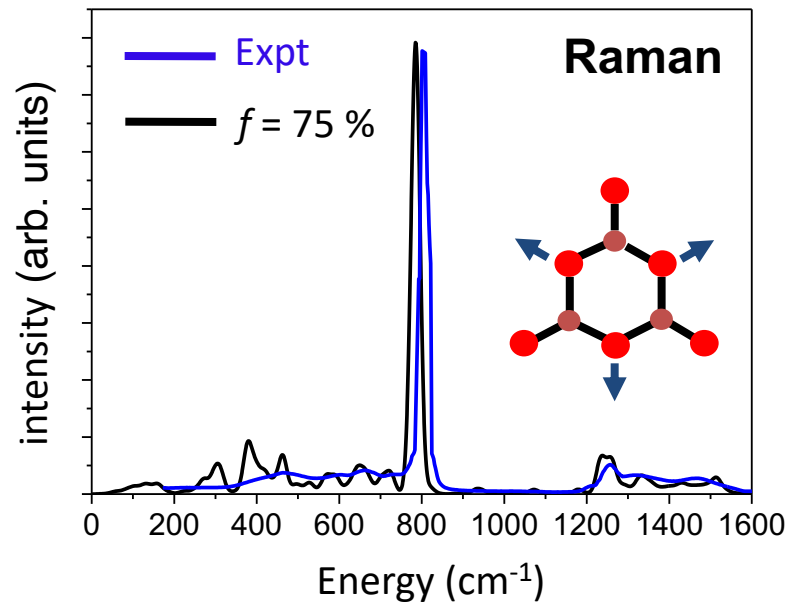
conventional numerical quench \rightarrow *Cannot follow the structural rearrangement*

Our previous works (summary)

G. Ferlat, T. Charpentier, A.P. Seitsonen, A. Takada, M. Lazzeri, L. Cormier, G. Calas, F. Mauri,
Phys. Rev. Lett., **101**, 065504 (2008)

From *first-principles* (DFT) calculations:

- liquid: dominated by triangles
- glass: dominated by boroxol rings ($\sim 65\text{--}75\%$)
- Reconciliation of numerical models with expts (diffraction, Raman, NMR)
- Previous underestimated values were due to methodological limitations (quenching rate)
- Confirmation of a **boroxol stabilisation energy**



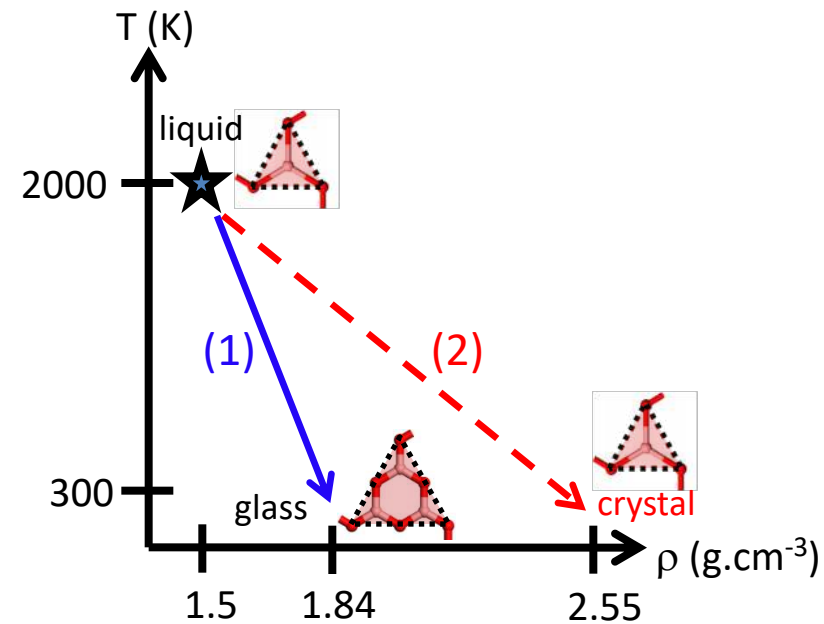
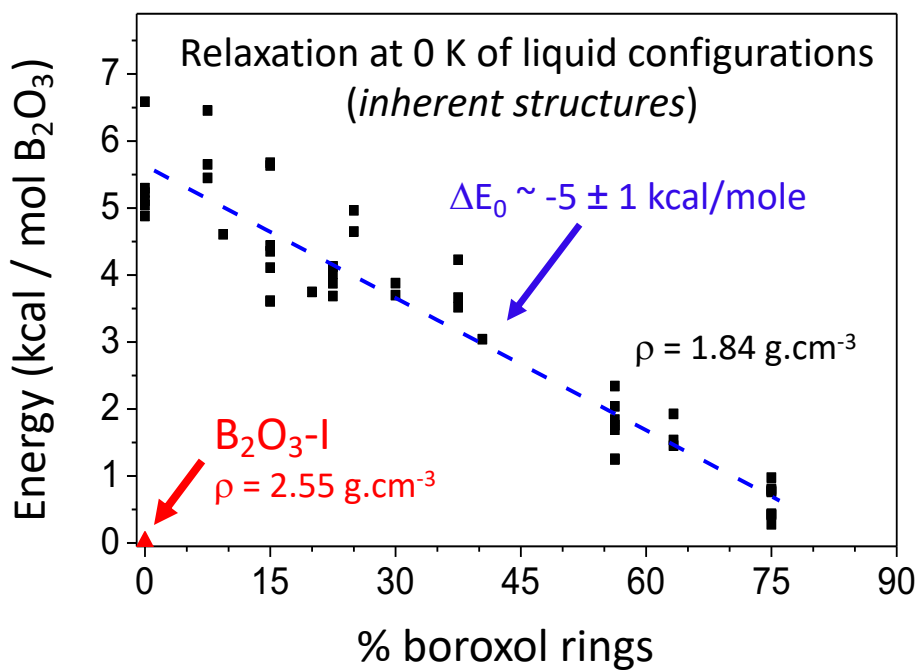
N.B. : the glass model was '*hand-made*' (by tweaking a Cs₂O-B₂O₃ crystal)

→ we still lack a (good) numerical model obtained from the liquid quench

Need for good (*many-body*) force-fields **and**
efficient sampling methods (*enhanced sampling*)

Our previous works (summary)

G. Ferlat, T. Charpentier, A.P. Seitsonen, A. Takada, M. Lazzeri, L. Cormier, G. Calas, F. Mauri,
Phys. Rev. Lett., **101**, 065504 (2008)



- ✓ Why does the liquid always follow path (1) (vitrification) rather than path (2) (crystallisation)?
- Crystallisation anomaly:** crystallisation from the liquid is **never** observed unless pressure is applied.

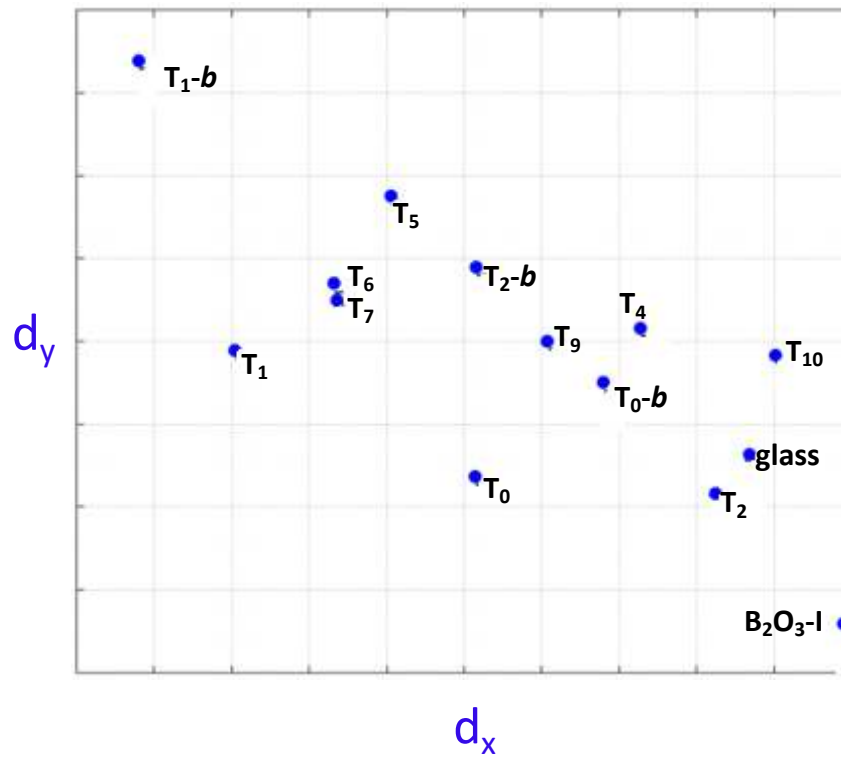
Work in progress: PIV metric

Using polarisable force-fields (previously calibrated from AIMD and tested against structural experiments)

O. Alderman et al., J. Phys.: Condens. Matter (2015)

A. Zeidler et al. Phys. Rev. B (2014)

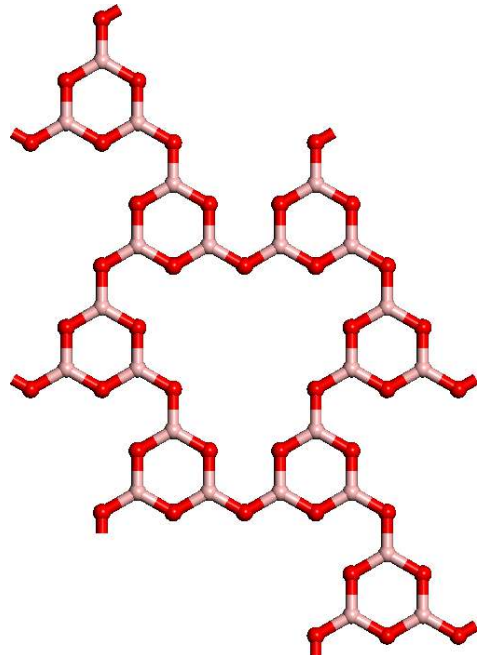
Map of topological distances using the PIV metric



✓ The PIV metric distinguishes B_2O_3 phases

B_2O_3 layers in borates

- ✓ The layers from our *graphite-like* B_2O_3 polymorphs are found in synthetised borates



T0-*b*

Motif: boroxol ($f = 100\%$)

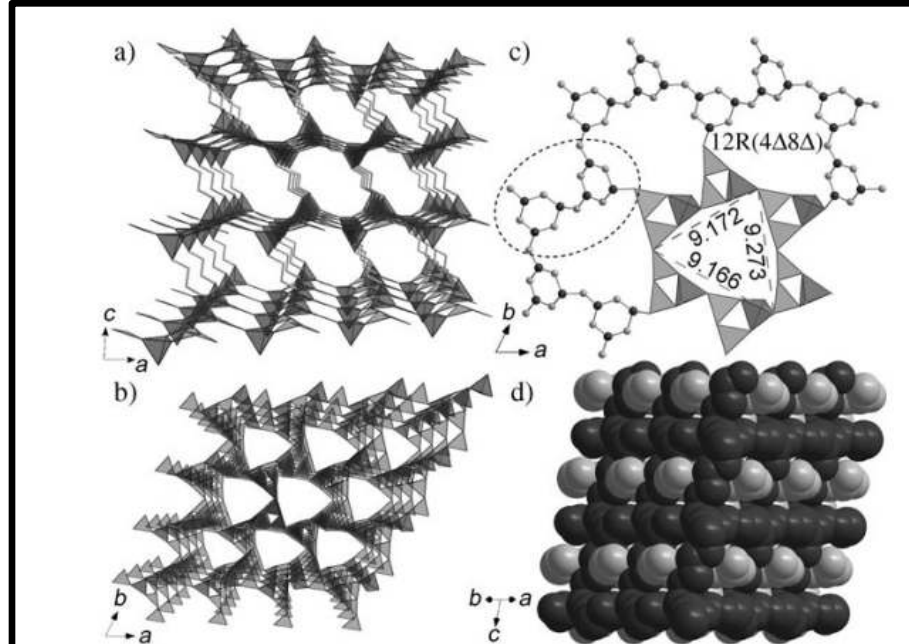


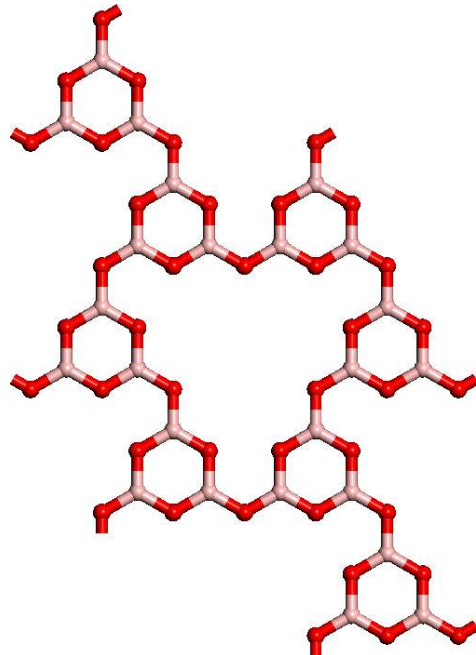
Figure 1. 3D open frameworks of **1** along the *b* (a) and *c* (b) directions, 2D layer of 3,12-membered rings with the dashed circle showing the FBB (c), and the twofold interpenetrating crystal structure (d).

The B_2O_3 layer in $B_6O_9(en)$ ($en =$ ethylenediamine)

Wang *et al.*, Angew. Chem. Int. Ed. **46**, 3909 (2007)

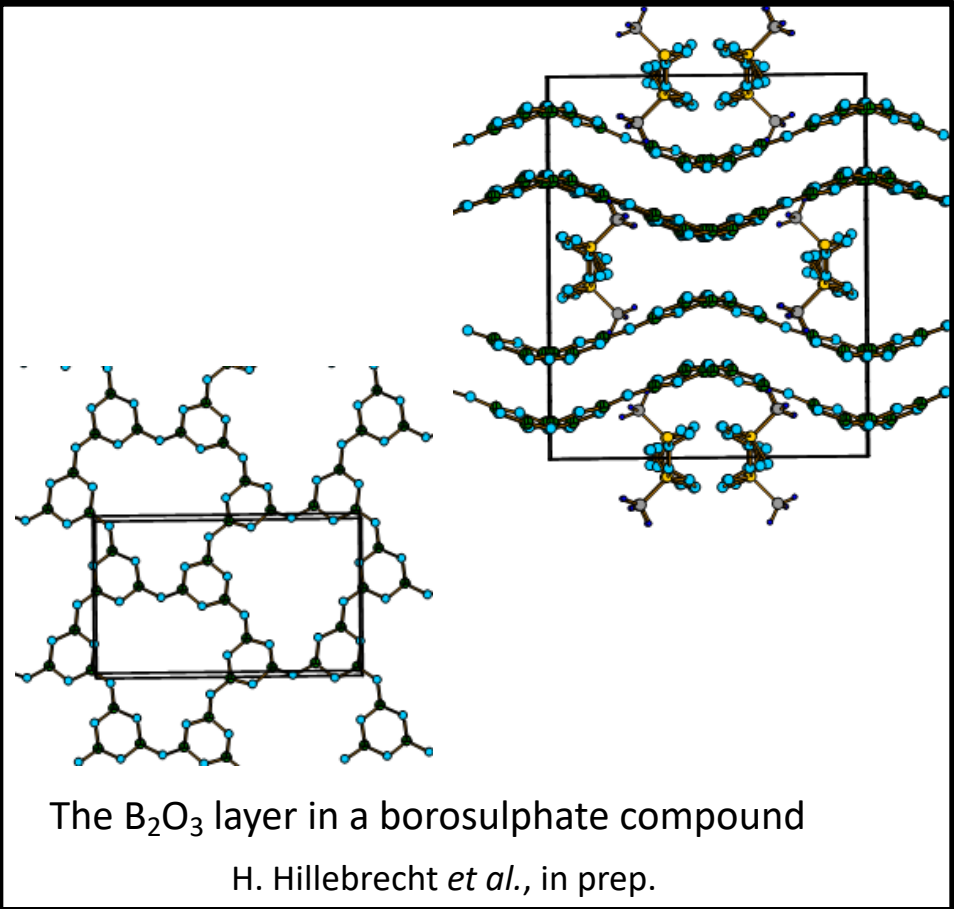
B₂O₃ layers in borates

- ✓ The layers from our *graphite-like* B₂O₃ polymorphs are found in synthetised borates



T0-*b*

Motif: boroxol ($f = 100\%$)



The B₂O₃ layer in a borosulphate compound

H. Hillebrecht *et al.*, in prep.

Other experimental routes ?

- Chemical Vapor Deposition techniques:
MOCVD, Atomic Layer Deposition (ALD), ...



Available online at www.sciencedirect.com
SCIENCE @ DIRECT®
Physica E 27 (2005) 319–324
www.elsevier.com/locate/physce



Crystalline boron oxide nanowires on silicon substrate

Qing Yang^a, Jian Sha^b, Lei Wang^a, Yu Zou^a, Junjie Niu^a,
Can Cui^a, Deren Yang^{a,*}

^aState Key Laboratory of Silicon Materials, Zhejiang University, 20 Yu Gu Road, Hangzhou 310027, People's Republic of China

^bDepartment of Physics, Zhejiang University, 20 Yu Gu Road, Hangzhou 310027, People's Republic of China

Received 26 November 2004; accepted 20 December 2004

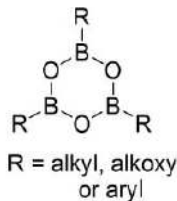
Abstract

Crystalline boron oxide nanowires have been synthesized on silicon substrates by chemical vapor deposition (CVD) process without the use of catalysts or templates. It is pointed out that the boron oxide nanowires are cubic and single crystalline, and the diameter of the nanowires is in the range of 20–80 nm. Some of the nanowires branched, and the diameters of the branches and stems of the branched boron oxide nanowires are in the range of 20–80 and 100–200 nm, respectively. The crystallinity, morphology, and structure features of the as-prepared boron oxide nanowires were investigated by field emission scanning electron microscopy, X-ray diffraction, transmission electron microscopy, and selected area electron diffraction. Furthermore, Raman spectrum and Fourier transform infrared spectroscopy of the nanowires were also investigated.

✓ cubic phase? That originally seen
in J. Am. Ceram. Soc., **18**, 55 (1935) ?

- Chemical synthesis using sol-gel techniques:

Starting from e.g. an alkyl (R)
substituted metaboric acid, $R_3B_3O_6$:



- Physical Vapor Deposition techniques:
Magnetron sputtering, IR irradiation, ...



Available online at www.sciencedirect.com
ScienceDirect
Thin Solid Films 515 (2007) 8723–8727
www.elsevier.com/locate/tsf



Analysis of magnetron sputtered boron oxide films

Dalibor Buc^a, Igor Bello^b, Maria Caplovicova^c, Milan Mikula^a, Jaroslav Kovac^a, Ivan Hotovy^a,
Yat Min Chong^b, Guei Gu Siu^{b,*}

^a Slovak University of Technology in Bratislava, Slovak Republic

^b City University of Hong Kong, Kowloon, Hong Kong

^c Comenius University in Bratislava, Slovak Republic

Available online 5 April 2007

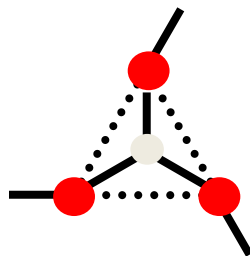
Abstract

Boron oxide films were grown on silicon substrates by radio-frequency (rf) unbalanced magnetron sputtering of a boron target in argon-oxygen gas mixtures with different compositions. Microscopic analyses show that overall boron oxide films are amorphous. The film prepared at oxygen/argon flow rate ratio >0.05 developed large crystallites of boric acid in localize areas of amorphous boron oxide matrices. These crystallites were unstable and at electron microscopic analysis they continuously transformed to a cubic B_2O_3 phase and then completely vanished leaving an underlying amorphous boron oxide film behind. The analyses indicate the coexistence of B_2O_3 , B_2O_5 crystallites and amorphous boron oxide matrices. Fourier transform infrared (FTIR) spectra revealed spectral bands of BOH, BO, BOB and BH groups. Nanohardness and elastic modulus of a film prepared at low oxygen concentration approach 30 and 300 GPa, respectively. These parameters however vary with deposition conditions.
© 2007 Elsevier B.V. All rights reserved.

- Physical synthesis at *negative pressure*
(Berthelot tubes)

Self-similarity

In a given structure:



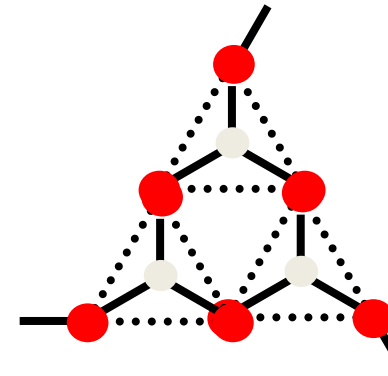
N atoms

length: L

volume: V

density: ρ

self-similar
↔
transformation



$N * 3$ atoms

$L * 2$

$V * 2^2$ (2D) or 2^3 (3D)

$\rho * 3/4$ (2D) or $3/8$ (3D)

$B_2O_3-I: \rho = 2.56 \text{ g.cm}^{-3}$

↔

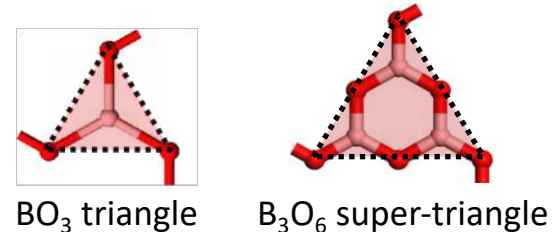
B_2O_3-I-b (3D unrelaxed) $\rho = 0.96 \text{ g.cm}^{-3}$

B_2O_3-I-b (relaxed) $\rho \sim 1.4 \text{ g.cm}^{-3}$

(potentially exhaustive) search

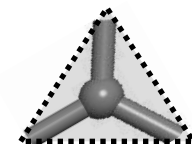
→ Using decoration of topological networks

- ✓ Relevant **building units** (for ambient polymorphs):



- ✓ Use of previously determined topological databases of **three-fold coordinated networks**

Winkler *et al.* (CPL, 2001): from **graph theory**, prediction of all possible **three-coordinated 3D** frameworks with up to 6 atoms in the primitive cell:
12 networks (originally applied to *sp*²-carbon structures)



+ 2D network of graphite : **13 networks**

- ✓ **Decoration** of the networks vertices by the relevant **building units**:

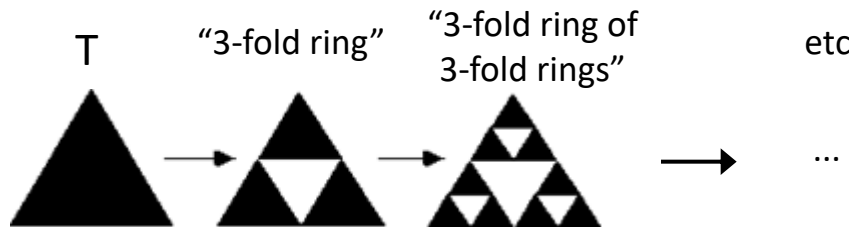


$2 * 13 - 1 = \mathbf{25}$ new B₂O₃ crystals
(with 10 to 135 atoms per unit cell)

- ✓ **Relaxation** (positions and unit cell) of the structures by ***first-principles*** calculations within Density Functional Theory (GGA-PBE, ultra-soft pseudos, PW basis, CASTEP code)

Some more predictions?

- Our search is not fully exhaustive since :
 - the number of nodes per unit cell is limited
 - 100 % of the nodes were decorated by a single type of decoration unit (triangle or boroxol). Mixtures (e.g. 50-50 %) could be considered.
 - Larger (self-similar) decoration units could be considered.

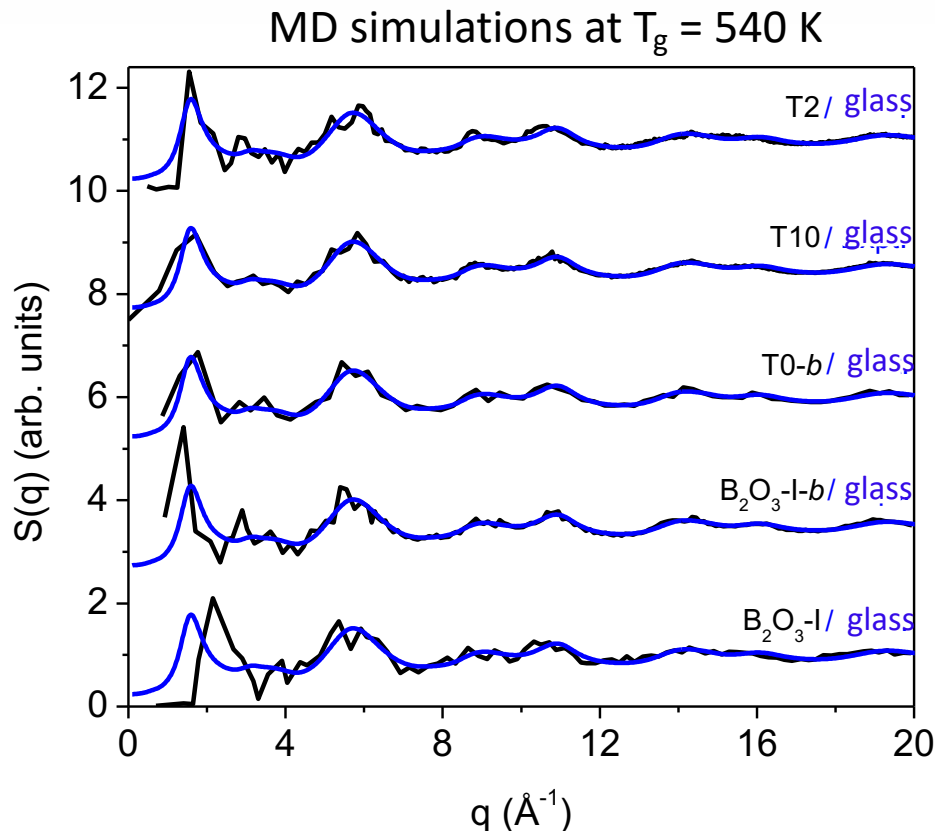


- Two additional predictions have since been published

F. Claeysens *et al.*, Adv. Funct. Mater., **23**, 5887 (2013)

- PCOD database : > 800 predicted B_2O_3 structures! (energies not determined)
<http://www.crystallography.net/pcod> (A. Le Bail, Univ. Le Mans, France)

New polymorphs versus glass: structure factors



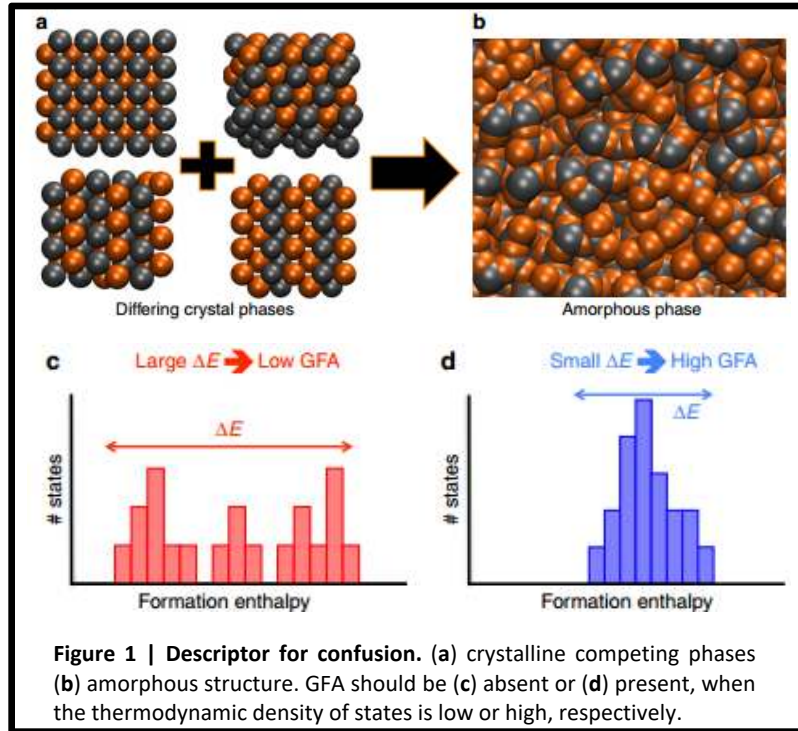
- ✓ Overall good match between the novel polymorphs' $S(q)$ and that of the glass. The novel crystals bear greater structural similarity with the glass than $\text{B}_2\text{O}_3\text{-I}$.

Glass expt. data: A. C. Hannon et al., JNCS 177 299 (1994)

Polymorphism and amorphisation

E. Perim *et al.*, Nat. Comm. 7, 12315 (2016)

"We postulate that the existence of **multiple phases with similar energies**, implying similar probabilities of being formed, but dissimilar structures, will lead to the formation of several distinct clusters, which will intimately compete and thus keep each other from reaching the critical size needed for crystallization."



Glass Forming Ability descriptor, evaluated by summing through structures i at fixed stoichiometry $\{x\}$

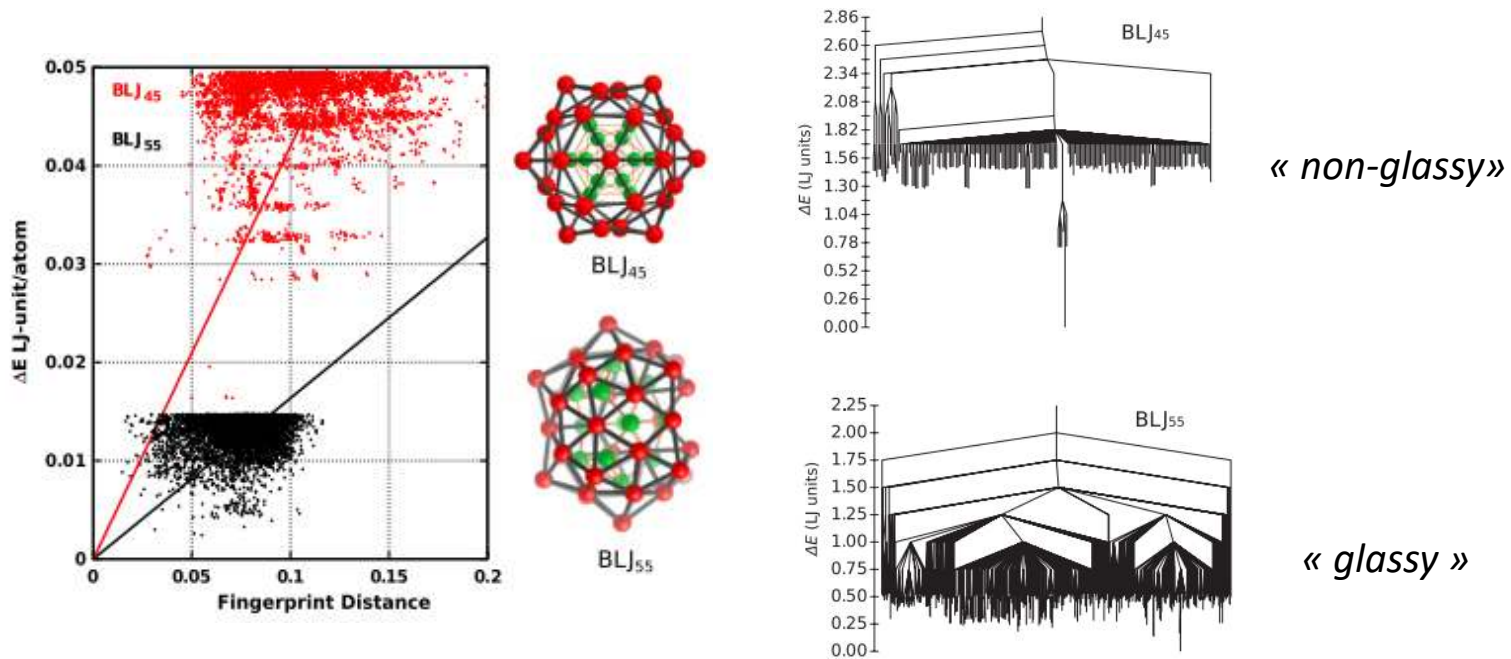
$$\chi_{GFA}(\{x\}) = \frac{\sum_i f(H_i)g(|\psi_i|)}{h(\{x\})}$$

Enthalpy proximity $f(H_i)$ = $\exp\left(-\frac{|H_i - H_0|}{k_B T_0}\right) \times$
 (to the ground state) $\begin{cases} 1, & H_i < 0 \\ e^{-H_i/k_B T_0}, & 0 \leq H_i < 50 \text{ meV} \\ 0, & 50 \text{ meV} \leq H_i \end{cases}$

Structure dissimilarity. To correlate properties of structures having different decorations of the underlying lattice, we use a lattice-free formalism, the expansion in local atomic environments (AEs)⁶⁴. ($g = 0$ for similar structures)

Polymorphism and energy landscape

S. De *et al.*, Phys. Rev. Lett. **112**, 083401 (2014)



« ... All the investigated clusters that were synthesized experimentally exhibit a nonglassy energy landscape. This suggests that a landscape of this type is a prerequisite for experimental synthesis. »

Common criteria for allotropes that have been experimentally isolated:

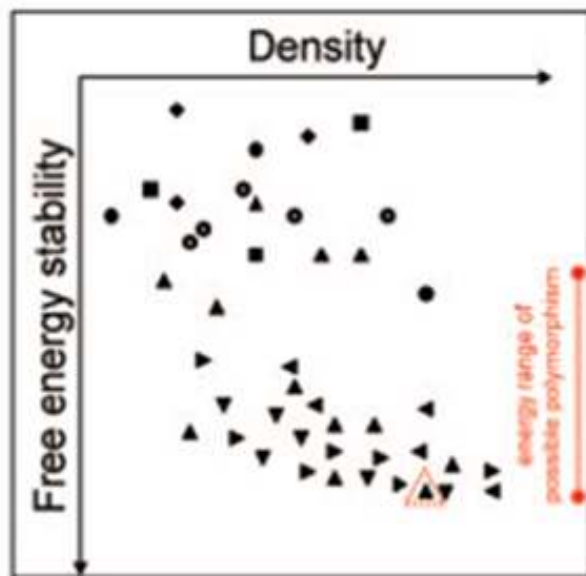
- occupy deep potential wells
- surrounding wells are higher in energy and/or « funneling » toward the stable form
- barriers to subsequent conversion are high

→ Structure lie at the apex of a disconnectivity graph, occupying a unique energetically isolated position

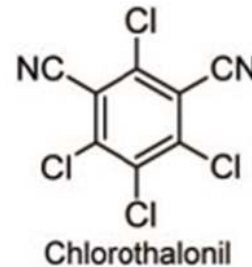
C. P. Ewels *et al.*, PNAS, **112**, 15609 (2015)

Polymorphism and ease of amorphization

Case (a): There are several polymorphs of similar energy



Examples (organic molecules):



from: S. L. Price, Accounts of Chem. Res. **42**, 117 (2009)

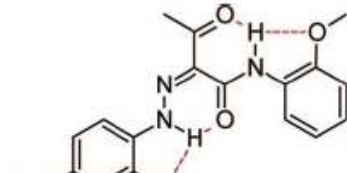
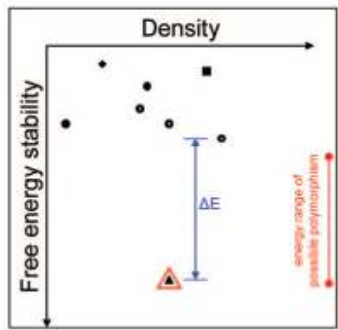
→ The system easily amorphizes (= hardly crystallizes a given polymorph)

This is typically the case for SiO₂, ...

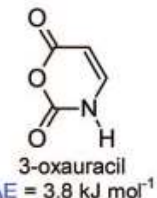
Polymorphism and the amorphisation

(a)

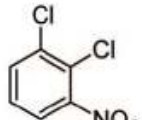
Monomorphic



$\Delta E > 12 \text{ kJ mol}^{-1}$



$\Delta E = 3.8 \text{ kJ mol}^{-1}$



$\Delta E = 1.8 \text{ kJ mol}^{-1}$

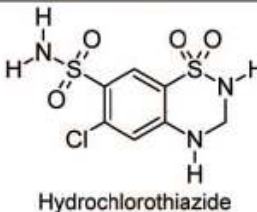
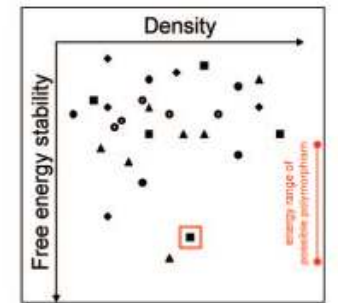
- (a) The lowest-energy polymorph is well separated from the others ($\Delta E \geq 10 \text{ kJ/mol} \sim 3 \text{ kcal/mol}$)

✓ monomorphic behaviour,
hard to vitrify (easy to crystallise)

This is typically the case for Si, Ge, ...

(b)

Predictive

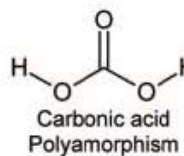
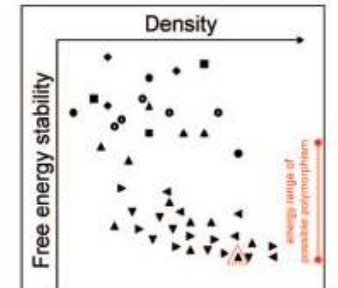


- (b) There is a small number of polymorphs (and they are structurally unrelated)

✓ these polymorphs may be observed

(c)

Tendency to disorder?



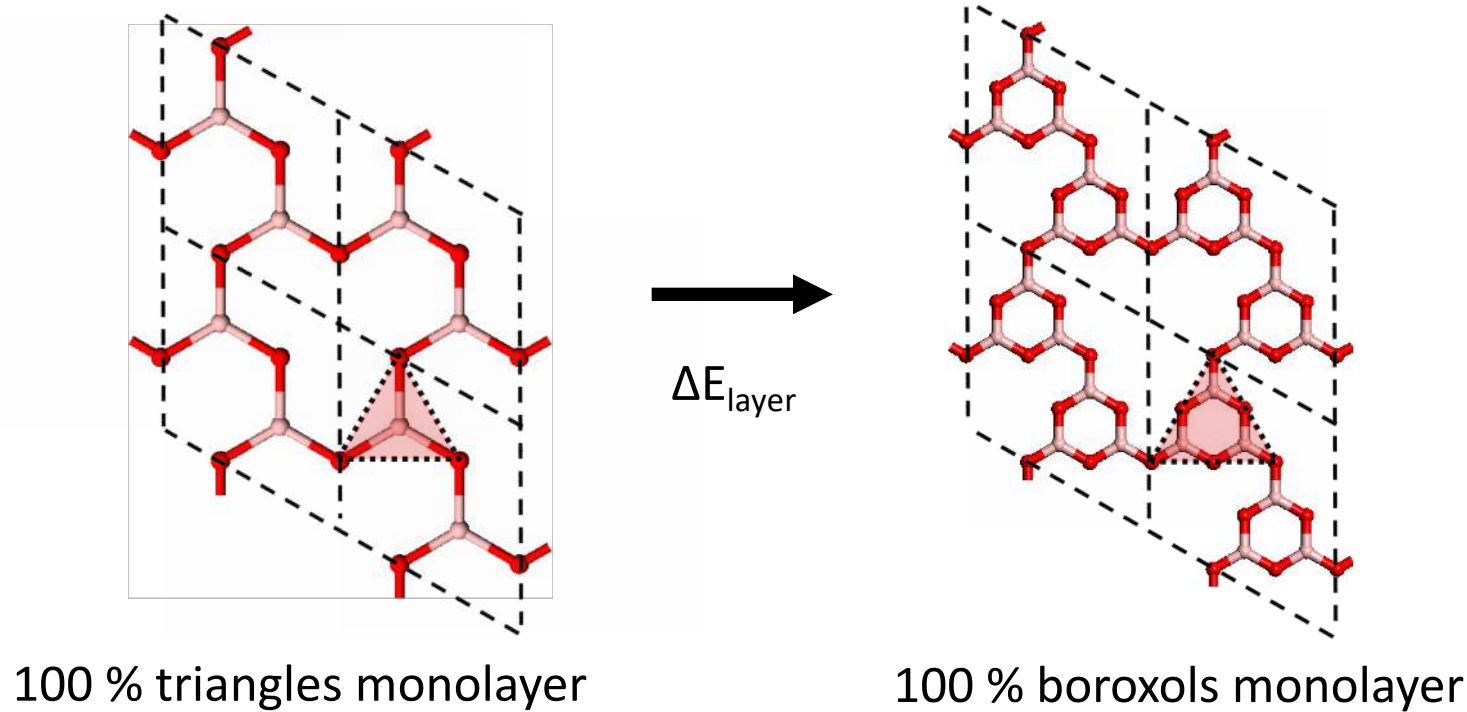
- (c) There are many polymorphs of similar energy

✓ easy to amorphise (hard to crystallise a given polymorph)

This is typically the case for SiO_2 , ...

Boroxol stabilisation energy

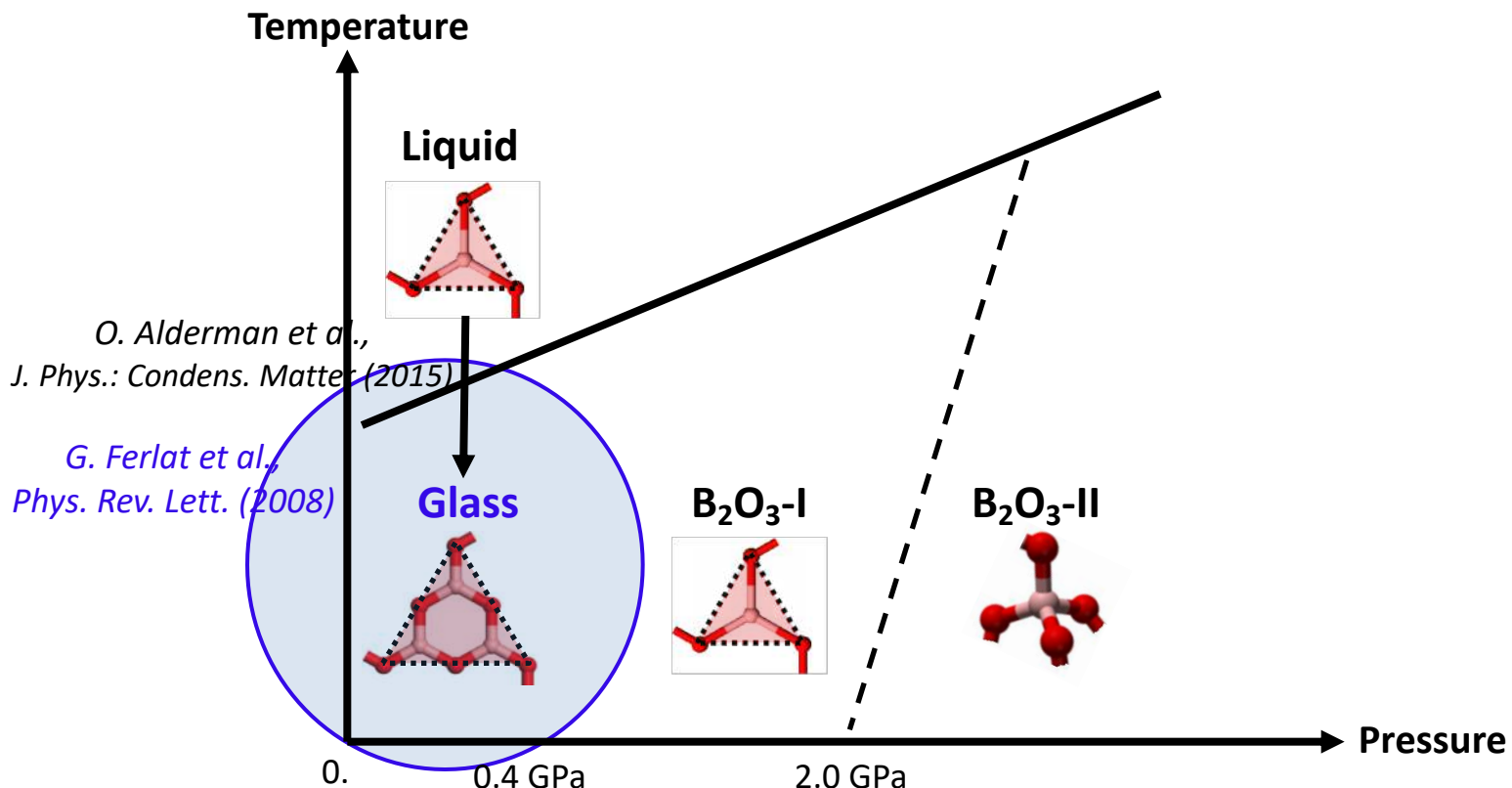
- « graphene » iso-structural layers



No relaxation (B-O-B angles = 120°): $\Delta E_{\text{Layer}} \sim -10.0 \text{ kcal / mole}$

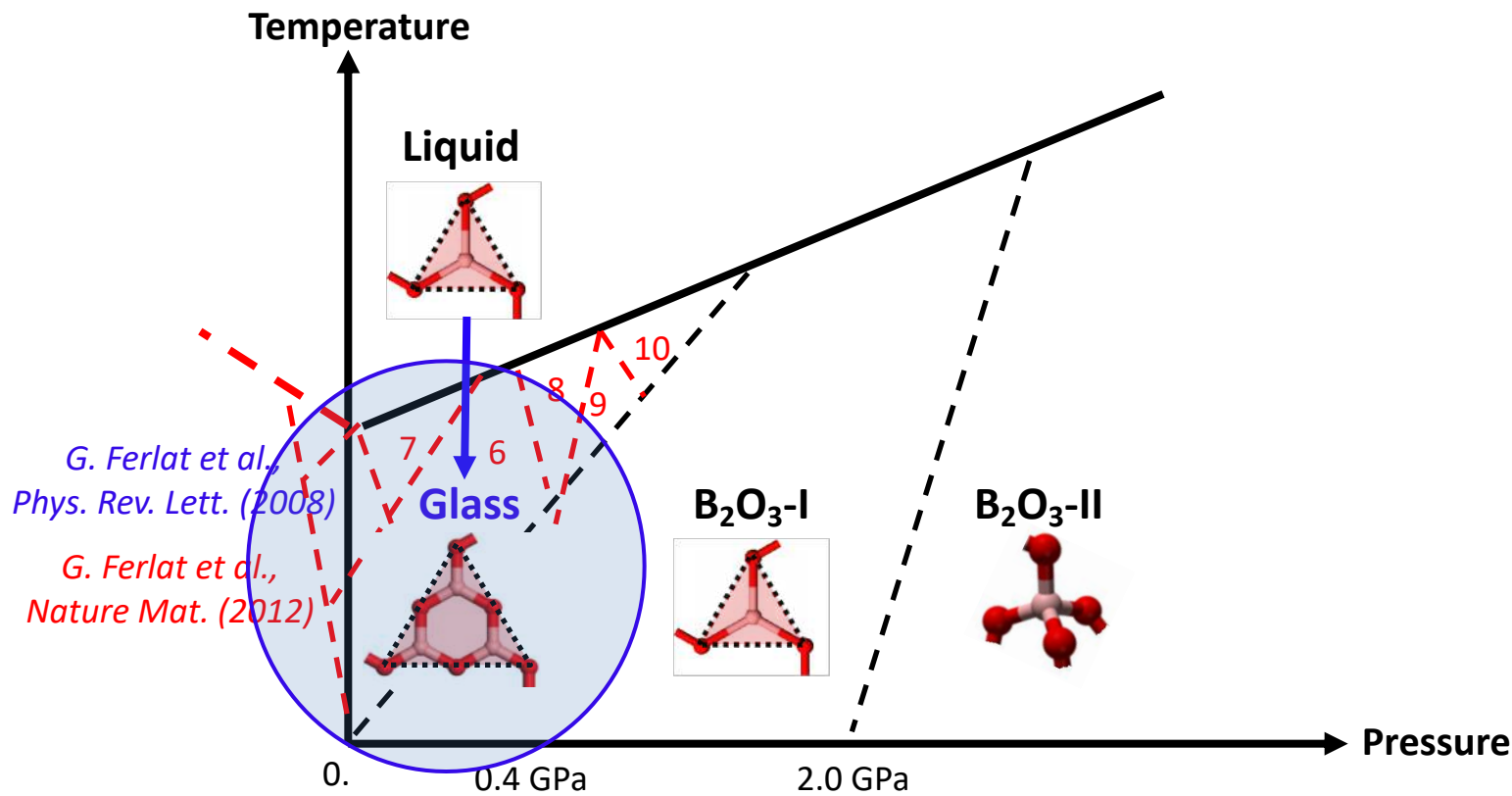
[After relaxation: $\Delta E_{\text{Layer}} \sim -1.0 \text{ kcal / mole}$]

Previous (MD) works: summary



✓ a **network-forming glass** with significant **medium-range order** (3-fold rings)

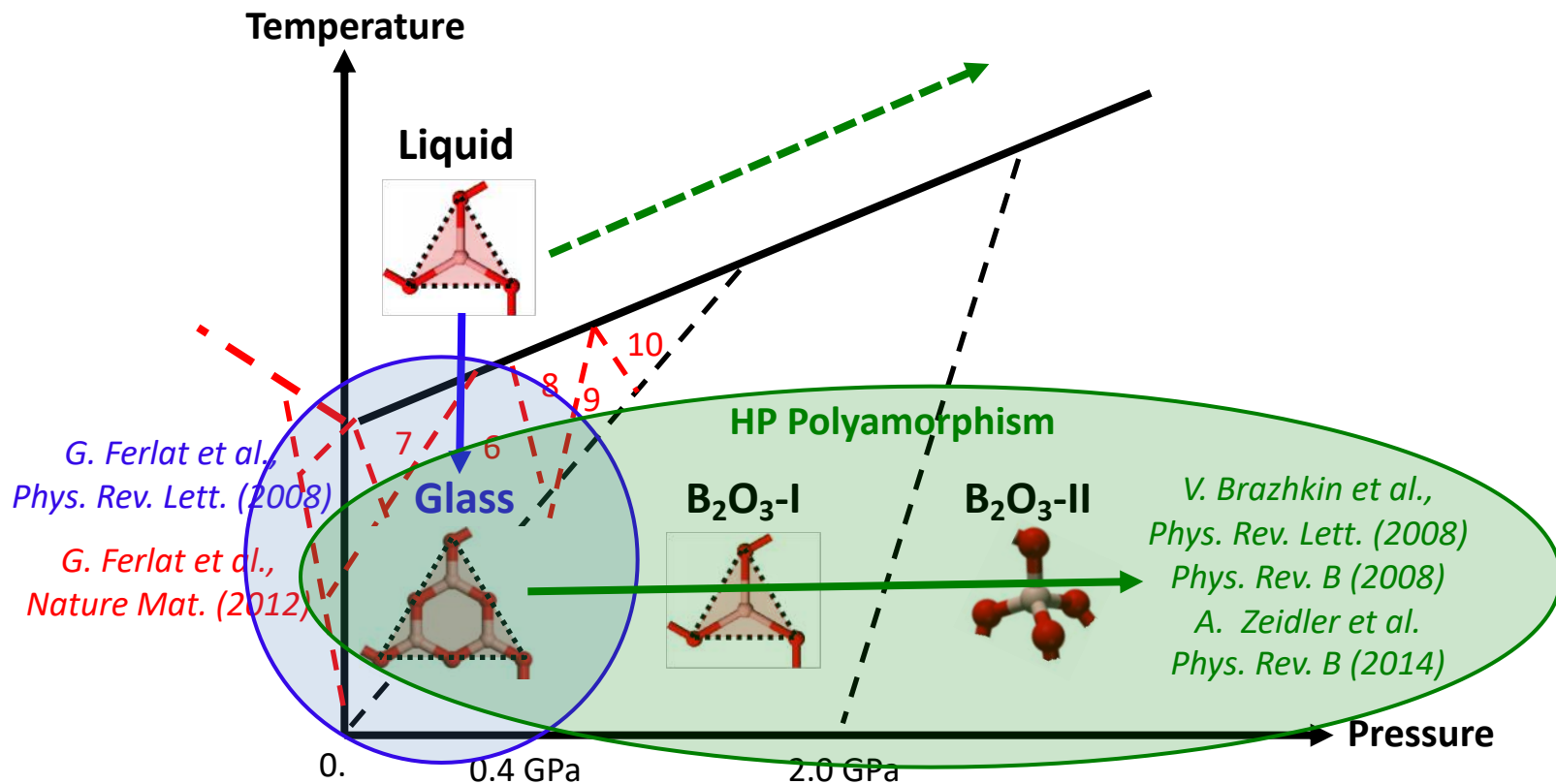
Previous (MD) works: summary



- ✓ a **network-forming glass** with significant **medium-range order** (3-fold rings)
- ✓ many (**new**) polymorphs structurally similar to the glass

Rings in network glasses: the B_2O_3 case. G. Ferlat. Chapter 14 in "Frontiers and challenges in molecular dynamics simulations of structurally disordered materials: from network glasses to phase change memory alloys", Springer (2015).

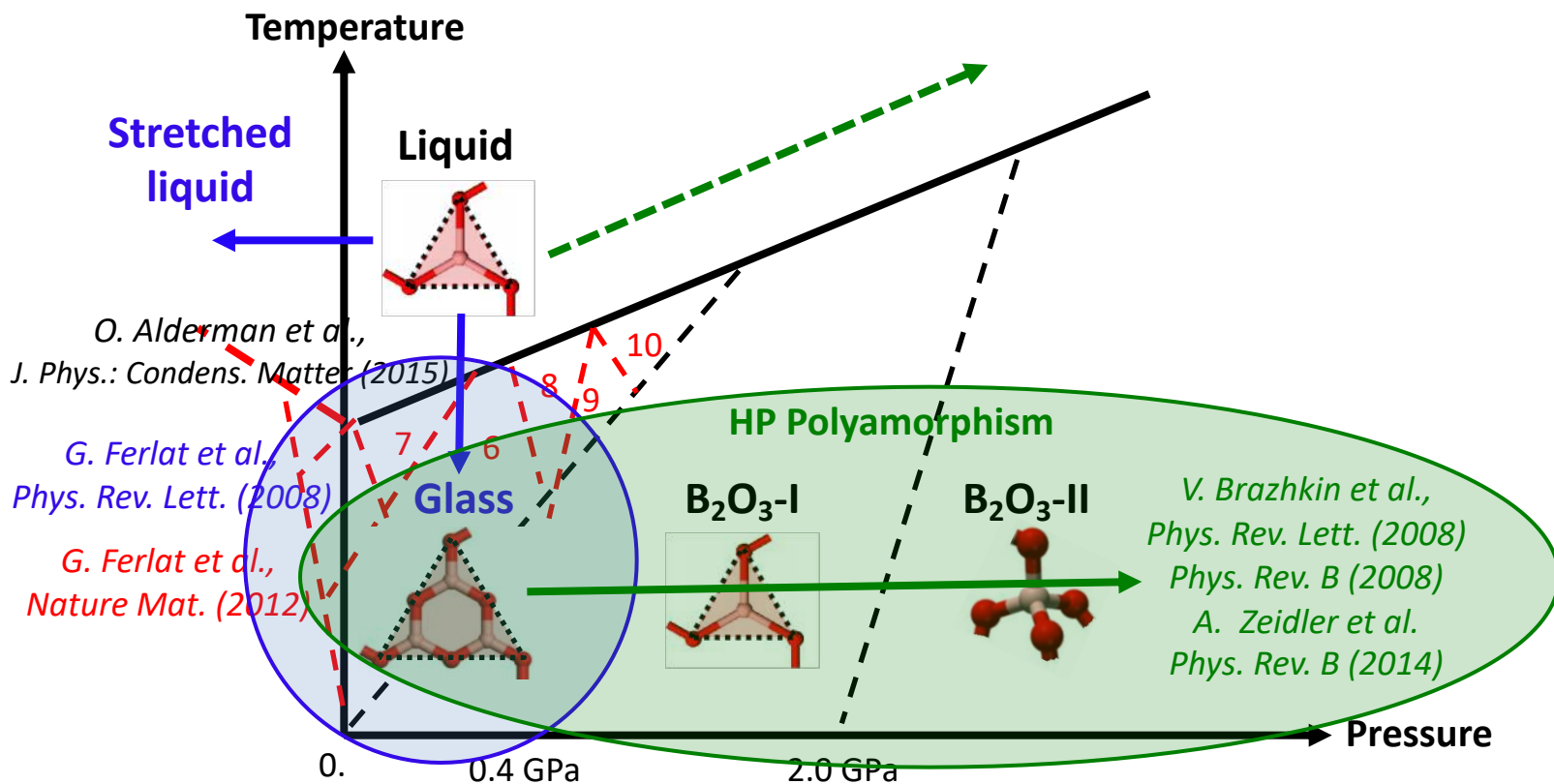
Previous (MD) works: summary



- ✓ a **network-forming glass** with significant **medium-range order** (3-fold rings)
- ✓ many (**new**) **polymorphs** structurally similar to the glass
- ✓ a system prone to polyamorphism and liquid-liquid transitions (?)

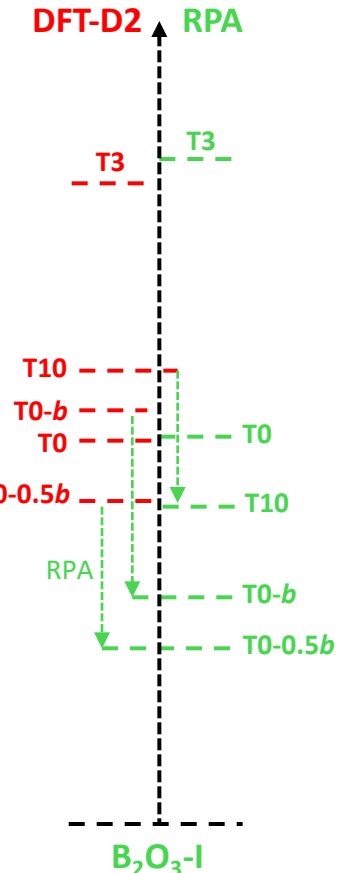
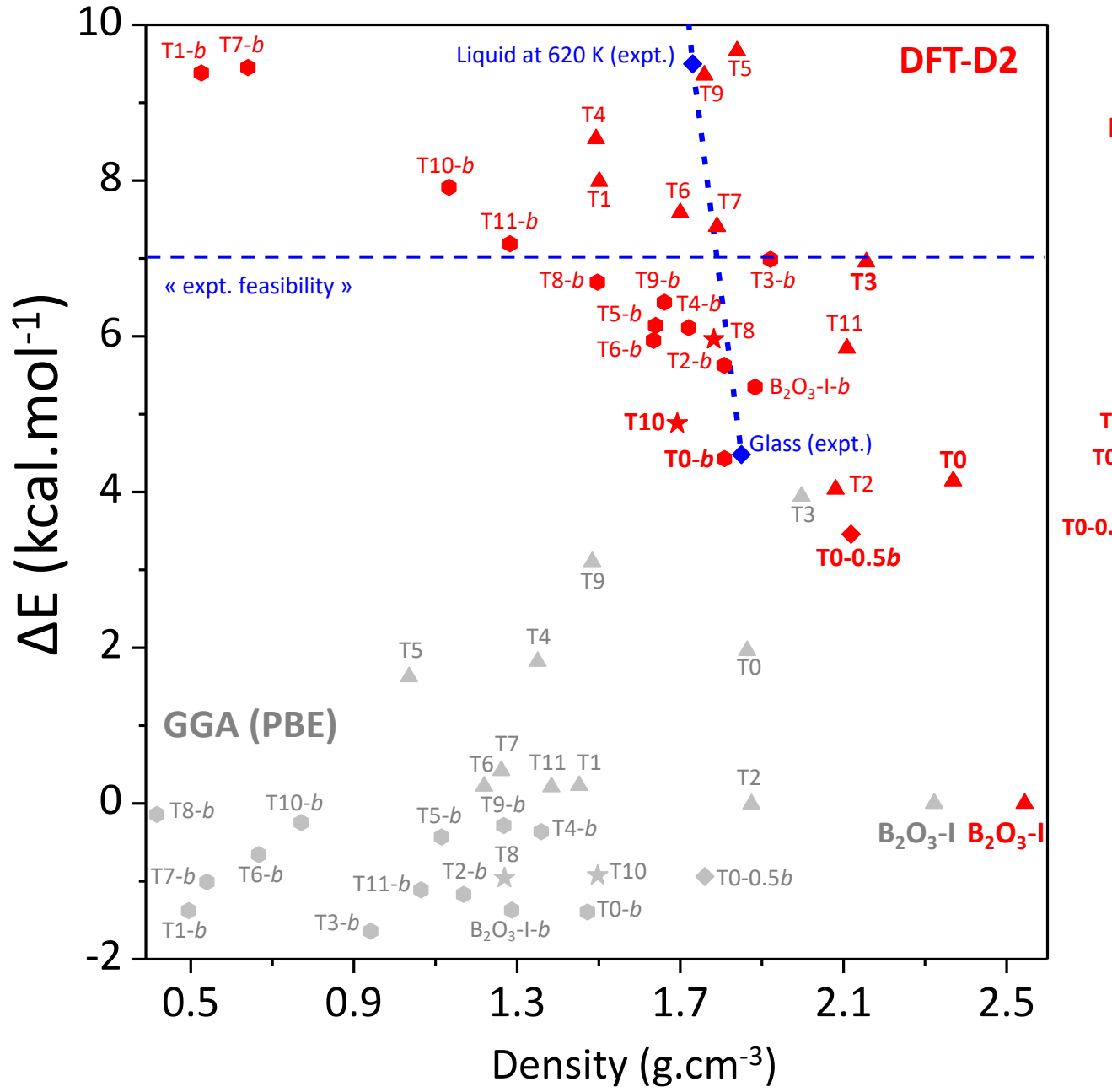
Rings in network glasses: the B_2O_3 case. G. Ferlat. Chapter 14 in "Frontiers and challenges in molecular dynamics simulations of structurally disordered materials: from network glasses to phase change memory alloys", Springer (2015).

Previous (MD) works: summary

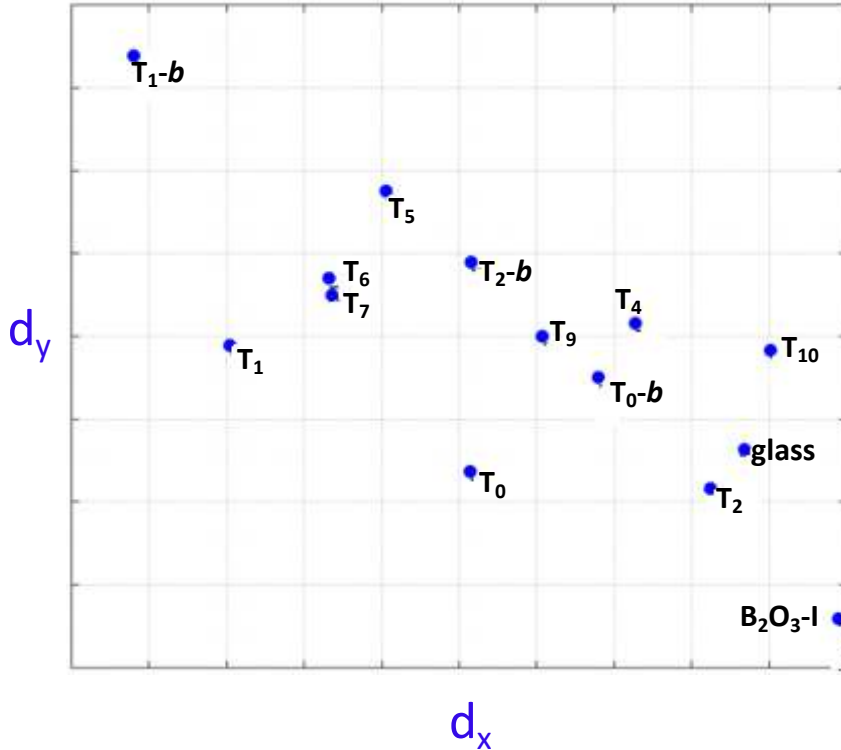


- ✓ a **network-forming glass** with significant **medium-range order** (3-fold rings)
- ✓ many (**new**) **polymorphs** structurally similar to the glass
- ✓ a system prone to polyamorphism and liquid-liquid transitions (?)

Rings in network glasses: the B_2O_3 case. G. Ferlat. Chapter 14 in "Frontiers and challenges in molecular dynamics simulations of structurally disordered materials: from network glasses to phase change memory alloys", Springer (2015).



Work in progress: PIV



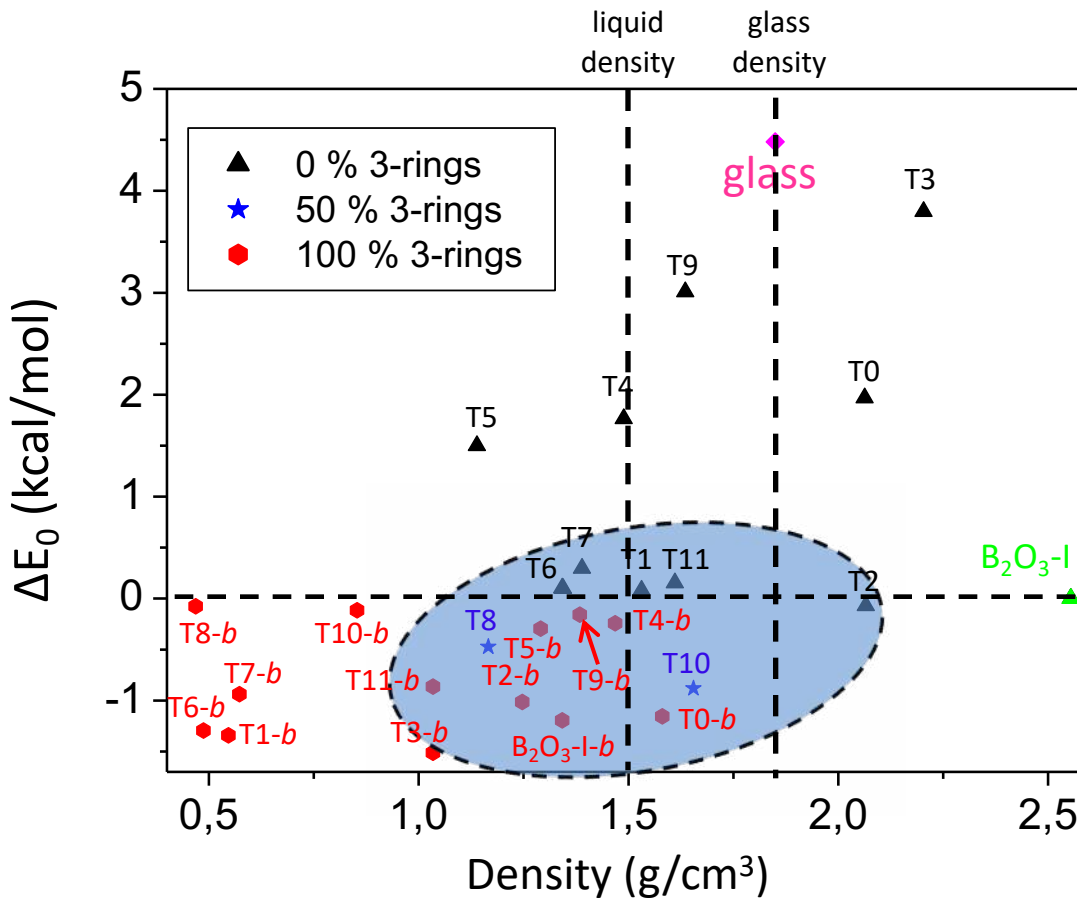
✓ The PIV metric distinguishes B_2O_3 phases

Starting from the PIV distances between all pairs of structures in a given set, for the sake of visualization and clarity, a two-dimensional map can be constructed employing the following Monte Carlo optimization algorithm. A representative point in a plane is assigned to each structure, initially with random position ($0 < x < 1$, $0 < y < 1$). Next, a cost function is defined as

$$U = \sum_{i < j} (\mathcal{D}_{ij} - d_{ij})^2, \quad (3)$$

where the sum runs over all pairs of structures and each harmonic term grows with the difference between the PIV distance \mathcal{D}_{ij} and the in-plane distance d_{ij} . In the case of liquid water and amorphous ices in Fig. 3, a set of 50 configurations is considered for each disordered phase but for the sake of clarity, a single point is shown for each phase, with \mathcal{D}_{ij} defined as the average distance between the configurations of phase i and those of phase j . U is minimized through a sequence of moves, each move consisting in the random displacement (maximum amplitude 0.0005) of one point in the plane. Moves are accepted or rejected according to a Metropolis criterion at thermal energy $kT = 1 \times 10^{-7}$ (in U units) until obtaining a Pearson's correlation coefficient = 0.999 between PIV distances and in-plane distances (in the case of water phases in Fig. 3, 10^5 moves were sufficient).

Energy-density (from DFT-GGA)

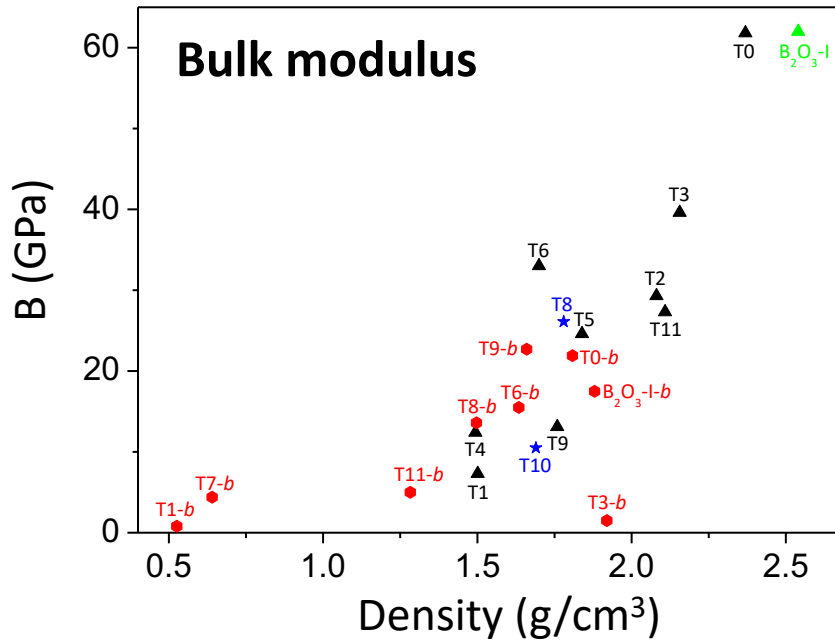


- ✓ Many low-energy crystals, most with high % of boroxols
 - ✓ Many of similar energy at densities ~ close to those of the liquid/glass
- This **rich polymorphism** induces the vitrification in a low-density glass

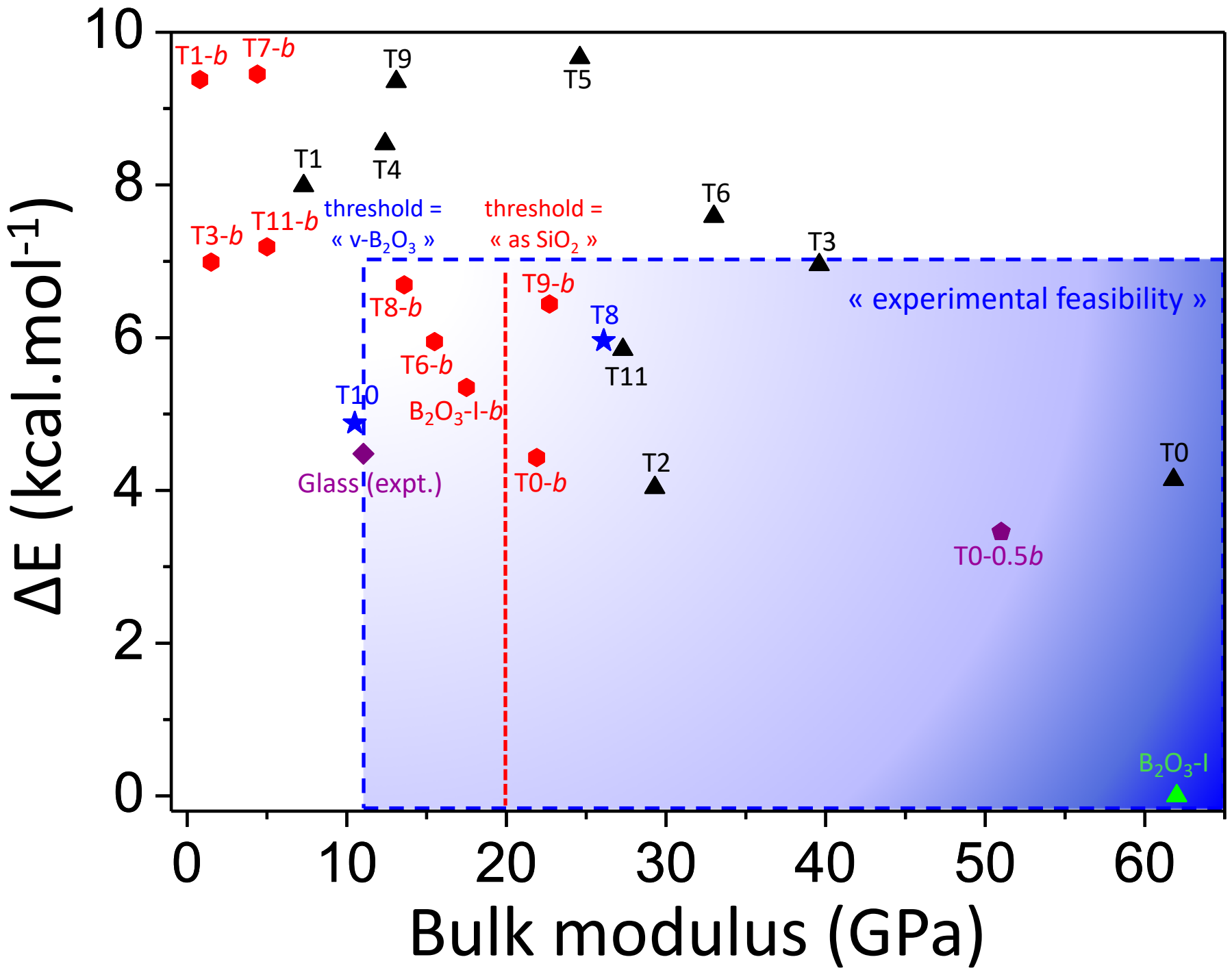
Work in progress: mechanical properties

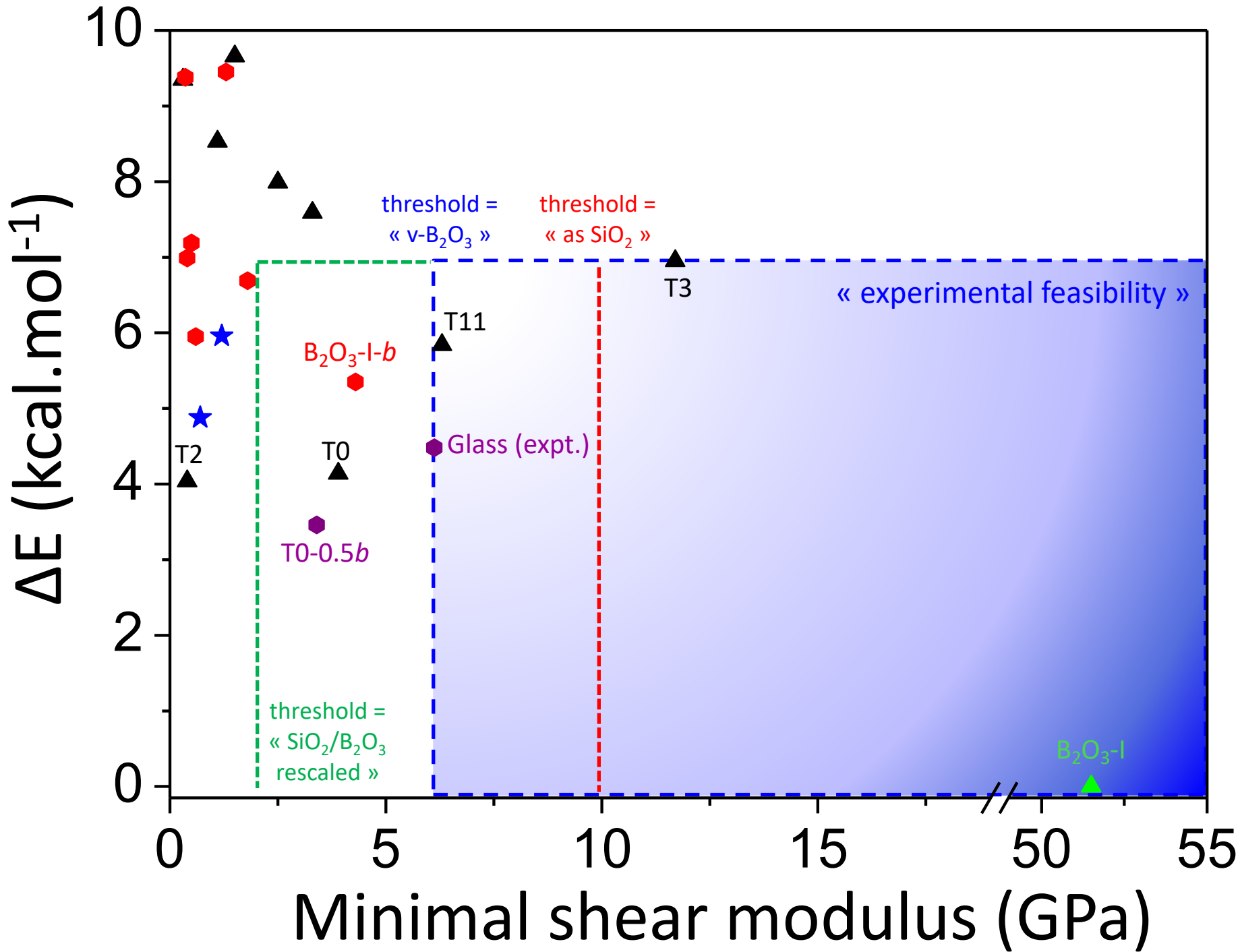
Coll. F.-X. Coudert (Chimie-ParisTech)

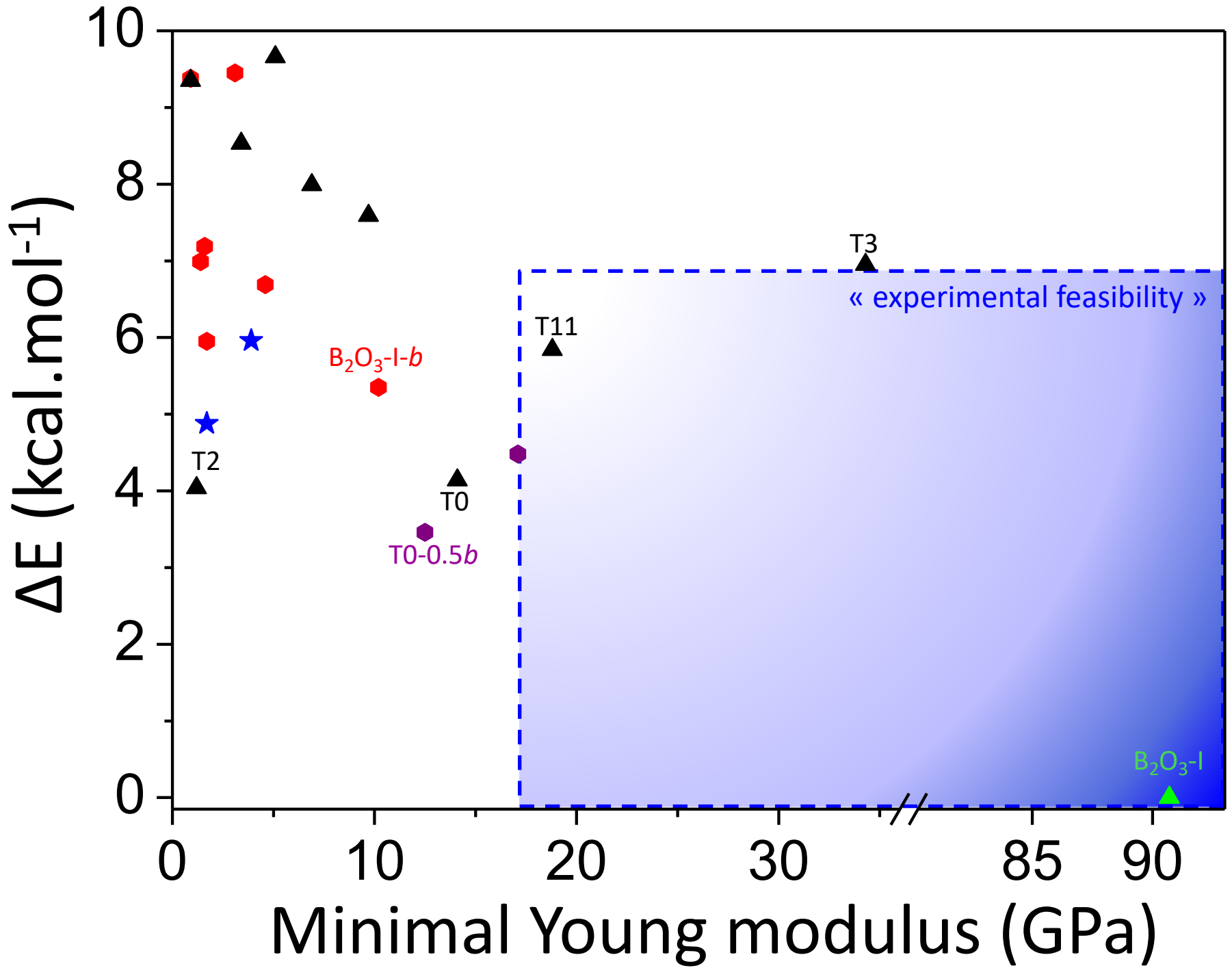
Computation of bulk, Young and Shear moduli + poisson ratio (and their anisotropy)



- ✓ most predicted polymorphs have **low** mechanical moduli (**low stiffness**)
- ✓ some show intriguing mechanical properties (*e.g. negative linear compressibility*)







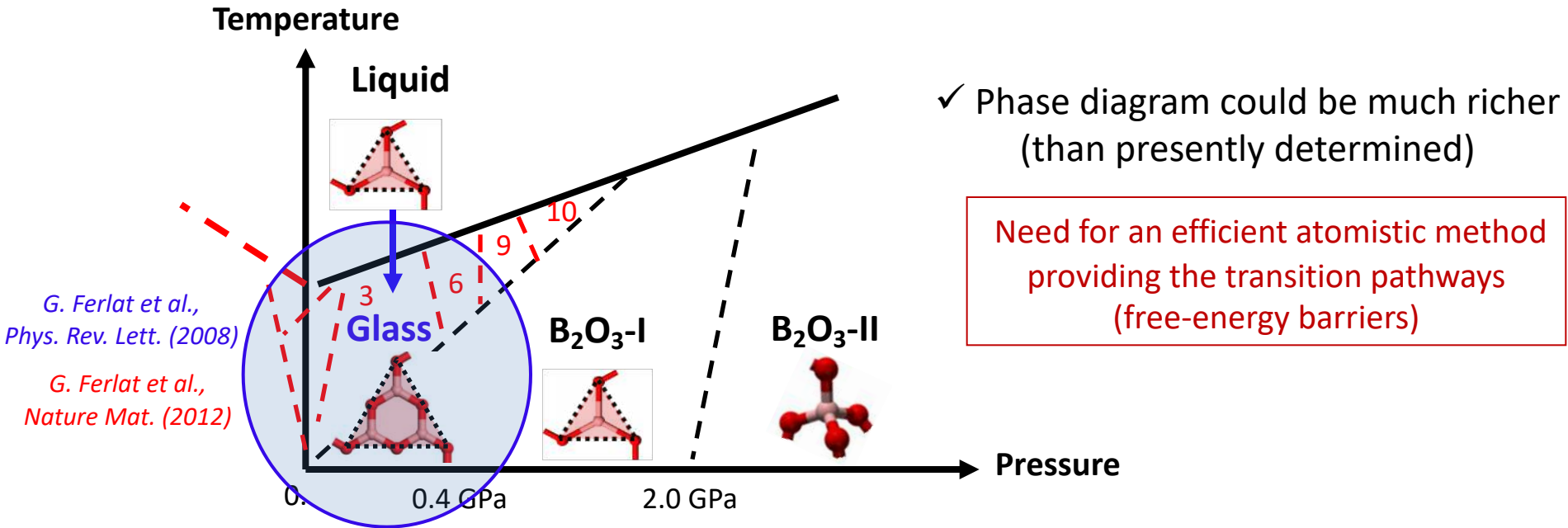
Conclusions

- Predictions of yet unknown crystals. This motivates renewed efforts to experimentally synthesise them (hints of possible synthesis do exist)
- The predicted crystals share structural similarities with the glass (low-density, high proportion of boroxol rings)
- Rich polymorphism + mechanical softness \leftrightarrow ease of vitrification
- Large flexibility of the B-O-B bonds. Importance of vdW interactions
- Evidence of a boroxol stabilisation energy of ~ 10 kcal/mol

Perspectives

- Exploration of the phase diagram: Metadynamics + PIV metric
collaboration F. Pietrucci (Sorbonne U.), M. Salanne (Sorbonne U.)

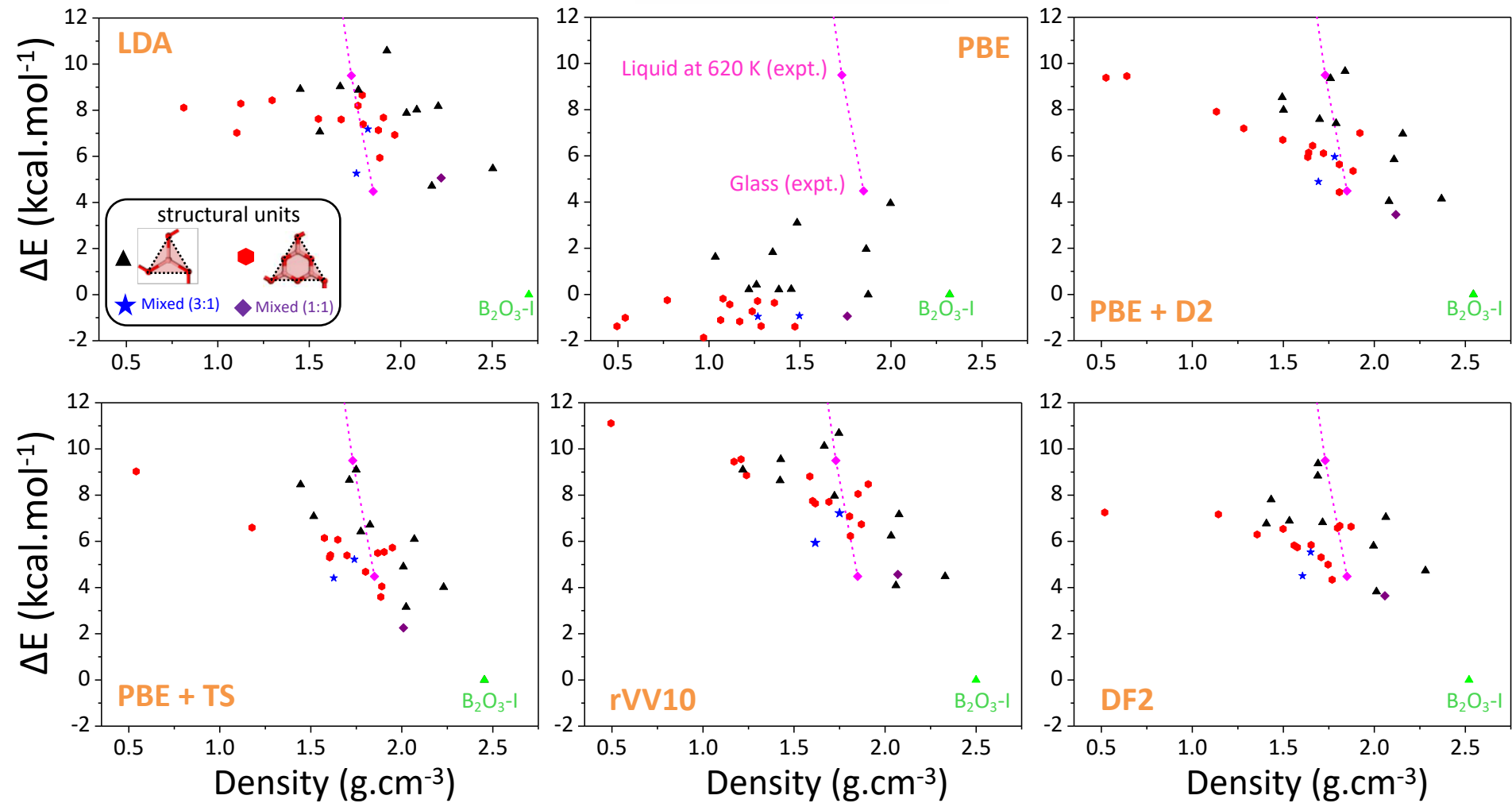
Perspectives



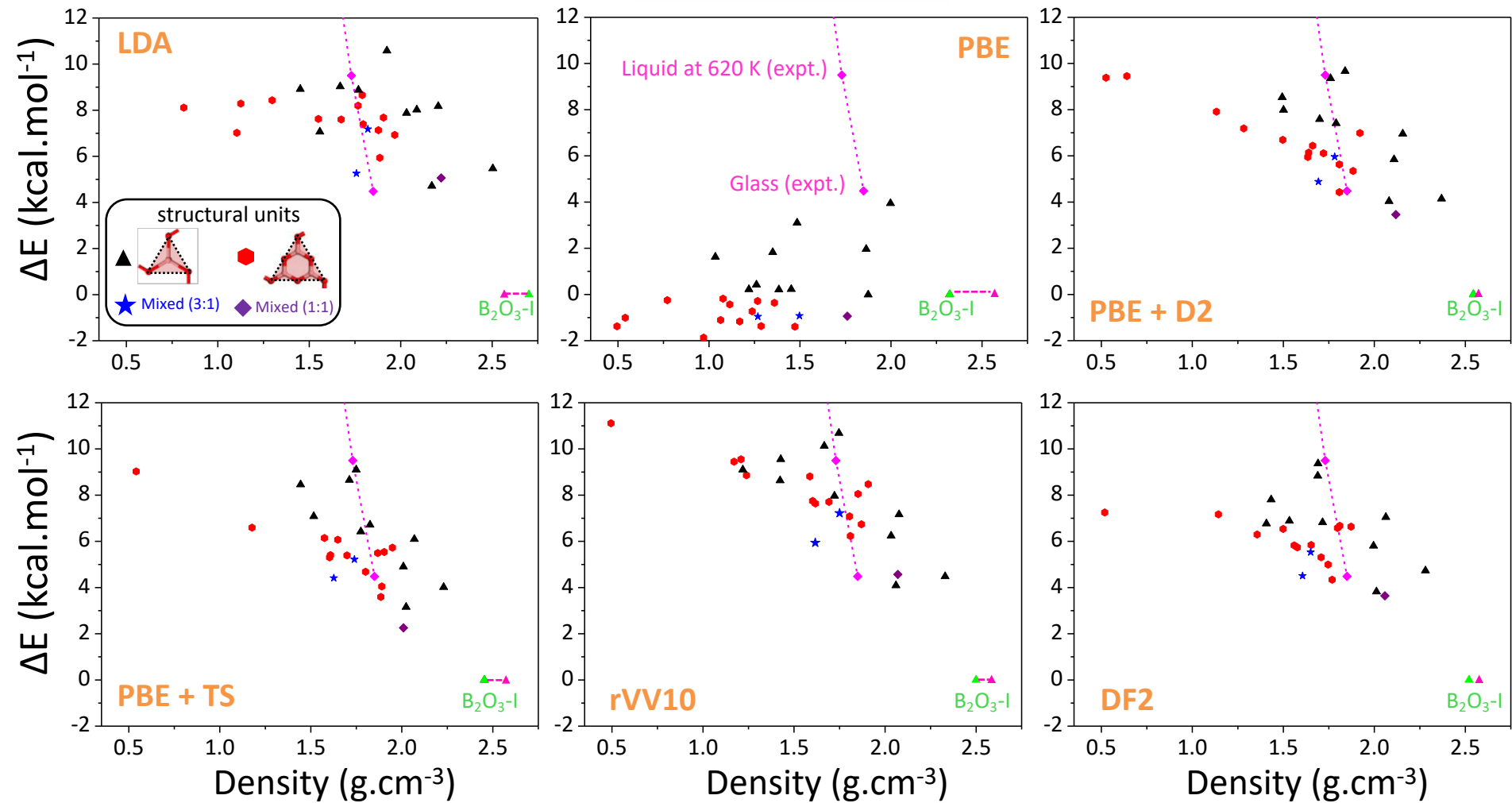
Perspectives: - determine the p-T conditions of stability for the novel phases
- track the structural transformations as the liquid is cooled down

- What are the **structural connections between the known and the novel crystals ?** (i.e. can we obtain a novel polymorph by e.g. shearing $B_2O_3\text{-I}$?)
- What are the **structural connections between the glass and the novel crystals ?** Can the glass be devitrified ? What is the glass **nanoscale organisation** ?

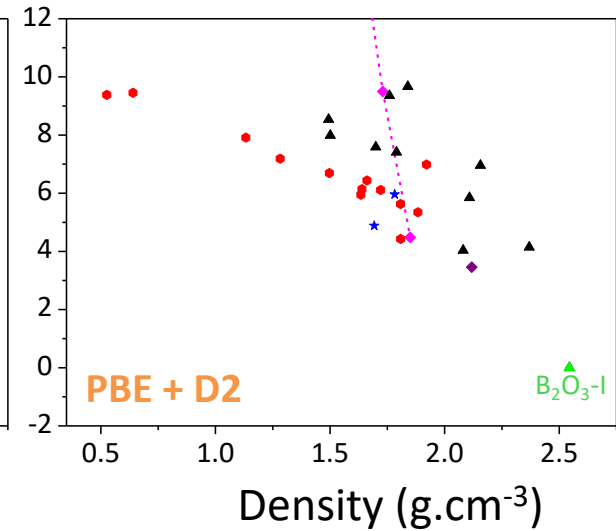
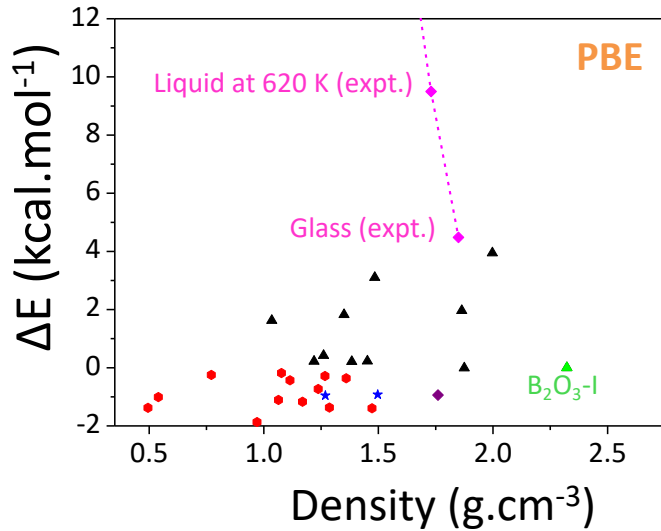
DFT scenario



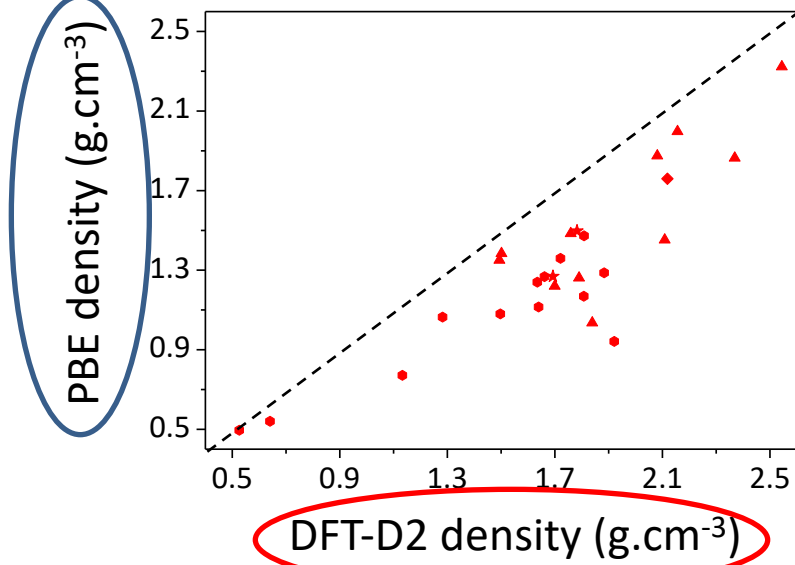
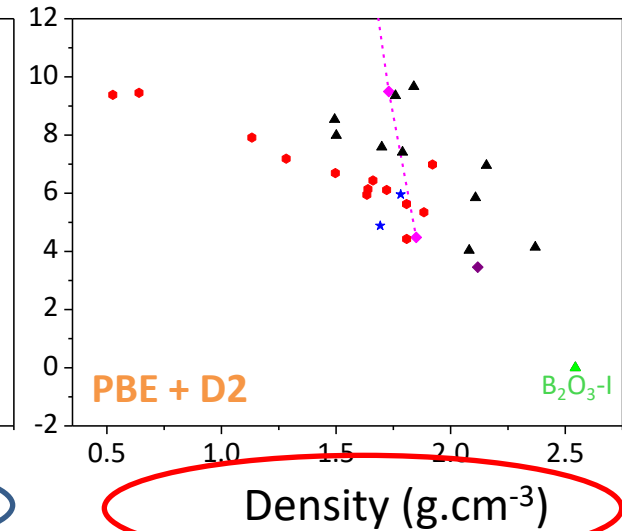
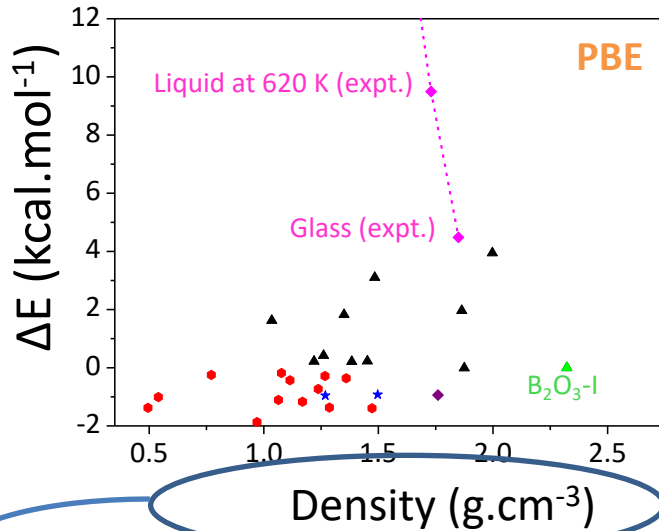
DFT scenario



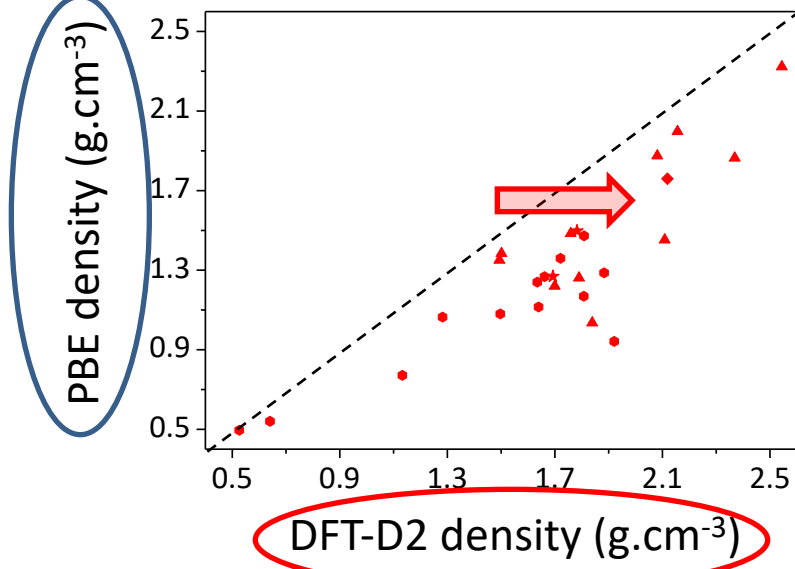
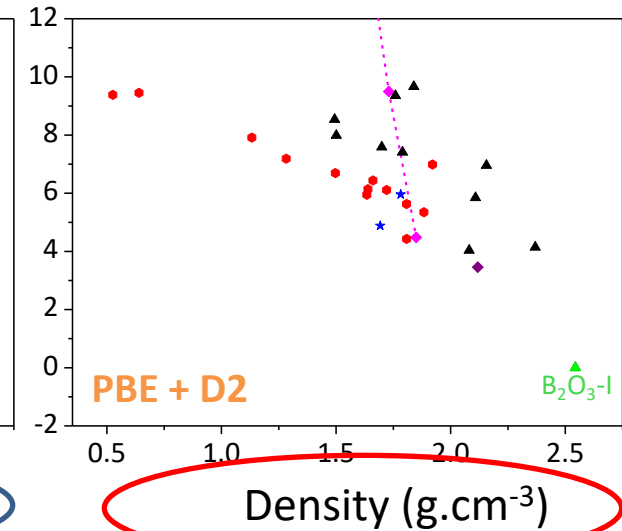
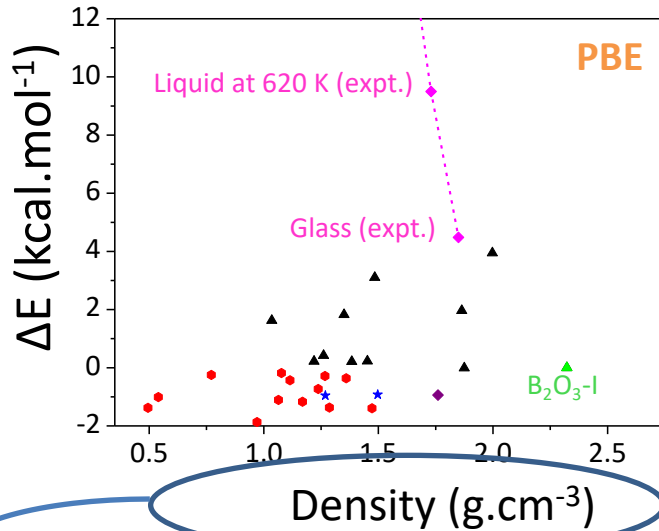
DFT-GGA versus DFT-D



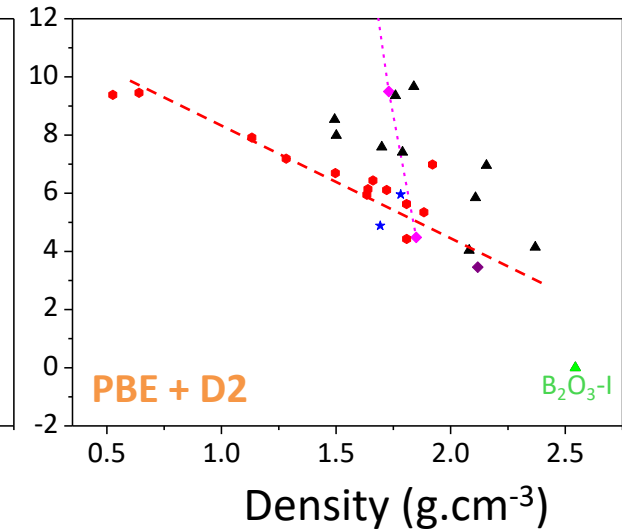
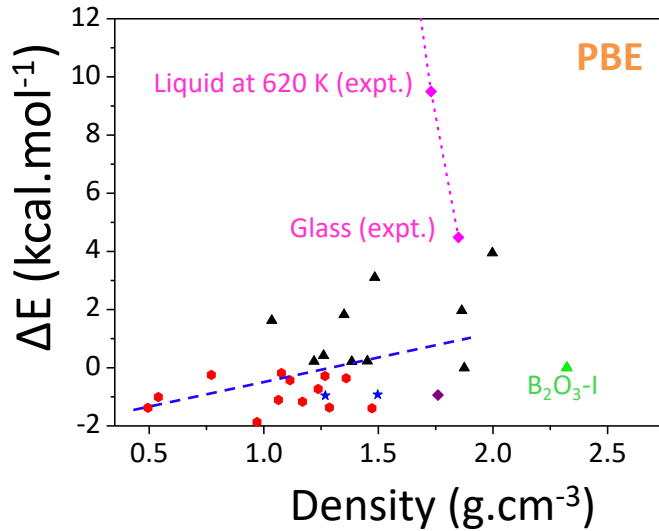
DFT-GGA versus DFT-D



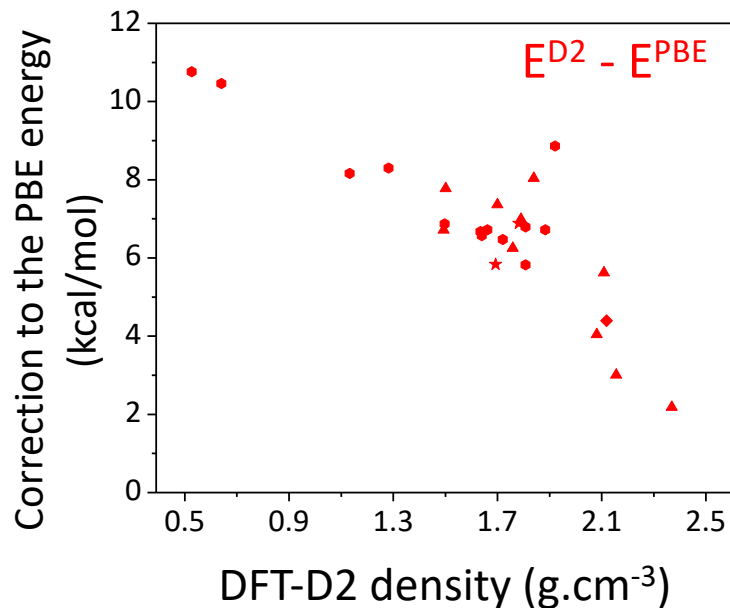
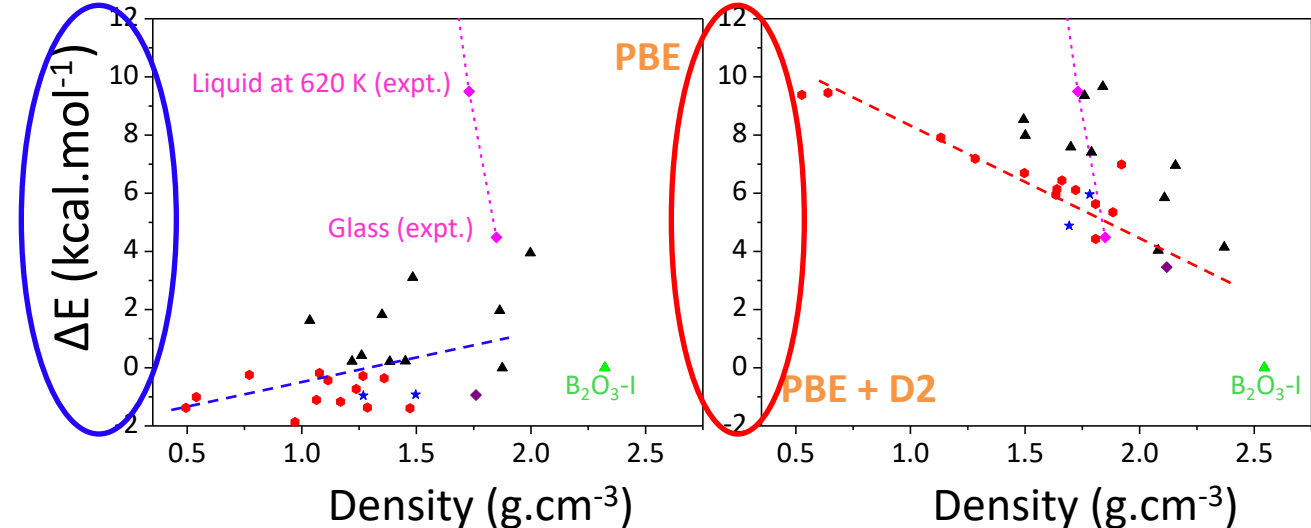
DFT-GGA versus DFT-D



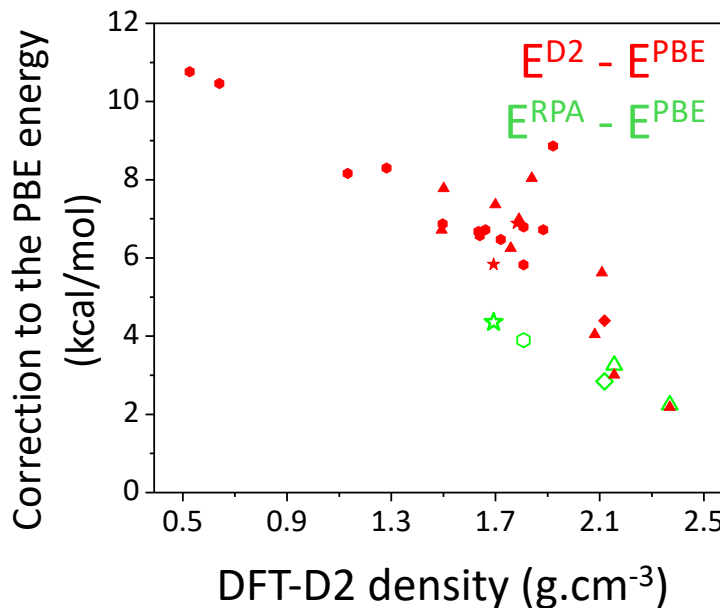
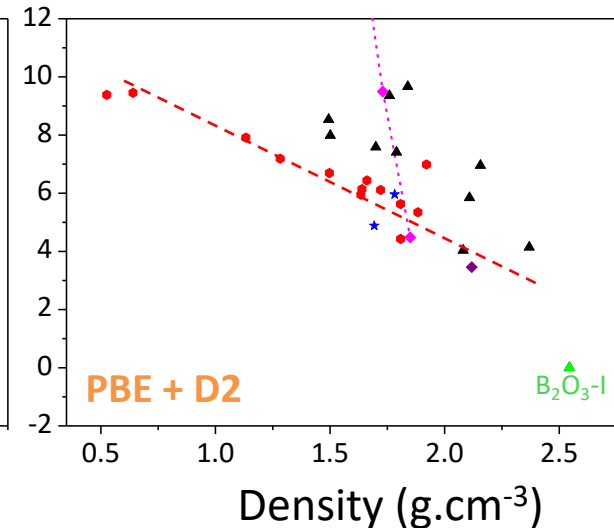
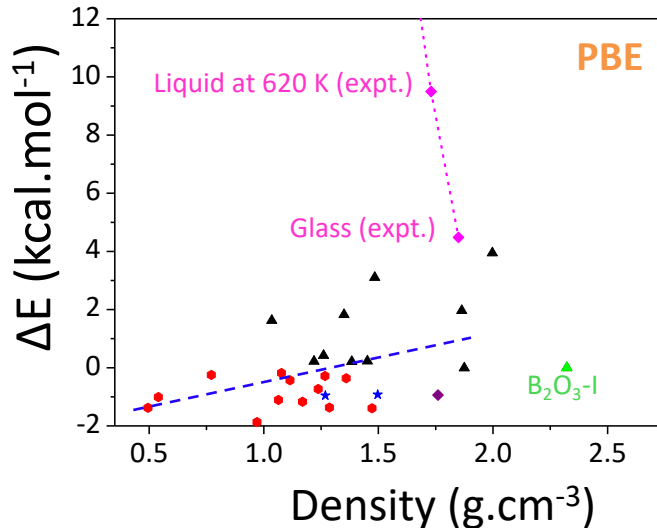
DFT-GGA versus DFT-D



DFT-GGA versus DFT-D



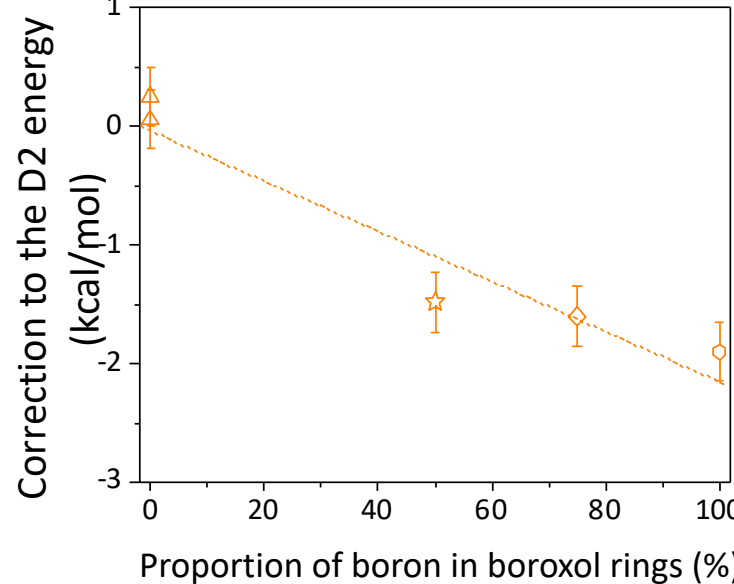
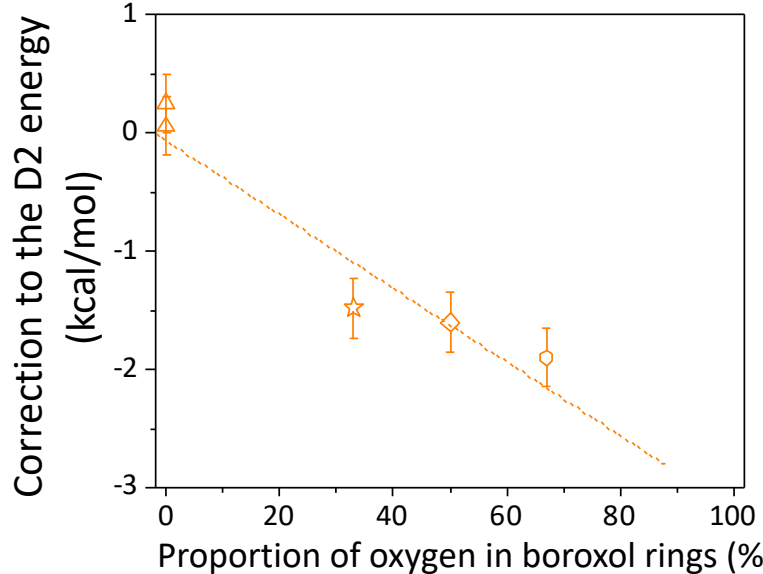
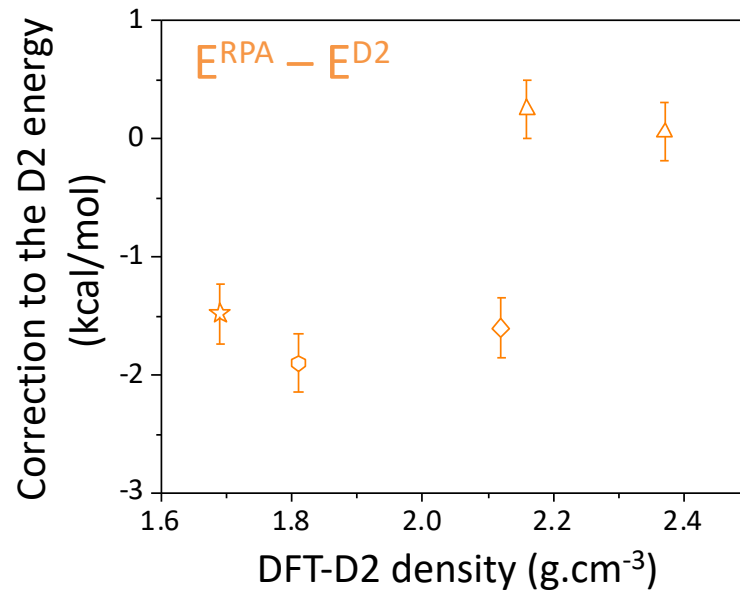
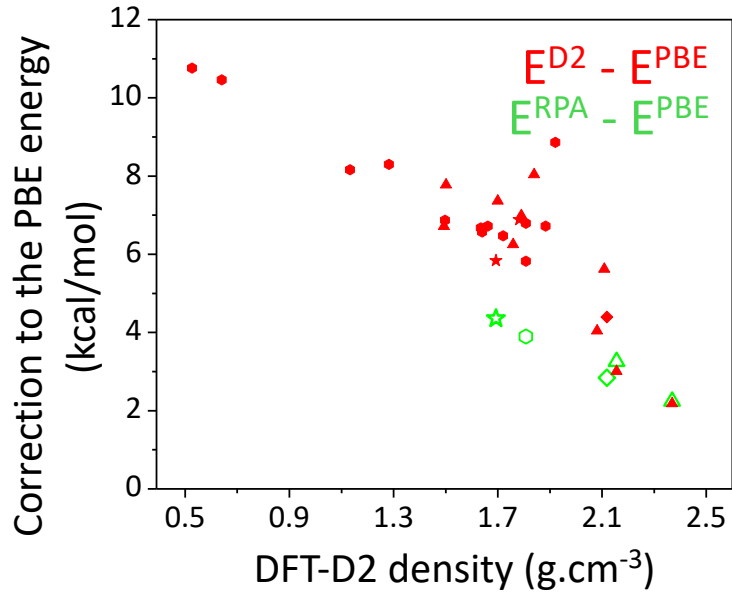
DFT-GGA versus DFT-D



vdW: increasing energy penalty
with decreasing density

Trend confirmed by RPA

Many-body beyond vdW



Polymorphism and ease of vitrification

Nature **257**, 370 (1975)

Strained mixed-cluster model for glass structure

C. H. L. Goodman

Standard Telecommunication Laboratories Ltd, London Road, Harlow, Essex, UK

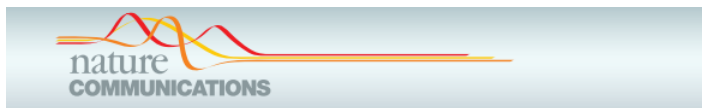
Many features of glass behaviour can be explained by a new approach to glass structure based on two ideas. First, glass-forming melts generate 'clusters' of structurally non-related polymorphs which associate on cooling but cannot nucleate and second, inter-cluster thermal strain can be relieved by subsequent 'plating-out' of modifier impurities.

Nature **260**, 35 (1976)

Non-crystallinity and polymorphism in elemental solids

RONG WANG
MARTIN D. MERZ

THIS paper shows a universal correlation of the non-crystalline state with polymorphism in elemental solids. This is demonstrated by a map constructed on a plot of the number of polymorphic forms (NPF) against the group number (GN) for all solid elements in the Periodic Table (Fig. 1). From this result, we propose that both the structure and occurrence of a non-crystalline solid are governed by the structures shown by crystalline states of the element.



ARTICLE

Received 29 Jan 2016 | Accepted 22 Jun 2016 | Published 2 Aug 2016

DOI: 10.1038/ncomms12315

Spectral descriptors for bulk metallic glasses based on the thermodynamics of competing crystalline phases

Eric Perim^{1,2,*}, Dongwoo Lee^{3,*}, Yanhui Liu^{4,*}, Cormac Toher^{1,2}, Pan Gong⁴, Yanglin Li⁴, W. Neal Simmons^{1,2}, Ohad Levy^{1,2}, Joost J. Vlassak³, Jan Schroers⁴ & Stefano Curtarolo^{1,2}

Metallic glasses attract considerable interest due to their unique combination of superb properties and processability. Predicting their formation from known alloy parameters remains the major hindrance to the discovery of new systems. Here, we propose a descriptor based on the heuristics that structural and energetic 'confusion' obstructs crystalline growth, and demonstrate its validity by experiments on two well-known glass-forming alloy systems. We then develop a robust model for predicting glass formation ability based on the geometrical and energetic features of crystalline phases calculated *ab initio* in the AFLOW framework. Our findings indicate that the formation of metallic glass phases could be much more common than currently thought, with more than 17% of binary alloy systems potential glass formers. Our approach pinpoints favourable compositions and demonstrates that smart descriptors, based solely on alloy properties available in online repositories, offer the sought-after key for accelerated discovery of metallic glasses.

QMC details

- Variational ansatz: Jastrow-Slater wave-function
- Pseudos-potentials of Burkatzki-Filippi-Dolg,
- Supercells of up to 60 atoms, special Baldereschi k -point

Geometry relaxation at VMC level:

- contracted basis set: $(6s4p)/[2s1p]$ for B and $(5s4p)/[2s1p]$ for O,
- fully optimised wave-function (Jastrow + Slater orbitals)

Energetics at LRDMC level

Large uncontracted basis set:

- for the determinant: $(10s10p1d)$ gaussian type orbitals for both B and O,
- for the Jastrow three- and four-body terms: $(2s2p1d)$ gaussian type orbitals

TurboRVB package